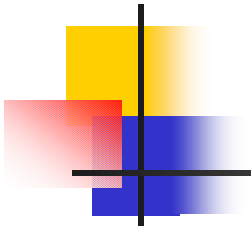

Neutrino beams and detectors

- Neutrino beams
  - Conventional neutrino beams
  - β beams
  - Neutrino factories
- Detectors
  - Cerenkov detectors: water, heavy water and scintillator
  - Liquid argon
  - Hybrid detectors: nuclear emulsions plus electronic detectors
  - Magnetized iron calorimeter
  - Low Z calorimeter

Working principle of a conventional neutrino beam

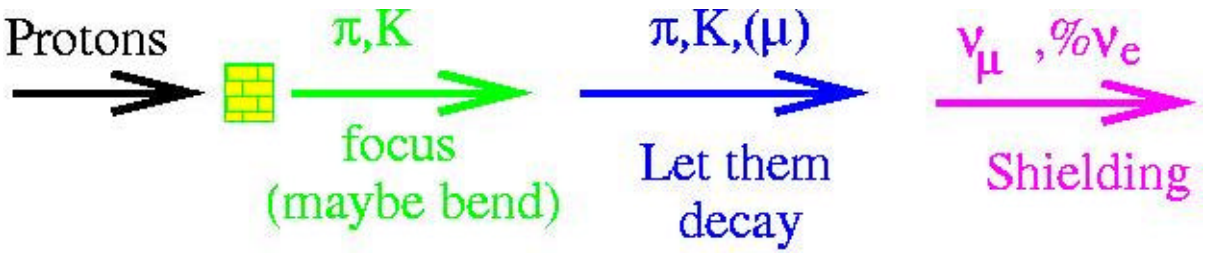

1. High energy protons (O(10 GeV) to O(100 GeV) are sent onto a target (typically Be, graphite) where π and K are produced copiously
2. π^+/K^+ (π^-/K^-) are focused and π^-/K^- (π^+/K^+) are defocused in order to obtain a ν_μ (anti-ν_μ) beam through a magnetic lens system
3. Focused hadrons are let decay into a "decay tunnel" to produce neutrinos of the wanted flavor (and not only)
4. A shielding is put at the end of the decay tunnel in order to absorb charged particles associated with the neutrino beam (this step is only true for exps located very close (L<1km) to the neutrino source)

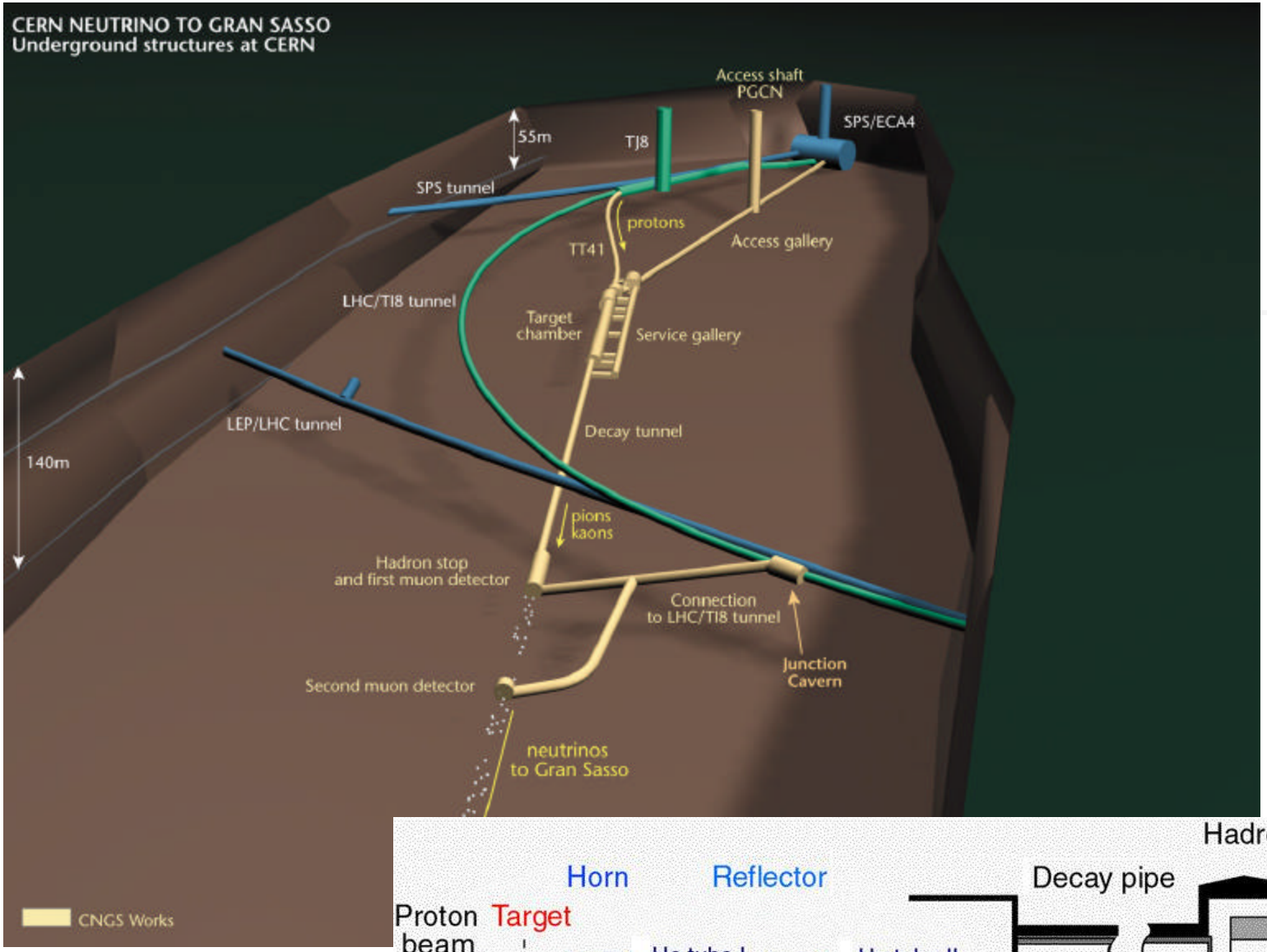

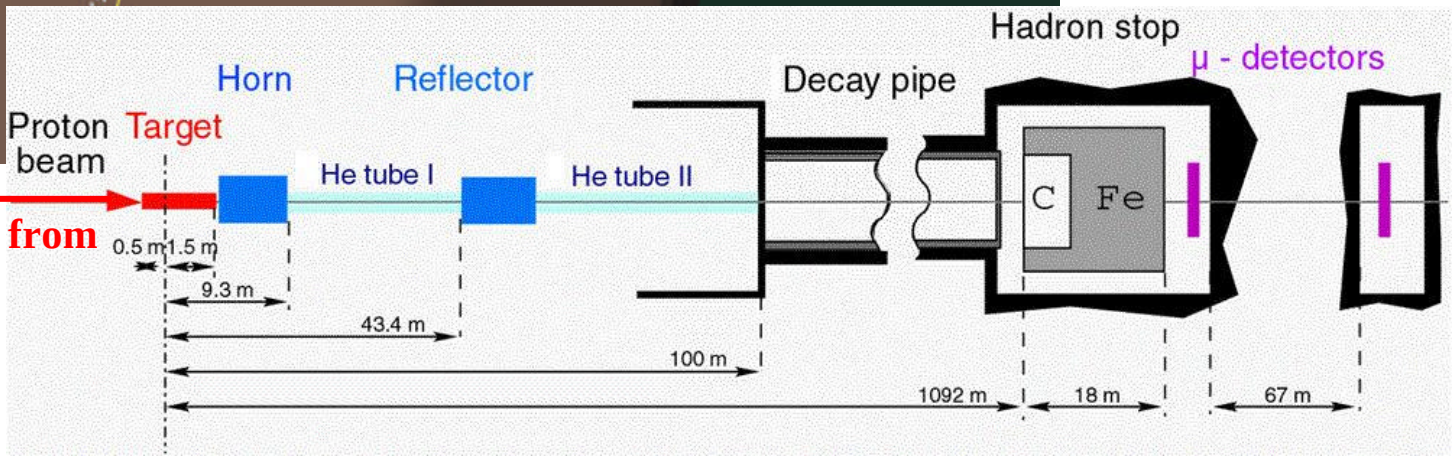

400 GeV proton beam from the CERN SPS

The magnetic focusing system (I)

Particles emerging from a source (the target) with a given momentum and angular distribution can be deviated into a parallel beam by means of the magnetic volume provided in the horn. This principle is illustrated below for 35 GeV positively charged particles leaving the CNGS target.

Those particles with very small angle at production will never cross the inner conductor into the magnetic volume and will therefore continue in a straight line. Particles with somewhat larger production angles travel inside the magnetic volume, the more so for the larger angles. Within a given range of angles, these particles all form a parallel beam at the exit of the horn. At even larger production angles, the field in the horn is insufficient and the particles are not deviated enough.

In order to deviate a larger number of particles produced at various energies and angles, a two-horn system, sometimes called horn and reflector, is needed.

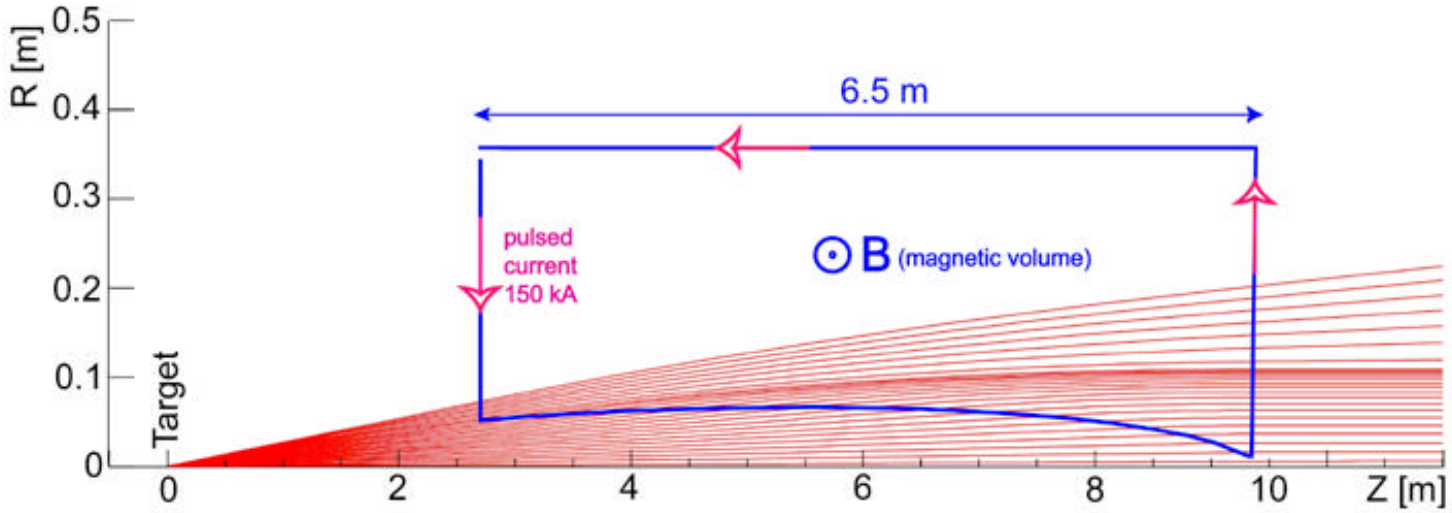

The magnetic focusing system (II)

The figure shows, for a few selected families of particles exiting the CNGS target, the action of horn and reflector on the trajectories. For a family of 35 GeV trajectories with production angles from 2.3 to 19.4 mrad, the horn alone achieves a parallel beam to Gran Sasso (middle), while for other energies or production angles, the action of the reflector is needed. (Note: "pt" stands for the transverse momentum of the particles.).

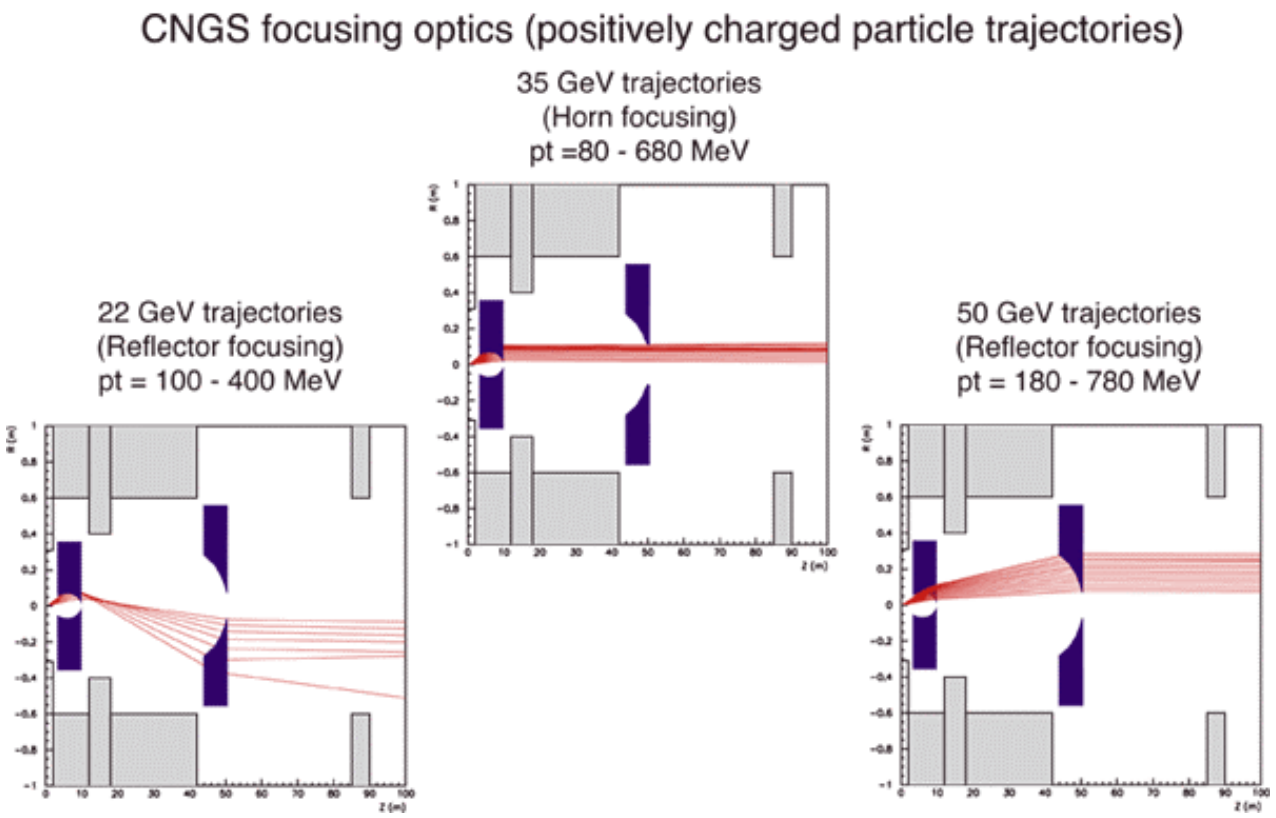

The magnetic focusing system (III)

Angular distribution upstream and downstream the horn

$\pi^+ (\rightarrow \mu^+ \nu_\mu)$

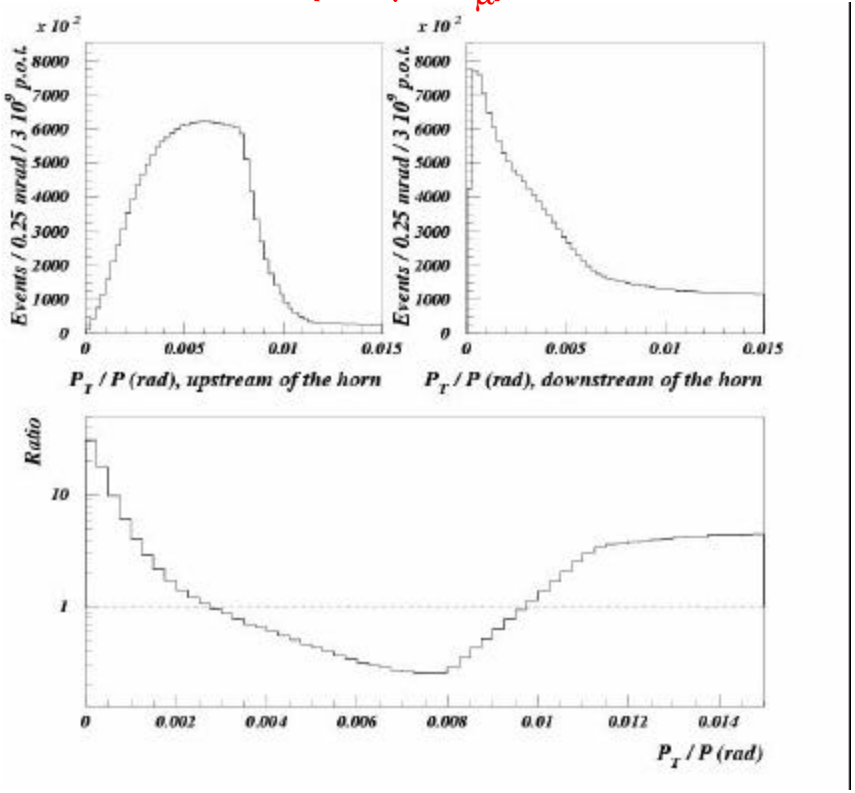

$\pi^- (\rightarrow \mu^- \text{anti-}\nu_\mu)$

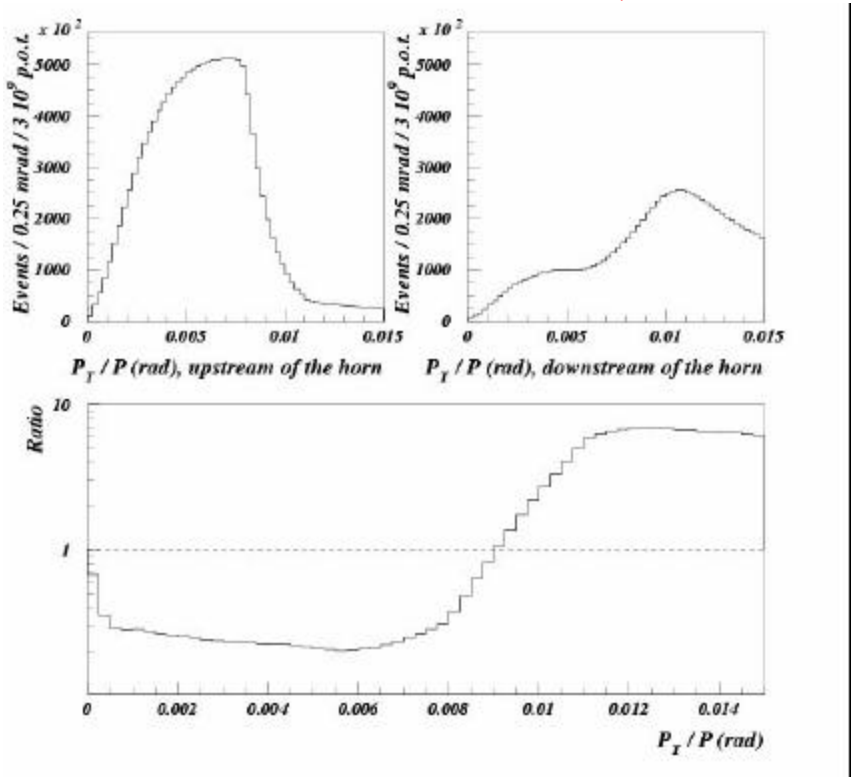

Three types of conventional neutrino beams

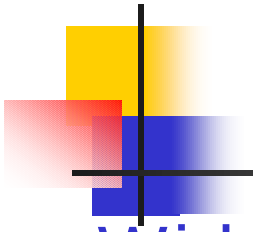

- Wide Band Beam
  - The magnetic lens system is supposed to collect as many hadrons as possible
    - $\Rightarrow$ “wide” neutrino energy spectrum
    - $\Rightarrow$ high neutrino flux
- Narrow Band Beam
  - The magnetic lens system is supposed to collect only hadrons with a given momentum
    - $\Rightarrow$ “narrow” neutrino energy spectrum
    - $\Rightarrow$ low neutrino flux
- Off-Axis beam
  - Reasonable compromise between the Wide and the Narrow approach

Working principle of the Off-Axis beam

- Quasi Monochromatic Beam
- x2~3 intense than NBB

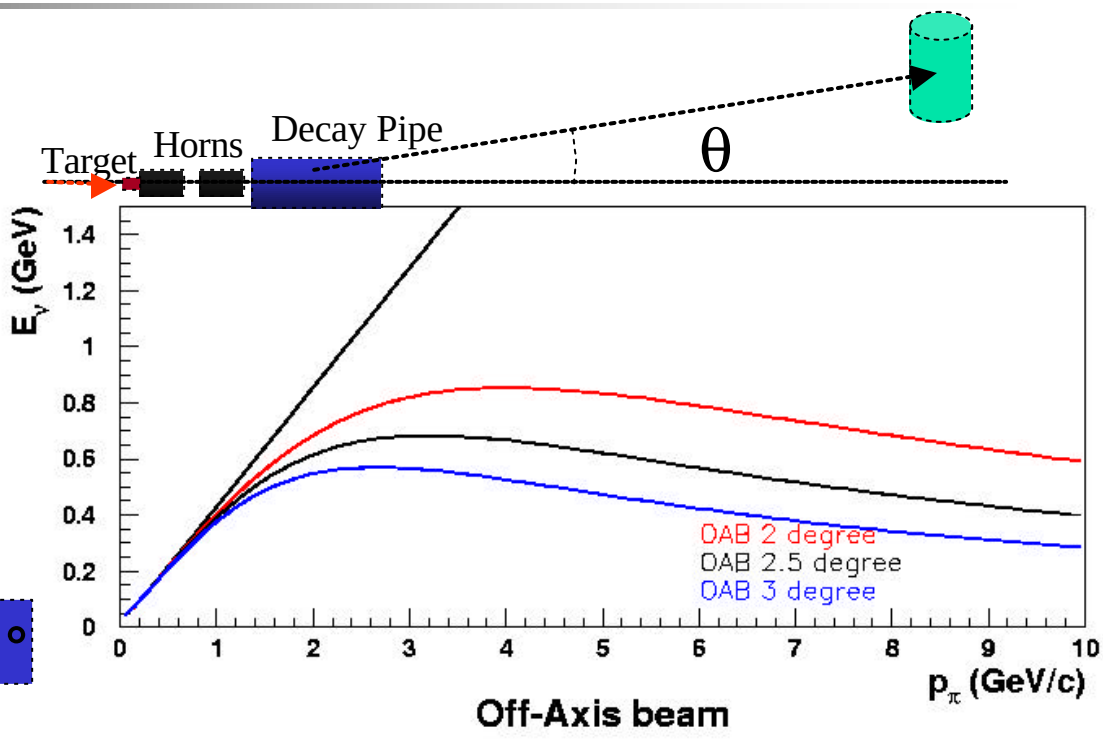

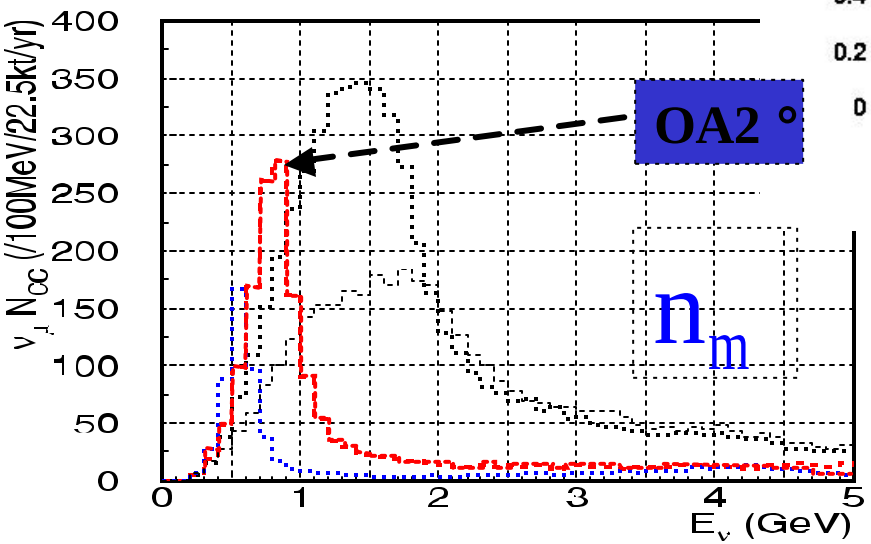

Problems with conventional neutrino beams in predicting fluxes and composition (I)

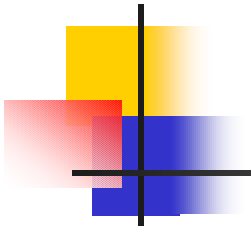

- Description of the proton beam
- Particle yield in the p-Target interaction
- Description of the focusing system
- Description of the particle trajectories after the focusing system (important to extrapolate from the decay point to the detector location)

Problems with conventional neutrino beams in predicting fluxes and composition (II)

- Use standard MC simulation : Geant, Fluka, Mars to full simulate target production + beamline (SLOW)
- Use dedicated parametrizations for secondary production in target (Sanford-Wang, Malensek, BMPT .... based on available data (Na56/SPY, ...) + simulation of beamline (FAST)
- Secondary components -> needs better knowledge of hadron production in the target
- More data needed on hadroproduction
- Two possible solutions
  - NOMAD approach (no close detector)
  - Two (or even more) detectors approach (near to far extrapolation)

Monitoring of the proton beam

The measured profiles of the incident proton beam, averaged over all years data taking, are larger than the target

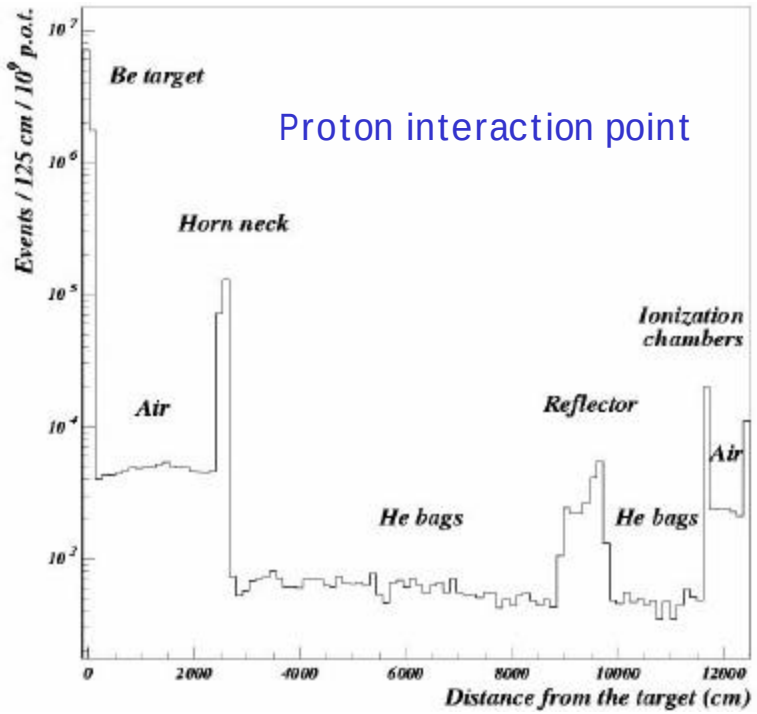

The vertical arrows indicate the edges of the target

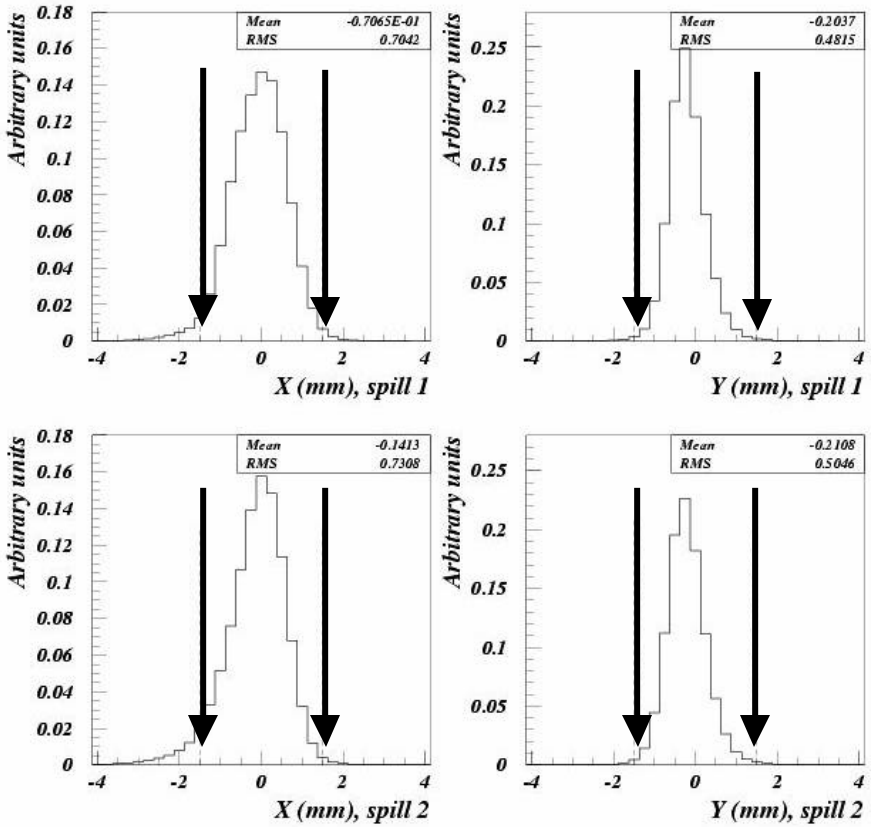

Particle production in p-Target interactions

- One of the most critical ingredients in the calculation of the neutrino flux and energy spectra is the hadron yield in p-Target interactions (in the example I'll discuss in the following, the WANF beam, Target=Be and E_p=450GeV)
- Only two exps measured the hadron yields: NA20 and NA56/SPY
- The results of these exps are used as benchmark for the MC simulation

FLUKA2000 vs DATA

FLUKA (histo) vs DATA (dots)

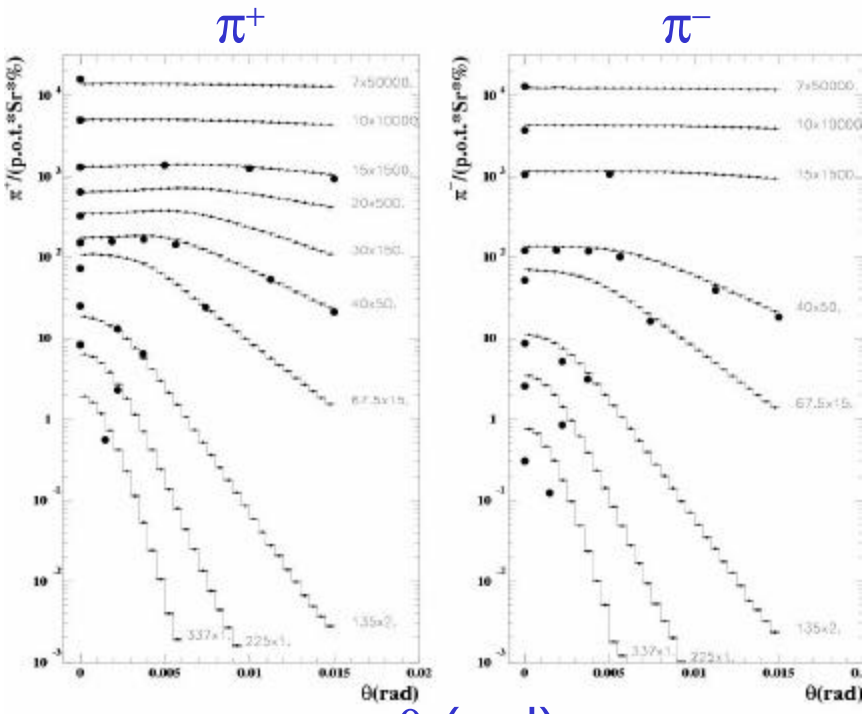

The reweighting functions for different hadrons obtained from NA20 and SPY

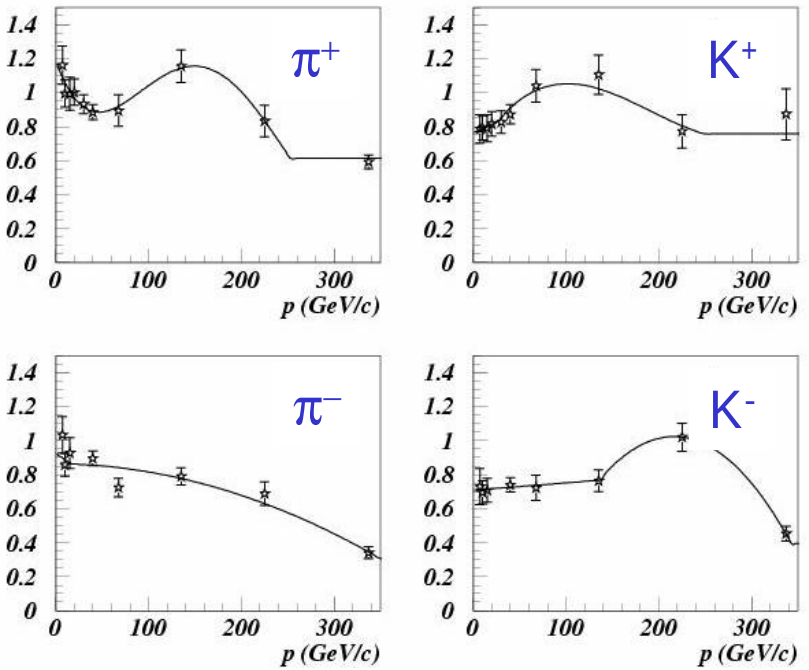

Beam composition as predicted with FLUKA2000

Table 2
Composition of the neutrino beam and its various species.

ν	Flux		Source							
			π^+ or π^-		K^+ or K^-		K^0_L		μ^+ or μ^-	
species	Abund.	$\langle E_\nu \rangle$	%	$\langle E_\nu \rangle$	%	$\langle E_\nu \rangle$	%	$\langle E_\nu \rangle$	%	$\langle E_\nu \rangle$
ν_μ	1.0	24.3	90.4	19.1	9.5	73.0	0.1	26.8	<0.1	11.4
$\bar{\nu}_\mu$	0.0678	17.2	84.0	13.8	12.8	38.1	1.9	26.9	1.2	17.0
ν_e	0.0102	36.4	–	–	68.0	41.8	17.8	30.3	13.6	16.8
$\bar{\nu}_e$	0.0027	27.6	–	–	25.1	22.8	68.2	30.4	3.5	11.1

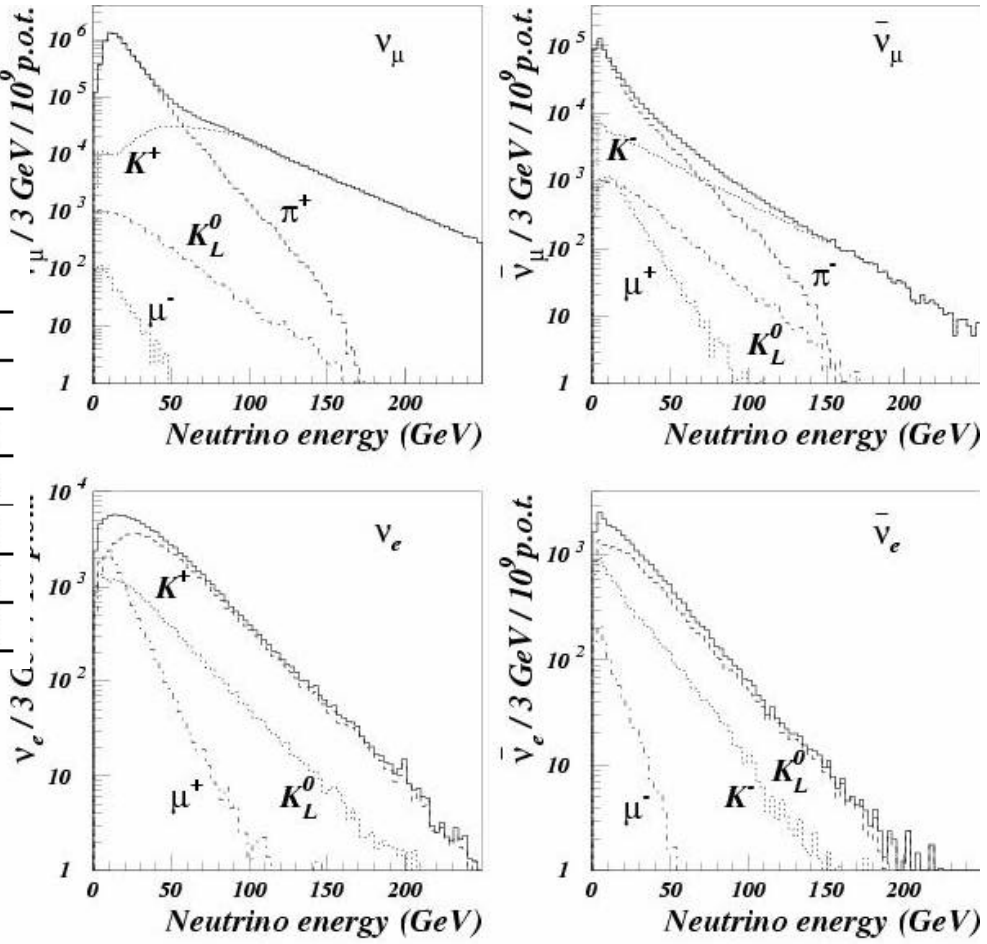

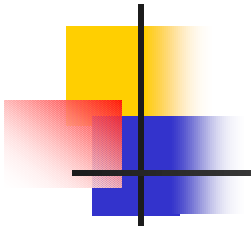

Systematic uncertainties (I)

- Uncertainty on the yields of particles from p-Be interactions
- Uncertainty on the yields of particles interactions other than p-Be
- Proton interactions downstream of the Be target
- Reinteractions in the Be target and downstream of the target
- Position and angular divergence of p beam
- Magnetic field in the horn and the reflector
- Inaccuracies in the simulation of the beam line elements
- Misalignment of the beam line elements

Systematic uncertainties (II)

Table 5
Summary of energy-independent relative systematic uncertainties in the ν_μ, $\bar{\nu}_\mu$, ν_e and $\bar{\nu}_e$ fluxes and in the ν_e/ν_μ ratio. The energy-dependent uncertainties are shown in Fig. 14.

Source of uncertainty	ν_μ	$\bar{\nu}_\mu$	ν_e	$\bar{\nu}_e$	ν_e/ν_μ
Yields of secondary particles	0.034	0.029	0.039	0.064	0.036
Proton interaction downstream of target	0.002	0.024	0.003	0.013	0.003
Reinteractions of secondary particles	0.014	0.070	0.017	0.067	0.018
Beam position and divergence	0.056	0.021	0.058	0.035	0.002
Horn current	0.004	0.004	0.001	0.001	0.005
Field in inner conductor	0.004	0.026	0.011	0.016	0.007
Amount of material	0.012	0.022	0.007	0.012	0.005
Horn misalignment	0.002	0.006	0.007	0.012	0.005
Collimator misalignment	0.003	0.020	0.008	0.013	0.005
Total	0.068	0.091	0.074	0.103	0.042

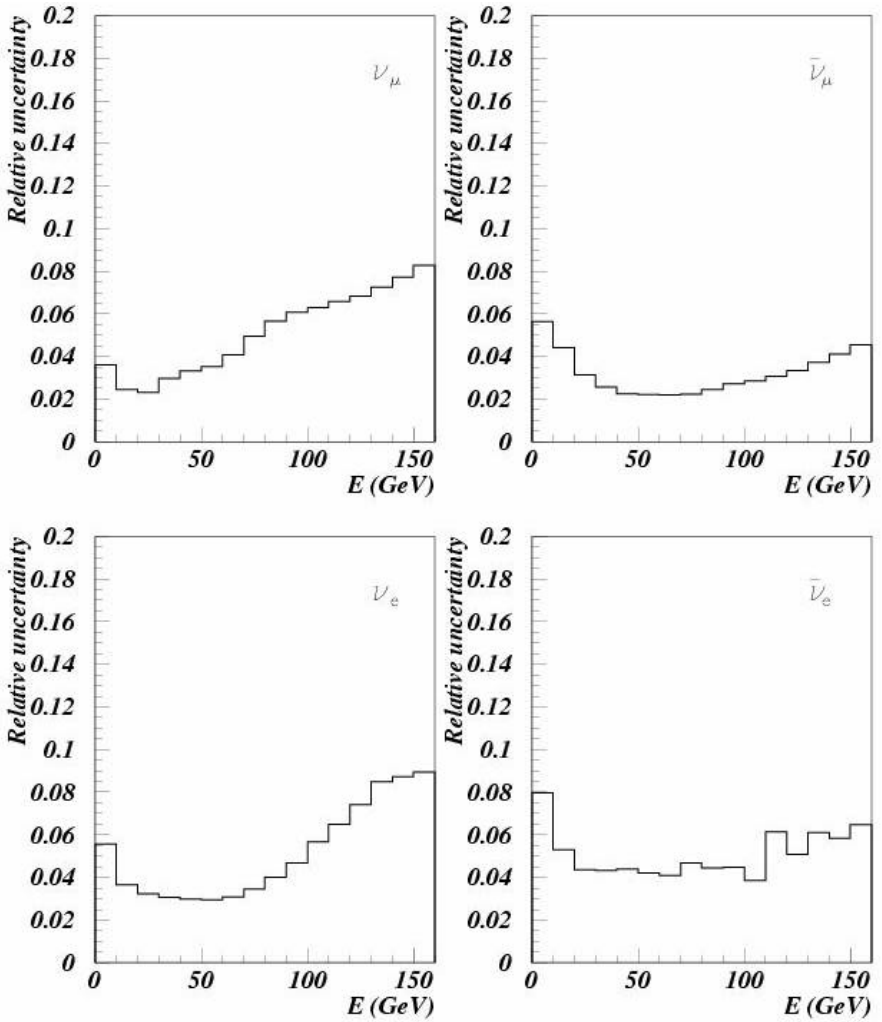

Data – Monte Carlo comparison

Neutrino interactions
in the NOMAD detector
when the beam is ran
in neutrino mode

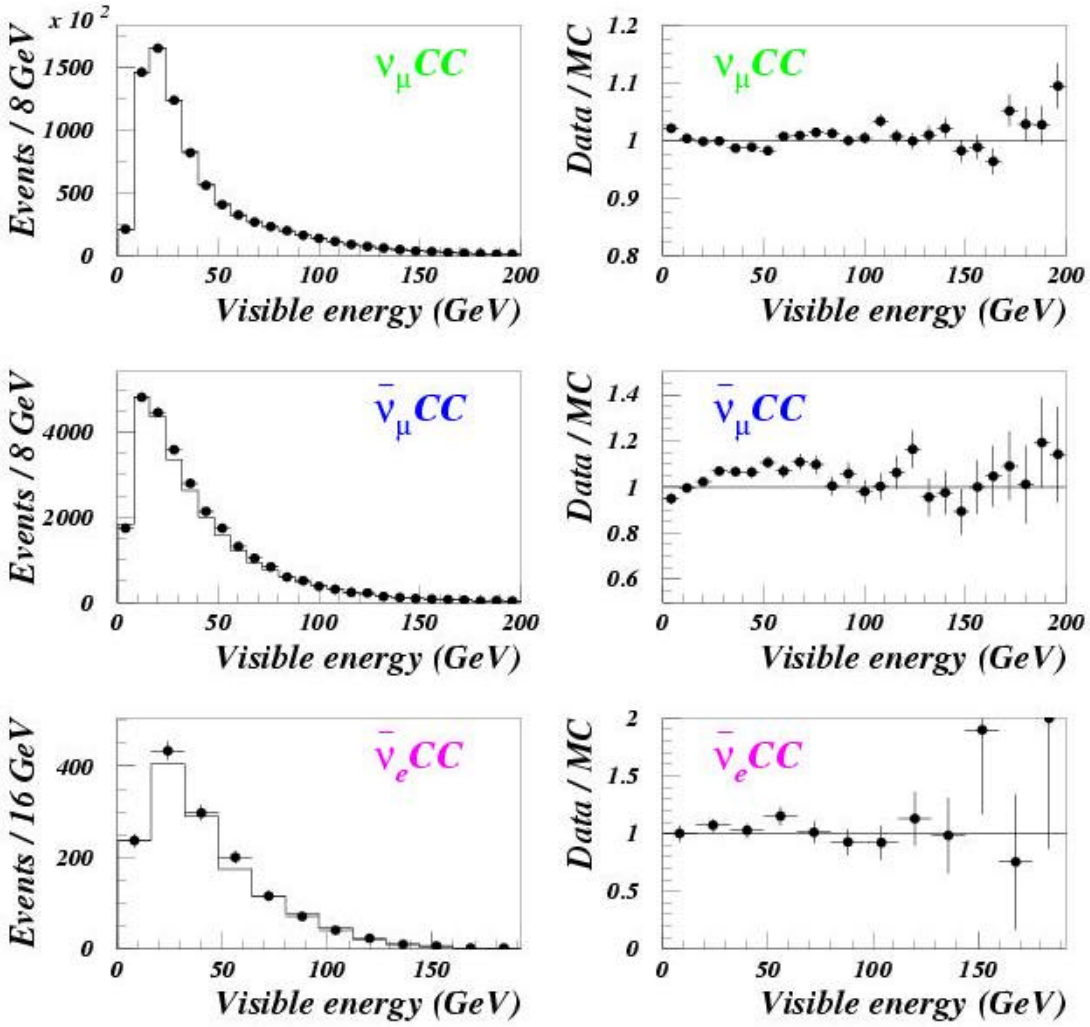

Data – Monte Carlo comparison

Neutrino interactions
in the NOMAD detector
when the beam is ran
in anti-neutrino mode

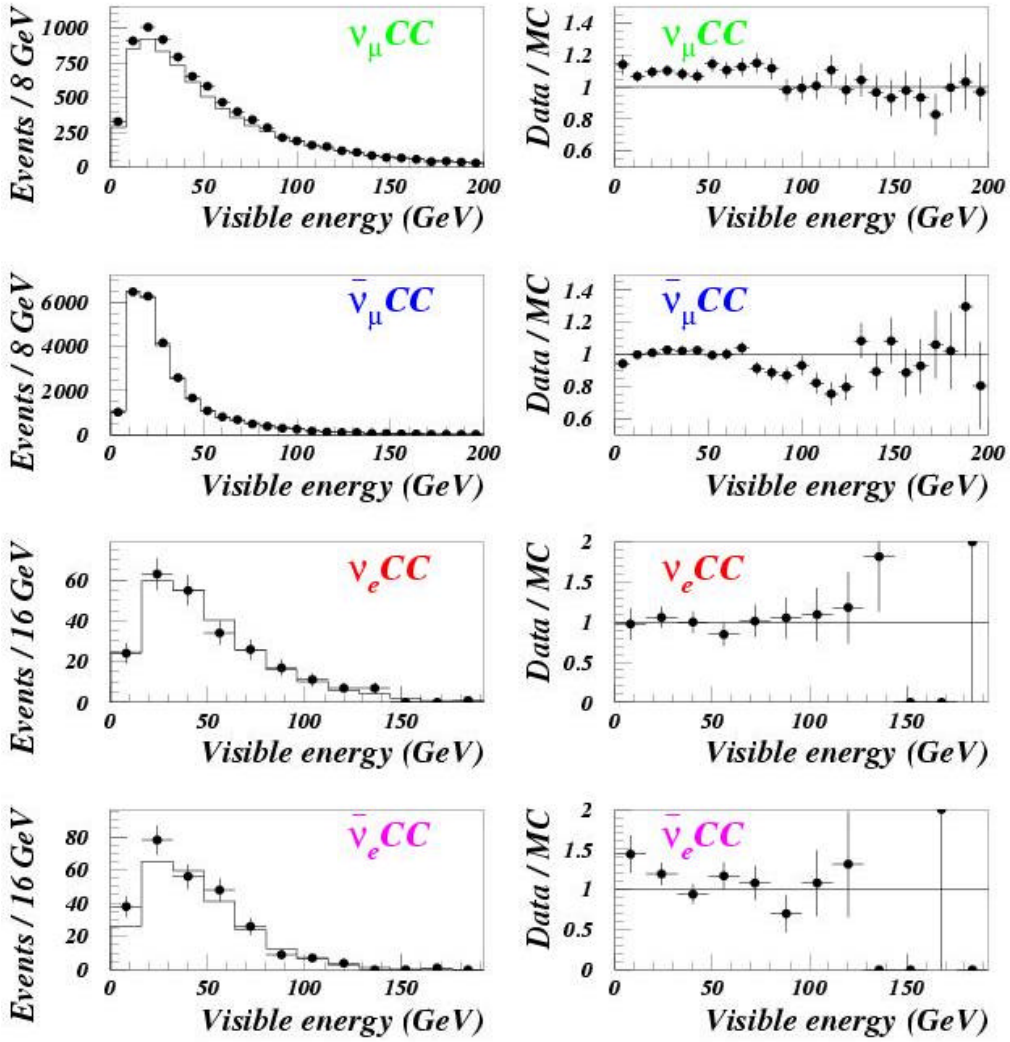

Data – Monte Carlo comparison

Neutrino interactions
in the NOMAD detector
when the beam is ran
in zero-focusing mode

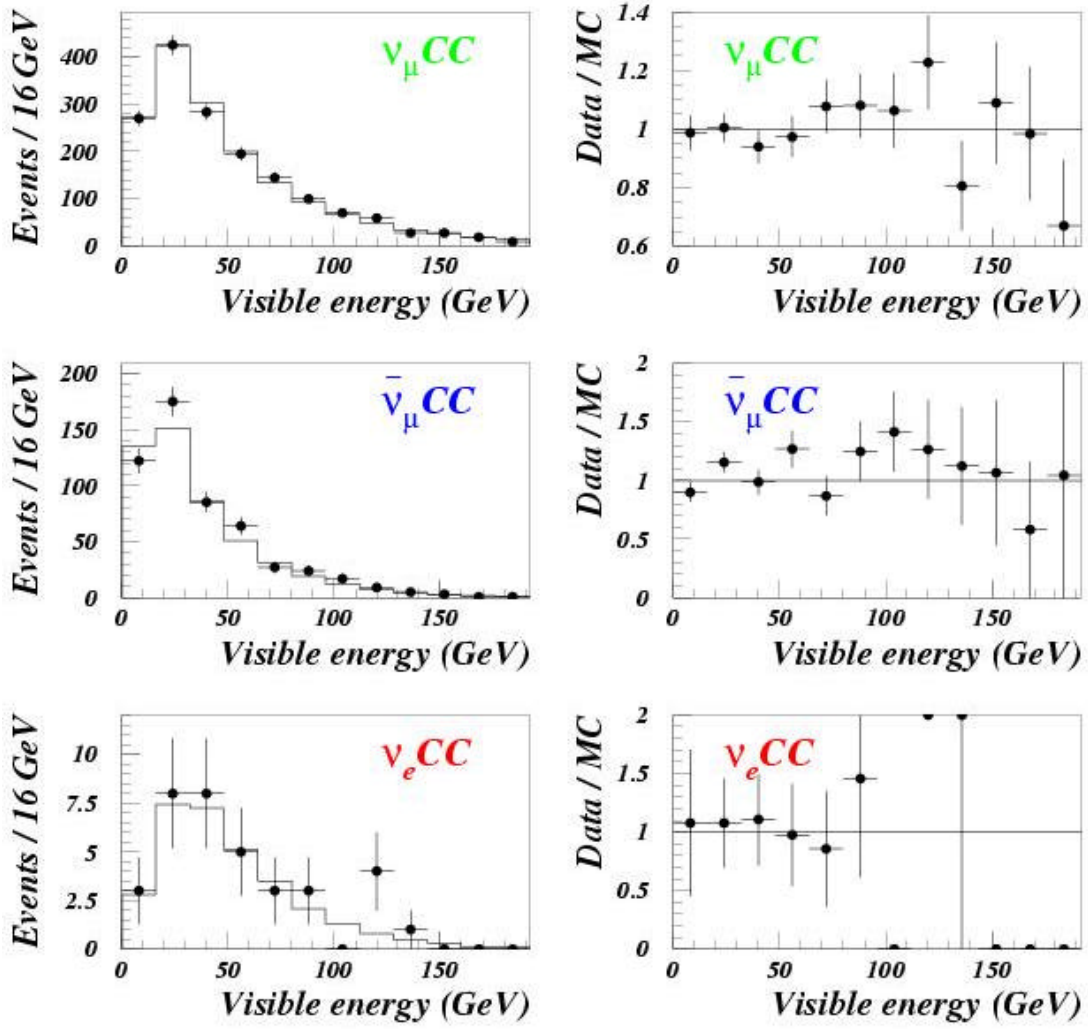

Data – Monte Carlo comparison

Neutrino interactions
in the NOMAD detector
when the beam is ran
in neutrino mode

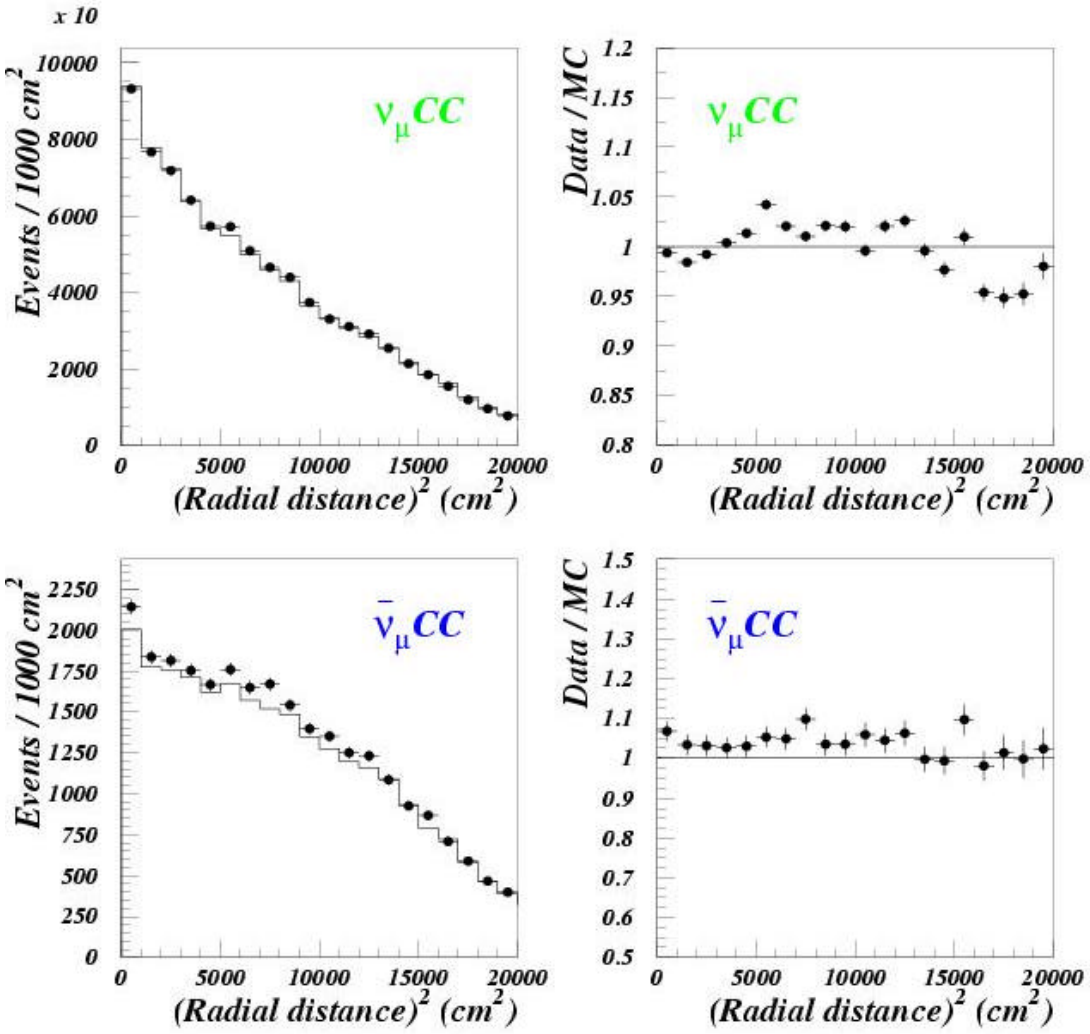

ν_μ/ν_e prediction as a function of E_ν

For some applications only the ν_μ/ν_e ratio is important
Energy-dependent uncertainty ranges from 4% to 7%
Normalization uncertainty is 4.2%

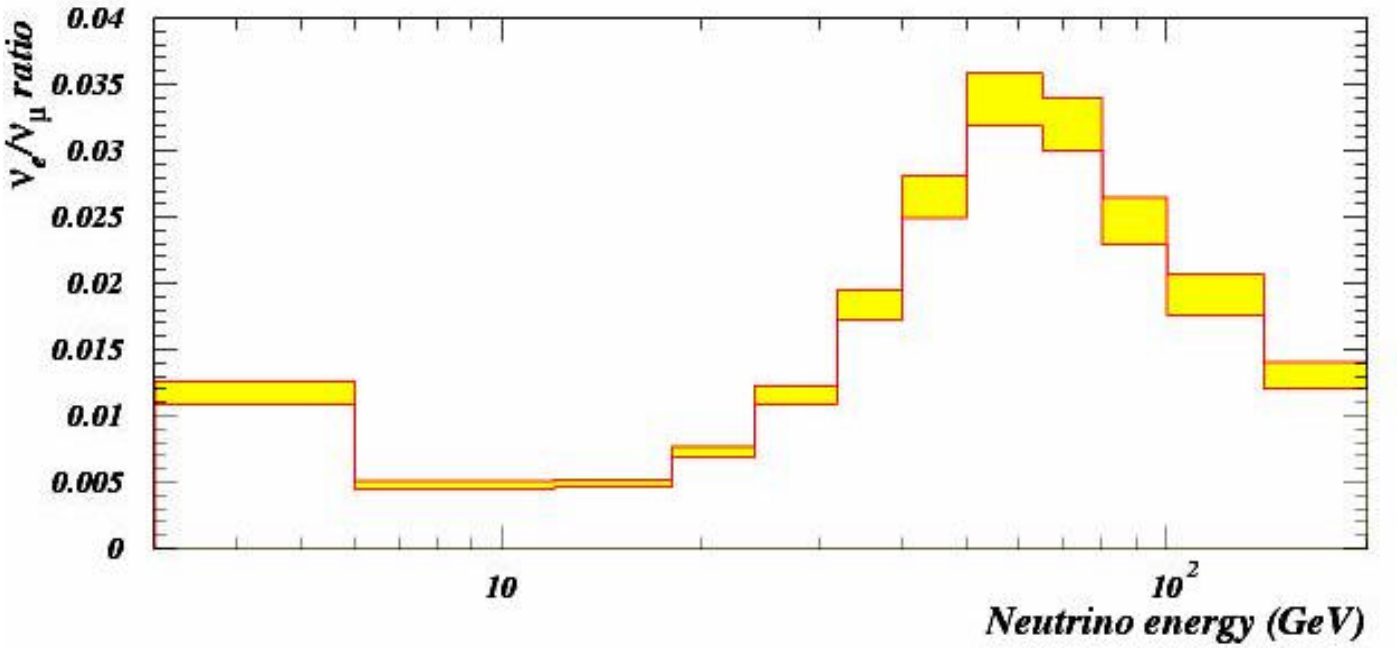

Conclusion on the approach à al NOMAD

- The fluxes of the four neutrino flavours were predicted with an overall uncertainty of about 8% for ν_μ and ν_e, 10% for anti-ν_μ, and 12% for anti-ν_e (energy-dependent and normalization errors combined)
- The uncertainty on ν_μ/ν_e ratio: energy-dependent ranges from 4% to 7%; the normalization is 4.2%
- The approach seems to work, but what to do when
  - the distance between the source and the detector is several hundred kilometres, I.e the position and angular divergence of the π/K beam is a crucial parameter?
  - a smaller systematic error is need, I.e. the cross-section of the processes we are looking at is very poorly known?

Measuring π angular distribution in real beamline

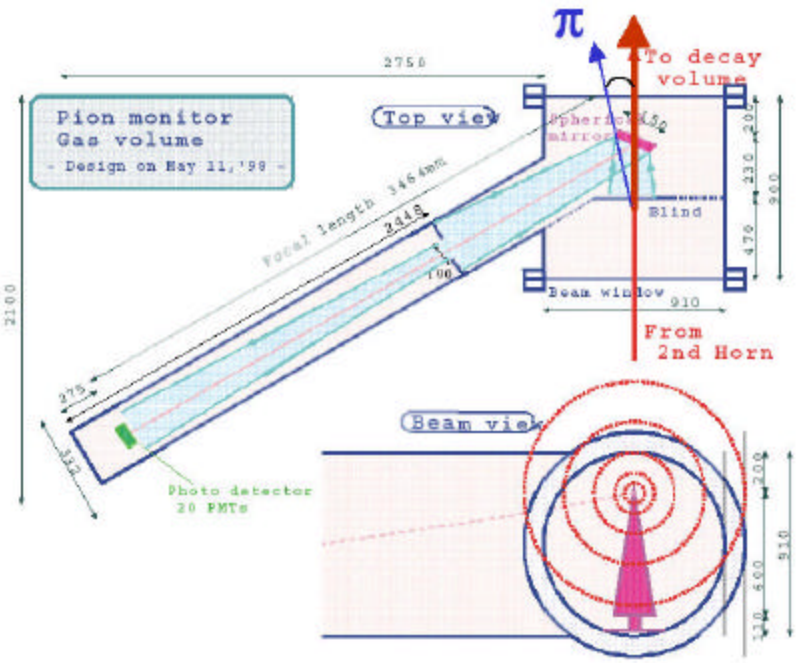

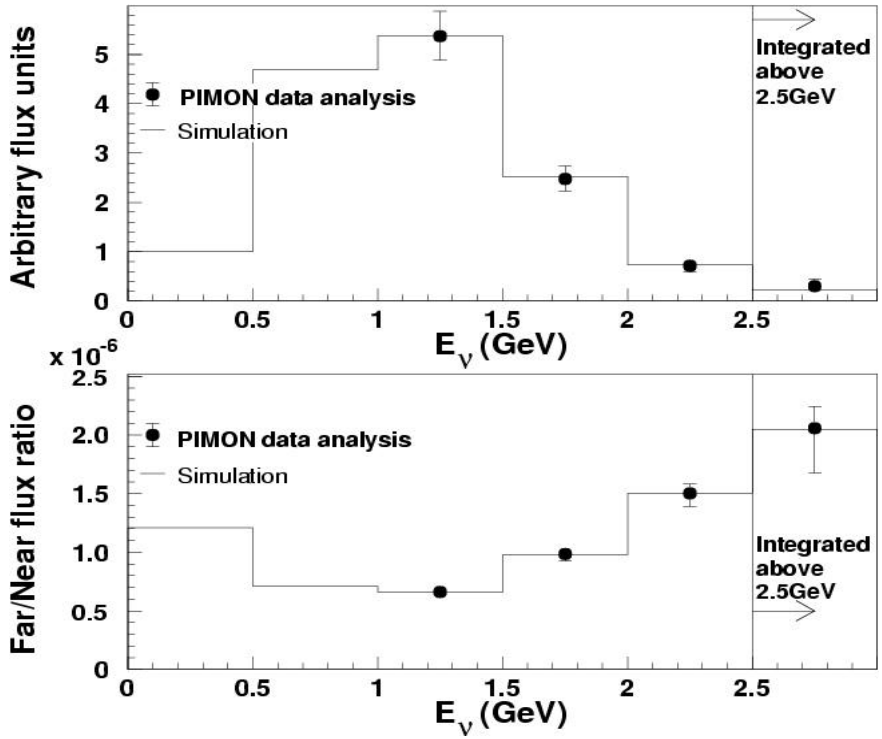

- K2K Gas cerenkov counter: measures angular distribution of π as function of momentum
- Located right after horns
- Works for pions above 2GeV

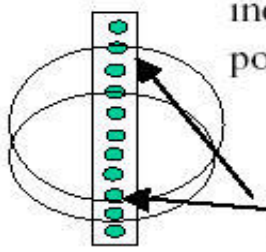

index of refraction : p_π threshold θ_π
position of ring : θ_π

p_π, θ_π gives two C-light peaks
fit with Σ (wi • C-light)

Translating from Near to Far

$$N_{\text{expected}} = N_{\text{observed}} \times \frac{1}{e_{ND}} \times R_{FD/ND} \times e_{FD} \times \frac{L.T._{FD}}{L.T._{ND}}$$

#evts expected at the Far Detector (FD)

#evts observed in the Near Detector (ND)

Live time correction using **p**roton **o**n **t**arget

$$R_{FD/ND} = \frac{\int \Phi_{FD} s_{FD} \mathrm{d}E}{\int \Phi_{ND} s_{ND} \mathrm{d}E} \times \frac{N_{FD}^{\text{target}}}{N_{ND}^{\text{target}}}$$

Event ratio R from MC calculation but, many tiny effects may increase the systematic uncertainty in the extrapolation...

Purpose of a near detector.

① Measure the quality of neutrino beam.

② Give a constraint to estimate the neutrino flux and the energy spectrum at the far detector location

③ Study neutrino interactions to estimate background events for oscillation analysis.

Measurements of the ν beam at the near detector.

1. Direction
2. Flux / Spectrum for ν_μ and ν_e
3. Profile
4. Stability
5. Event types (QE, single μ, NC π0 etc..)

As an example of the Near to Far extrapolation we refer to the JHF case

of CC events of various beams

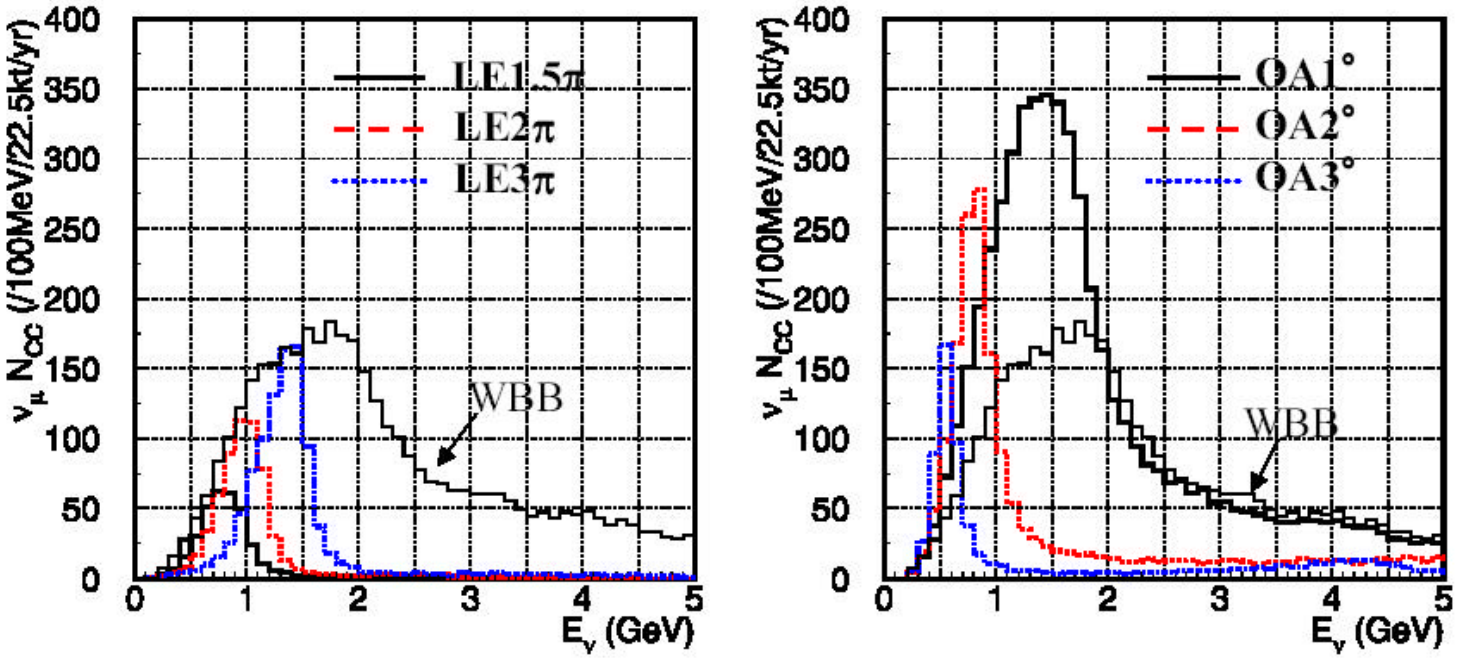

WBB:**5200** CC int./22.5kt/yr
NBB: **620** CC int./22.5kt/yr (2GeV/c π tune)
OAB: **2200** CC int./22.5kt/yr (2degree)

Spectrum difference btw. near and far

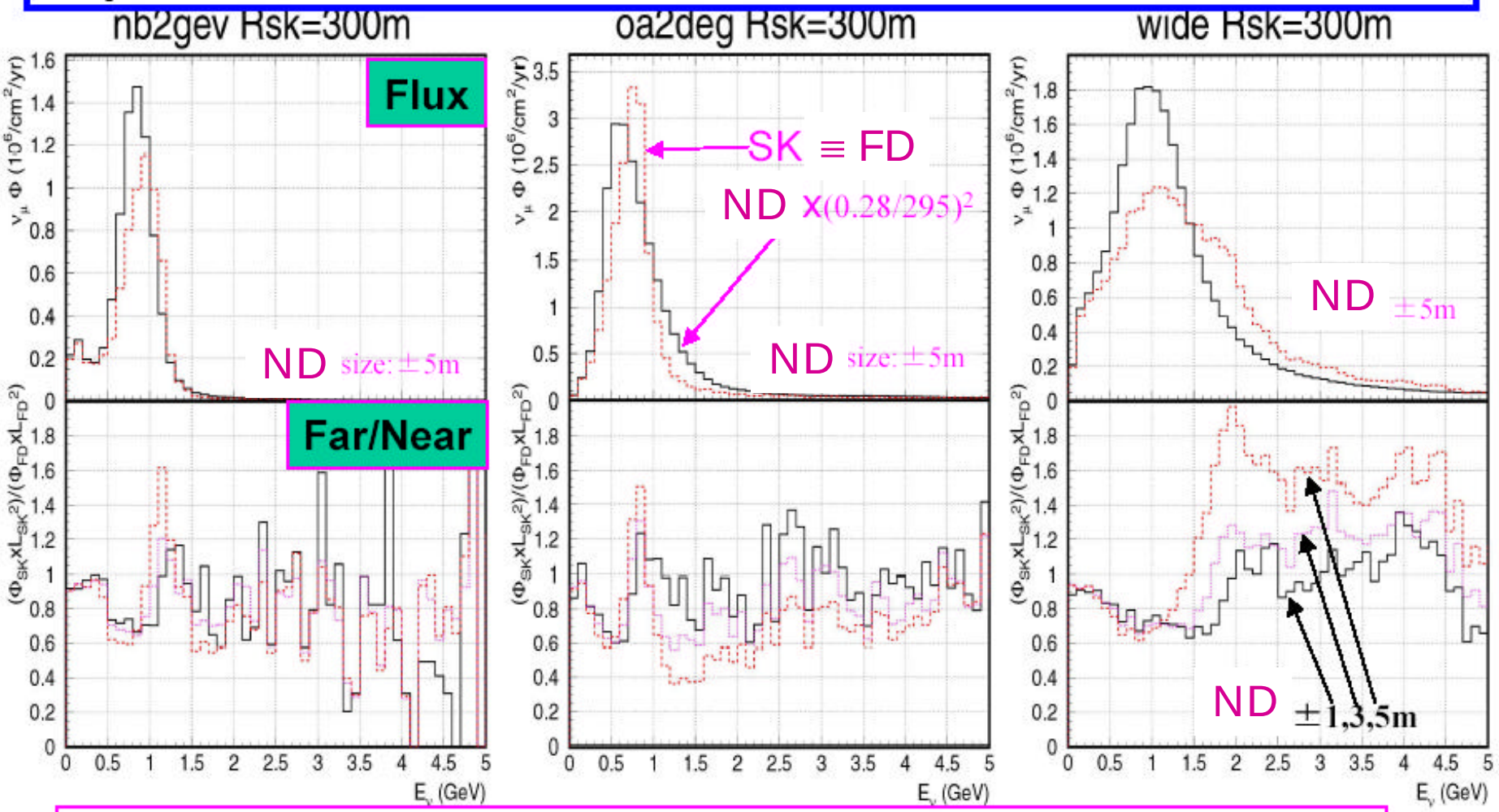

- Peak energy shift → serious syst.
- dependence of high energy side or ND size → Handle to estimate correction
- Low energy side does not depend on ND size

Near/Far ratio (finite decay pipe length)

Decay vertex (z) dist. of parent pions

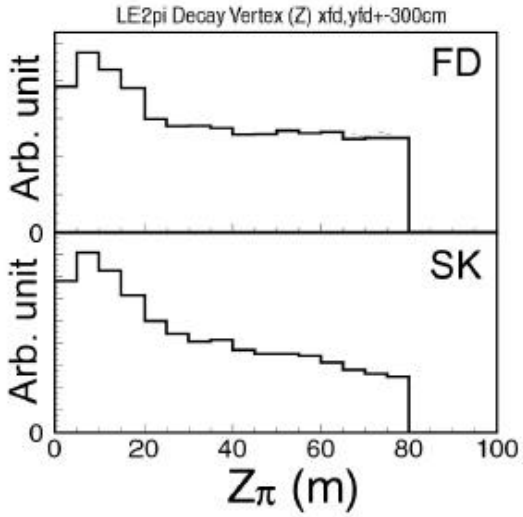

More downstream pion contribute to FD (solid ang)

The effect of finite decay pipe length observed in wide E_ν range >300MeV

Change decay pipe length???
Observe ν at large angle???

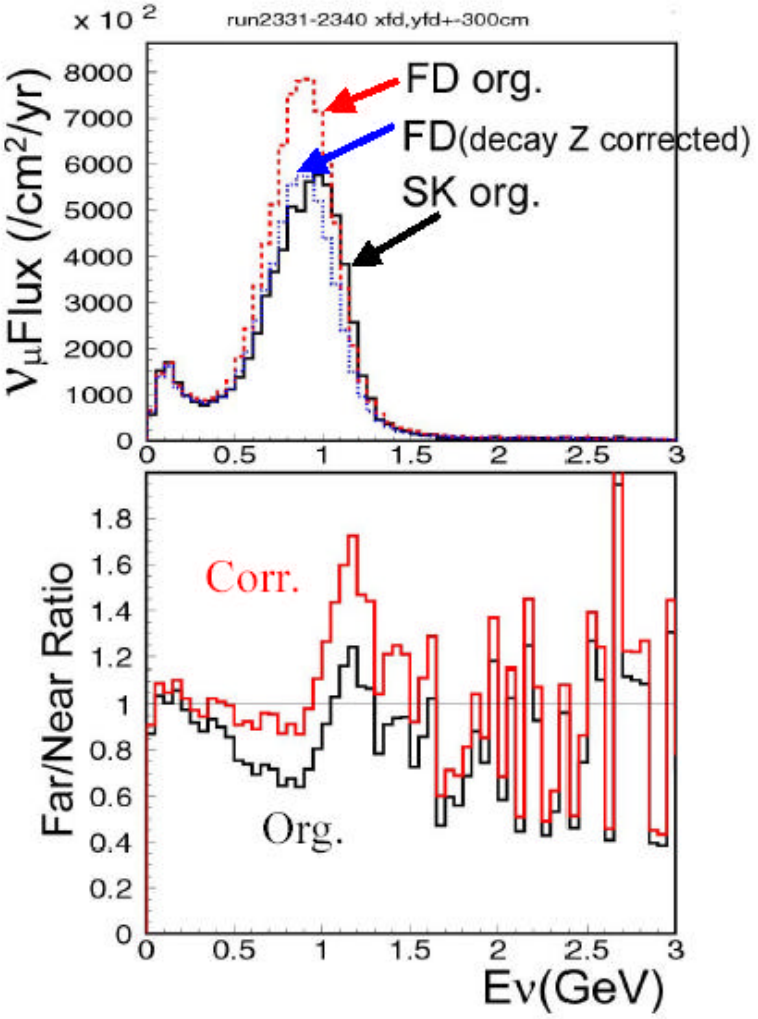

Far/near ratio @ various Z

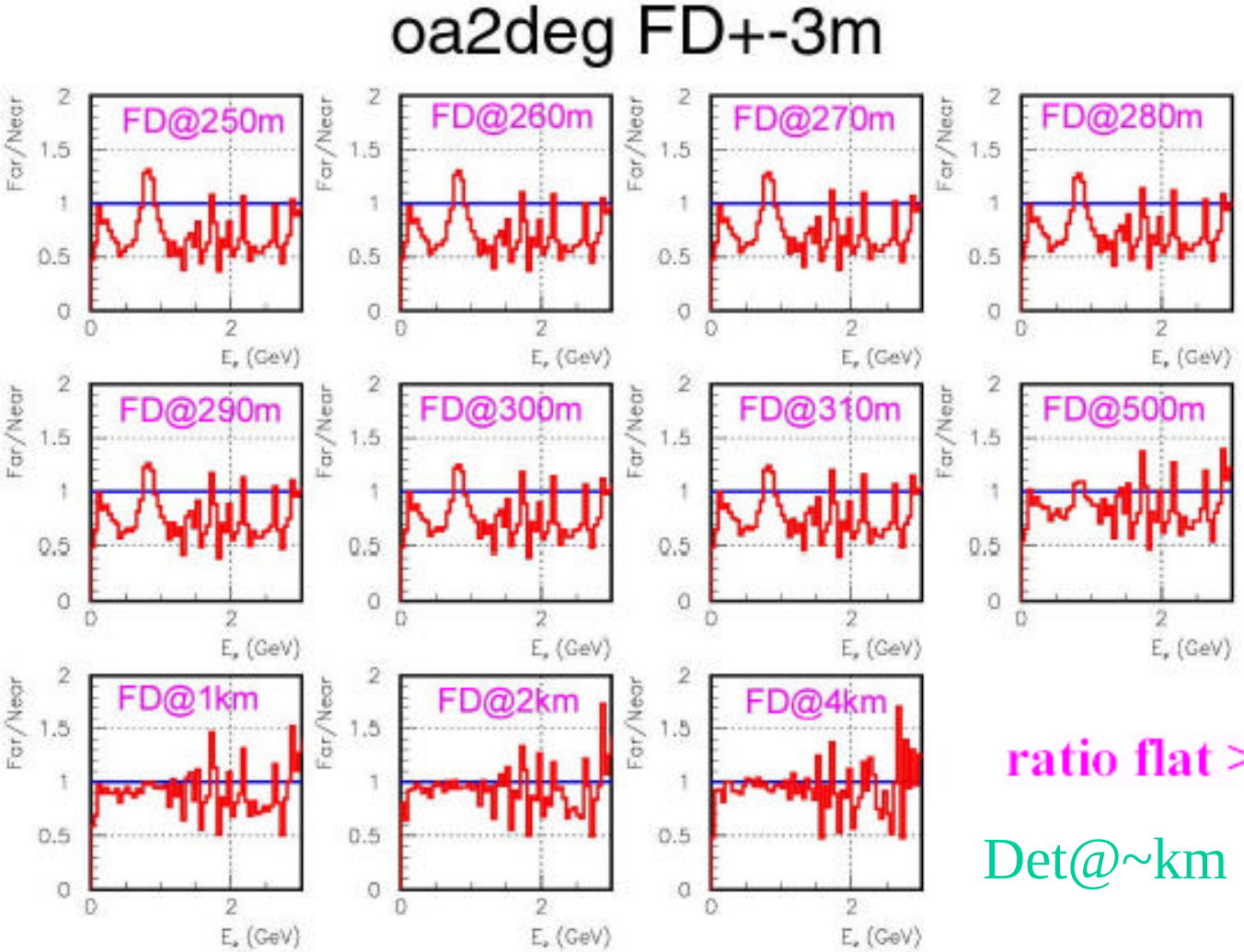

ratio flat >~1km

Det@~km "Ultimate" Solution!

Conclusion:

Criteria for a "Good neutrino beam monitor"

- Event rate of the far detector (neglecting the volume):
  Event-rate(near) × { $(L_{near}/L_{far})^2 + \varepsilon$ }

ε should be as small as possible

Near detector should be as similar as possible to the Far detector (Super-Kamiokande)

Water Cherenkov detector

Near detector position should not be too near to the neutrino production region.

$L_{near} > 1$km

Focussing Properties

ν are produced by weak "decay" of a parent: $\mu,\pi,K,$nucleus.
We assume the decay to be isotropic at rest and call E_0 the rest frame energy of the ν

The focussing properties are given only by:

- the divergence of the parent "beam"
- the Lorentz transformations between different frames

$$P_T = p_T$$
$$P_L = \gamma (p + p \times \cos\theta)$$

from which, on average

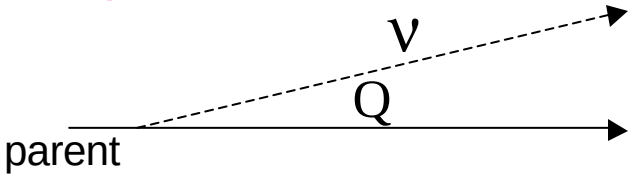

$\Theta \approx 1/\gamma$ (it depends ONLY on parent speed!)
$E \approx \gamma E_0$

and, in the forward direction,
$E \approx 2\gamma E_0$ (same rest-frame spectrum shape multiplied by 2γ)

The BETA-BEAM

1. Produce a radioactive ion with a short beta-decay lifetime
2. Accelerate the ion in a conventional way (PS) to “high” energy
3. Store the ion in a decay ring with straight sections
4. By its β–decay, ν_e ($\bar{\nu}_e$) will be produced

Muons:
γ~500
E_{cms}~34 MeV
QF~15

- SINGLE flavour (ν_e)
- Known spectrum/intensity
- Focussed (1/γ)
- Low energy (E_ν = 580 MeV)

^{6}He Beta-:
γ~150
E_{cms}~1.9 MeV
QF~79

^{18}Ne Beta+:
γ~250
E_{cms}~1.86 MeV
QF~135

The “quality factor” QF=γ/E_{cms} ($N_{int} \propto \gamma/ E_{cms}$) is bigger than in a conventional neutrino factory. In addition, ion production and collection is easier. Then, 500000X more time to accelerate.

Anti-Neutrino Source

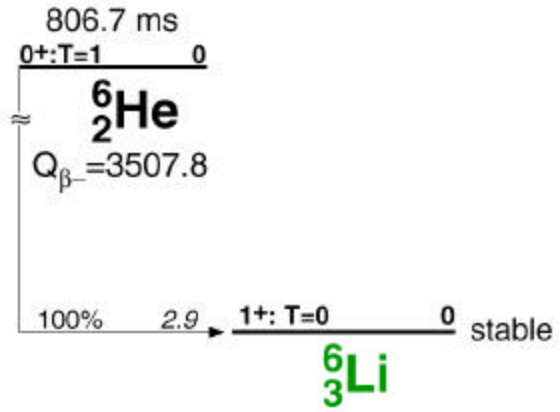

Consider $^6He^{++} \rightarrow {}^6Li^{+++}\ \bar{\nu}_e\ e^-$

$E_0 \approx 3.5078$ MeV T/2 ≈ 0.8067 s

1. The ion is spinless, and therefore decays at rest are isotropic.

2. It can be produced at high rates, I.e. 5×10^{13} ^{6}He/s

3. The neutrino spectrum is known on the basis of the electron spectrum.

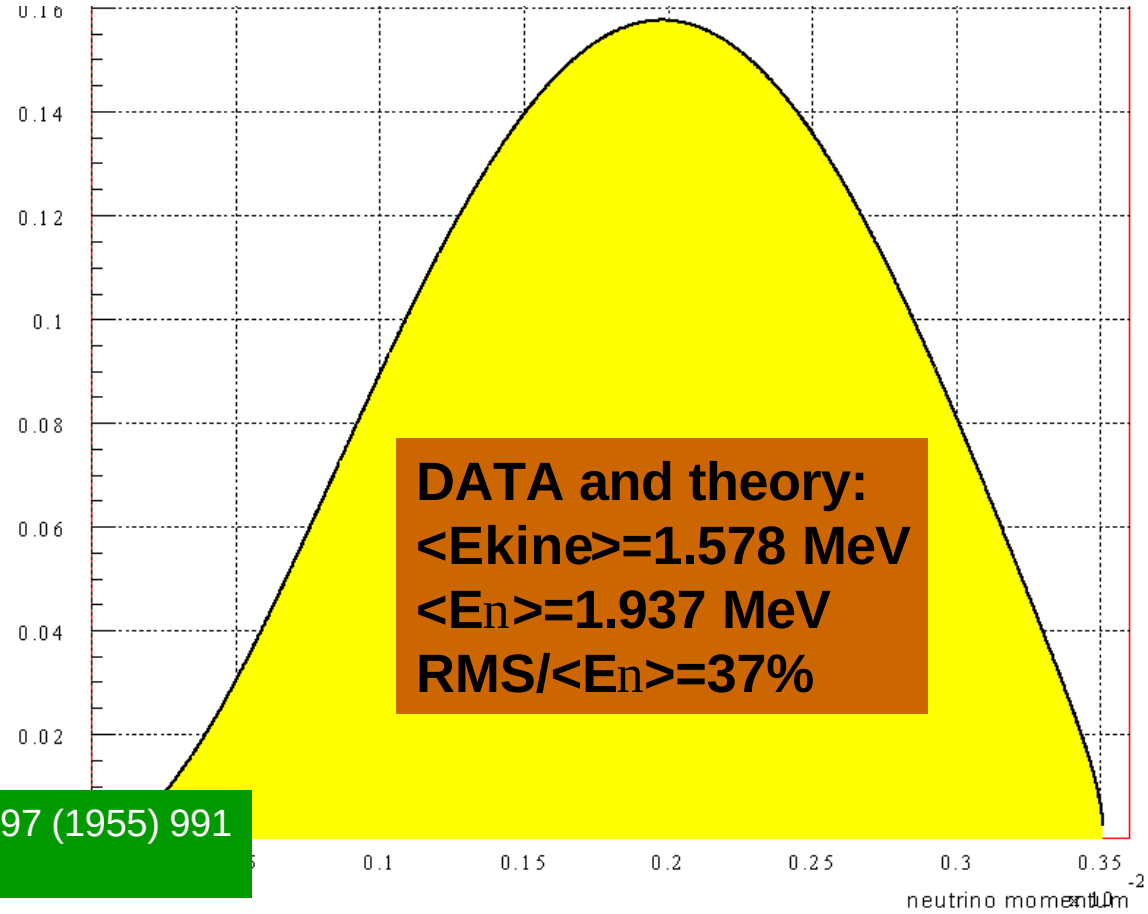

B.M. Rustand and S.L. Ruby, Phys.Rev. 97 (1955) 991
B.W. Ridley Nucl.Phys. 25 (1961) 483

Neutrino Source

Possible neutrino emitter candidate: ^{18}Ne

The same technology used in the production of ^{6}He is limited in the ^{18}Ne case to 10^{12} ions/s.
Despite it is very reasonable to assume that a dedicated R&D will increase this figure, this intensity is used as "today" reference.

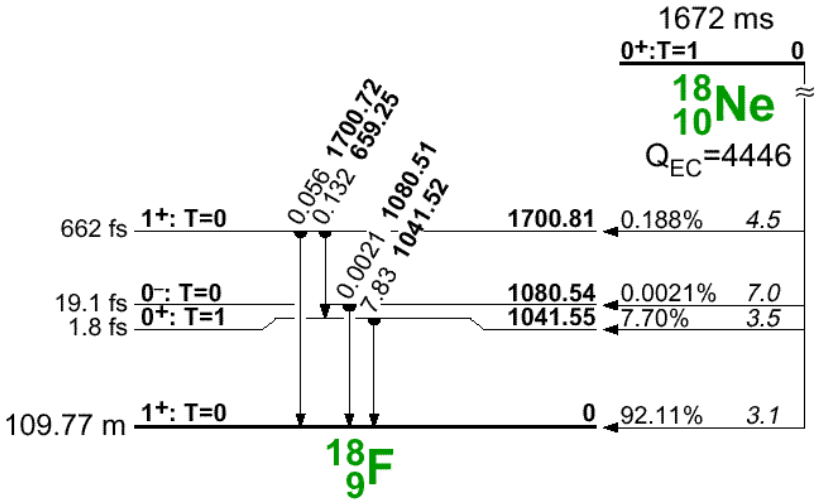

CERN baseline scenario

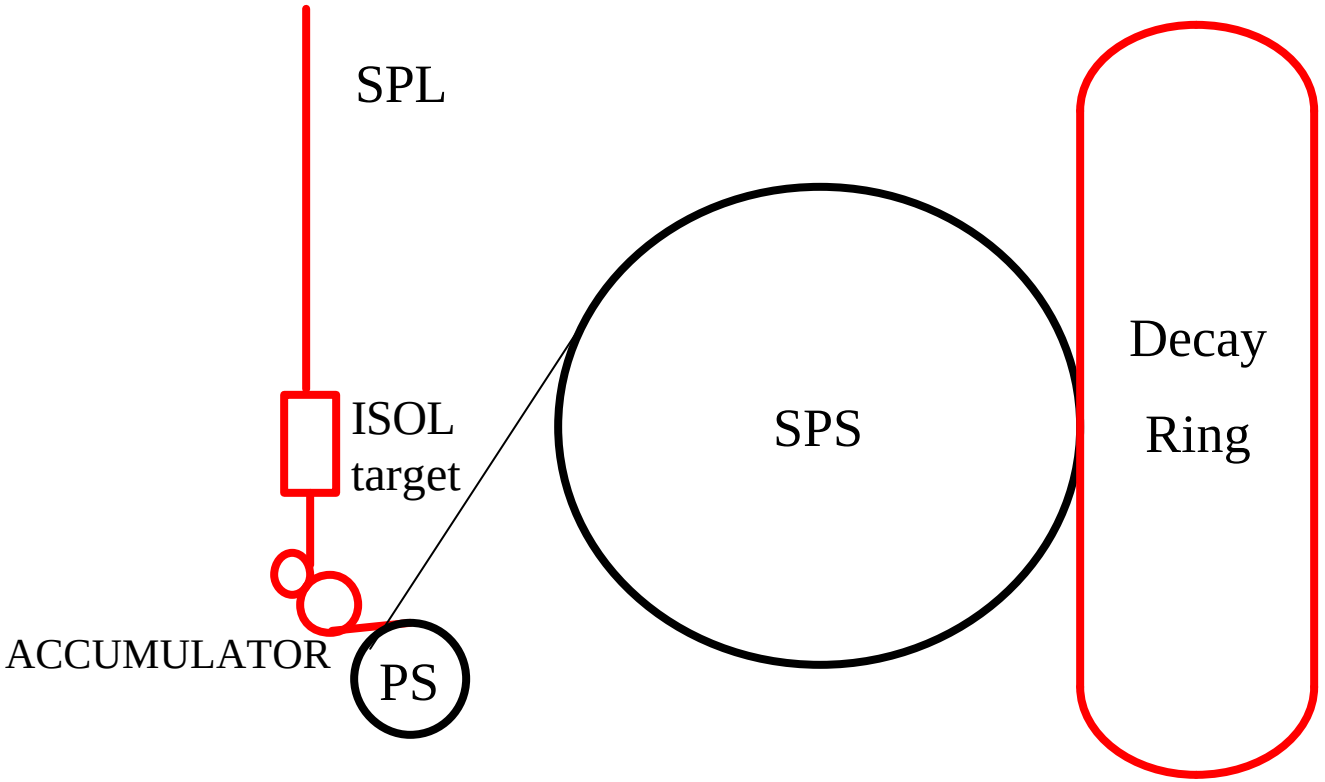

Decay ring

$B\rho = 1500$ Tm

$B = 5$ T

$L_{ss} = 2500$ m

Studies are made on EXISTING CERN machines. Why? Much more detailed knowledge exists, the best way to identify possible problems and limitations.

Neutrino Factories

- The ultimate tool for probing neutrino oscillation, based on muon decays (NOT π DECAY !!!)
  - Enormous luminosity
  - Exceptional purity
  - Perfect knowledge of spectrum
  - Flavor of initial neutrino tagged by charge
- Caveats:
  - Technical challenges to muon acceleration
  - Cost

- Proton drivers
- Targetry
- Particle production measurements
- RF manipulation
- Cooling
- Muon acceleration

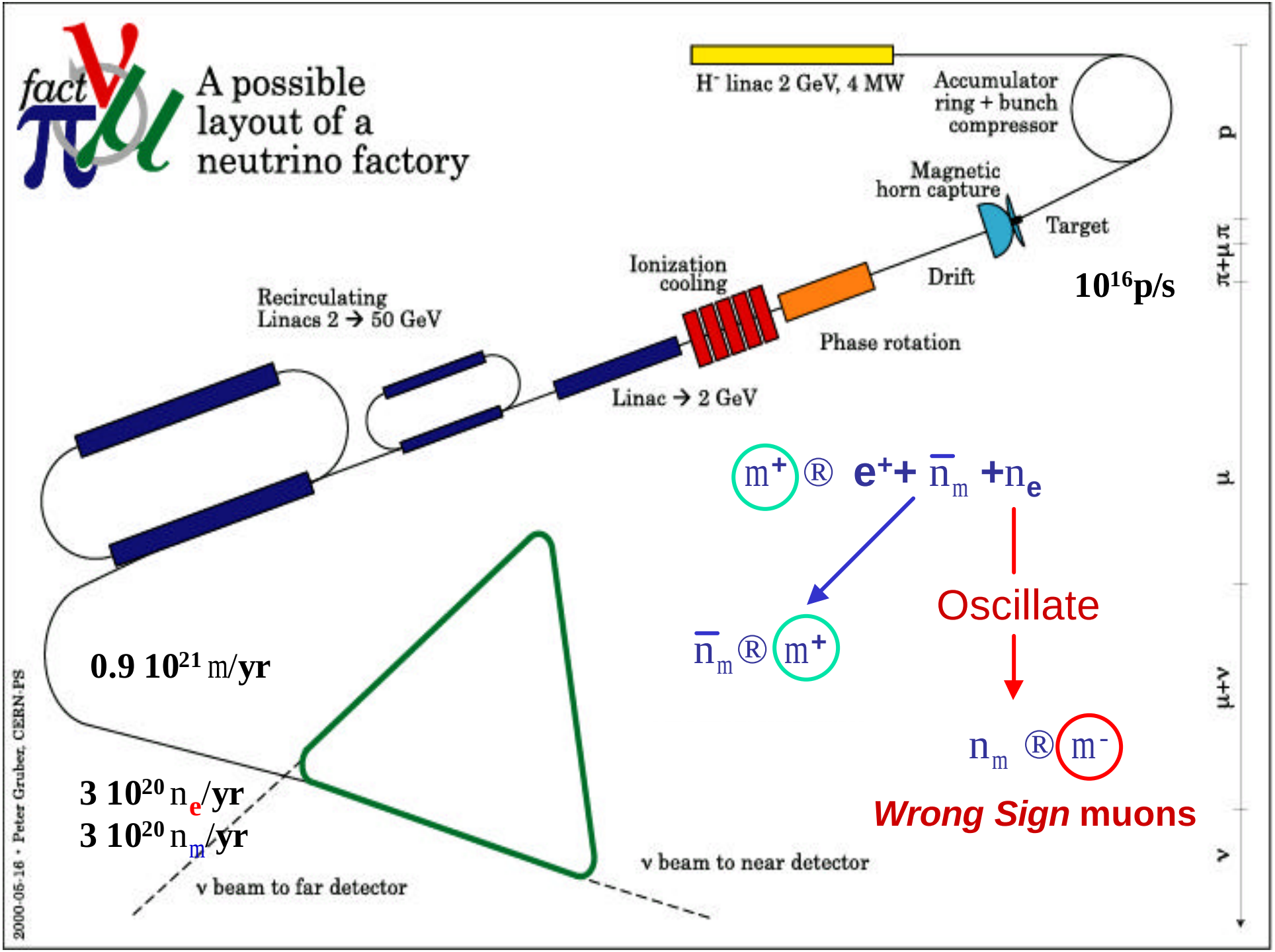
A possible layout of a neutrino factory
H⁻ linac 2 GeV, 4 MW
Accumulator ring + bunch compressor
Magnetic horn capture
Target
Drift
Ionization cooling
Phase rotation
Recirculating Linacs 2 → 50 GeV
Linac → 2 GeV
10¹⁶p/s
m⁺ ® e⁺+ n̄m +ne
n̄m ® m⁺
Oscillate
nm ® m⁻
Wrong Sign muons
0.9 10²¹ m/yr
3 10²⁰ ne/yr
3 10²⁰ nm/yr
ν beam to far detector
ν beam to near detector
2000-05-16 · Peter Gruber, CERN-PS
p
π+μ+ν
μ
μ+ν
ν

Advantages of Muon Storage Ring

- Both ν_e and ν_μ species in beam:
  - A way to get well understood, high-intensity source of ν_e's
    $\nu_e \rightarrow \nu_\tau$ or $\nu_e \rightarrow \nu_\mu$
- High intensity allows:
  - Probe small mixing angles
- Long distances
  - Start to see earth matter effects for oscillations involving ν_e's
  - Reach solar neutrino region with accelerator beams

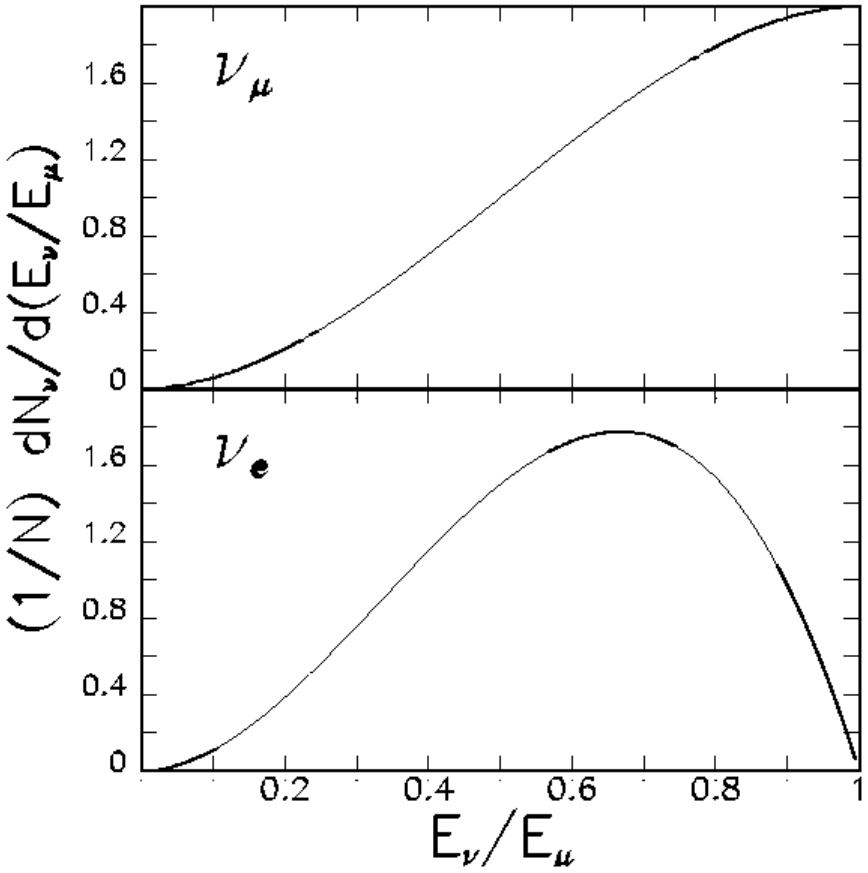

Comparison with Conventional ν Beam

Experiment (L = 732 km)	CC Rates (per kt–yr) ν_μ	$\bar{\nu}_e$
MINOS (WBB)		
Low Energy	458	1.3
Medium Energy	1439	0.9
High Energy	3207	0.9
μ–ring		
10 GeV	2200	1300
20 GeV	18 000	11 000
50 GeV	2.9×10^5	1.8×10^5
250 GeV	3.6×10^7	2.3×10^7

Rate ~ E^3

ν - Factory Beam Parameters

- High Rate Beam:
  - 10^{20} - 10^{21} muon decays/yr
  - ν rates higher than conventional beams for $E_{storage}$ > ~20 GeV
  - Rate in detector ∝ E^3 ⇒ High storage ring energy ~ 50 GeV

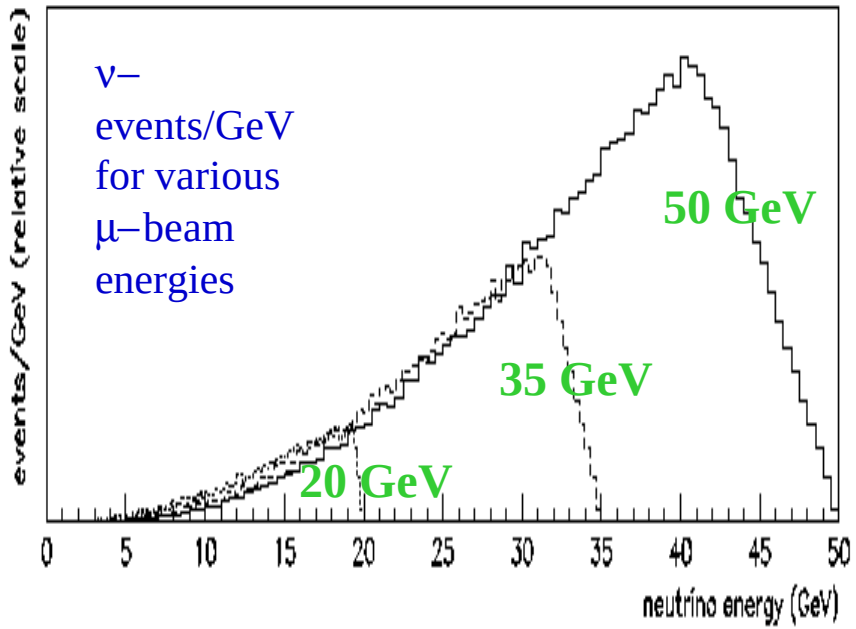

Measurement Uncertainties at Neutrino Factory

In general, MUCH SMALLER than Conventional Beams

- Flux Uncertainties come from:
  - current of muons in the ring
  - divergence of muon beam
  - Energy
  - Polarization (usually unpolarized)
- Cross Section Issues
  - Energies are higher, in DIS regime
  - Energy resolution good (>10GeV)
  - ν production of charged particles well-modeled—less important

Cerenkov light

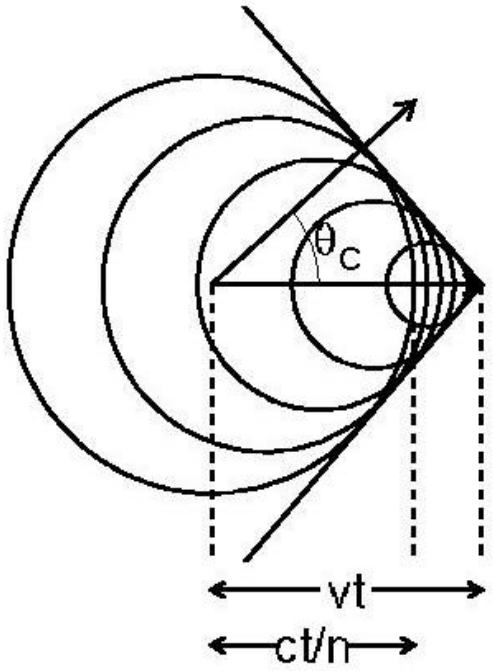

$$b \equiv \frac{v}{c}$$

$$b > \frac{1}{n}$$

As particles move faster than the speed of light in that medium, they emit a "shock wave" of light

$$q_c = \cos^{-1}(1/n(l))$$

$$p_{threshold} = \frac{m}{\sqrt{n^2 - 1}}$$

- For water, n(280-580nm)~1.33-6
- Threshold Angle: 42°

Event Reconstruction

- Vertex Point fit: time of flight should be as sharp as possible
- Define set of in-time tubes
- Look for rings until you're done
- Particle ID
- Corrections to Vertex
- Energy Reconstruction
- Decay Electron Finding

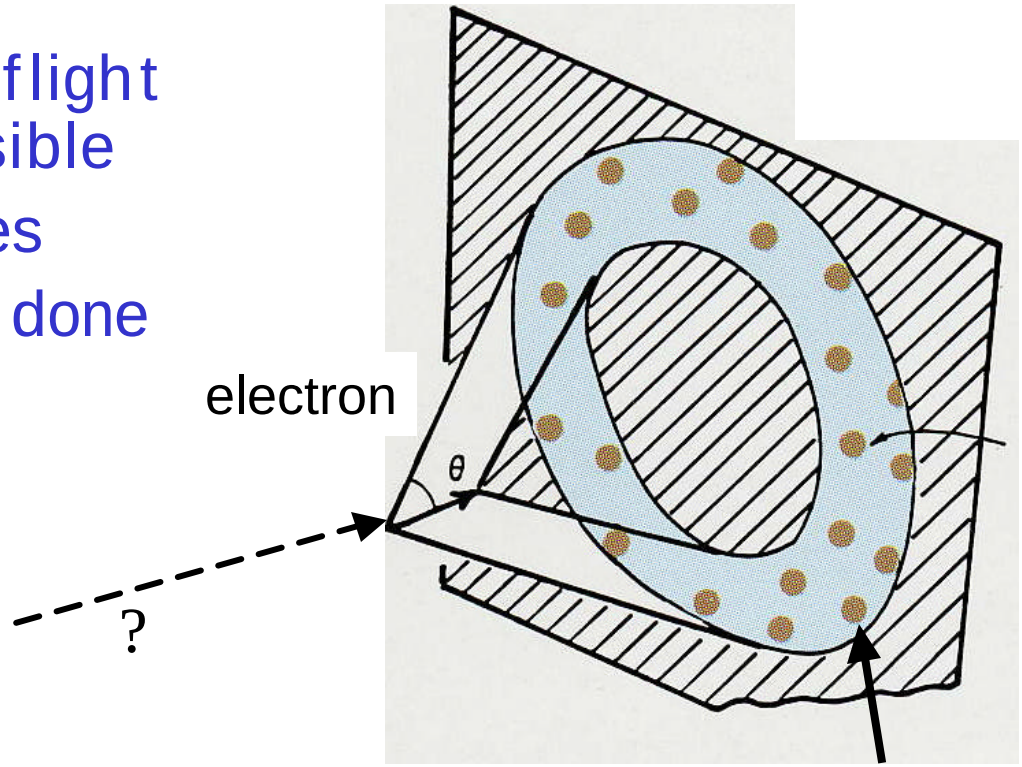

Time: vertex position

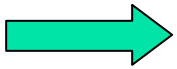

direction

Pulse height: energy

Particle ID w/Cerenkov

From side

Ring

short track, no multiple scattering

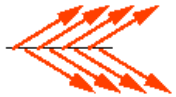

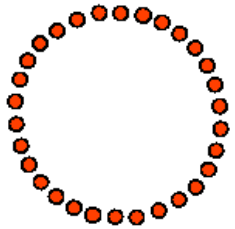

Sharp Ring

electrons: short track, mult. scat., brems.

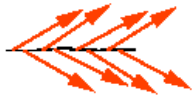

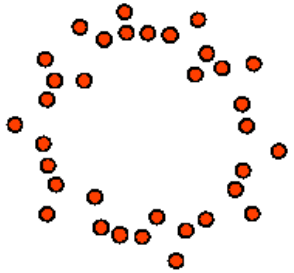

Fuzzy Ring

muons: long track, slows down

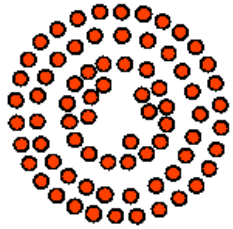

Sharp Outer Ring with Fuzzy Inner Region

neutral pions: 2 electron-like tracks

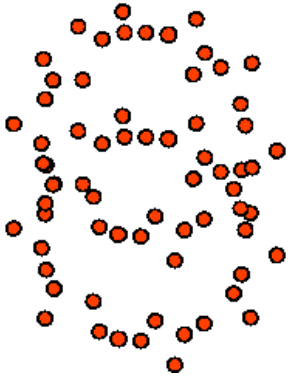

Two Fuzzy Rings

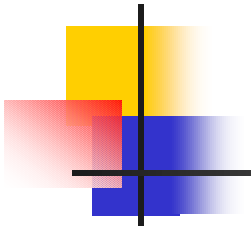

Which kind of media can be used?

- Water
  - Solar neutrinos, atmospheric neutrinos, conventional beams (E_ν<1GeV), β-beams
- Heavy water
  - Solar neutrinos
- Liquid scintillator
  - Reactor neutrinos, conventional beams (E_ν<1GeV)

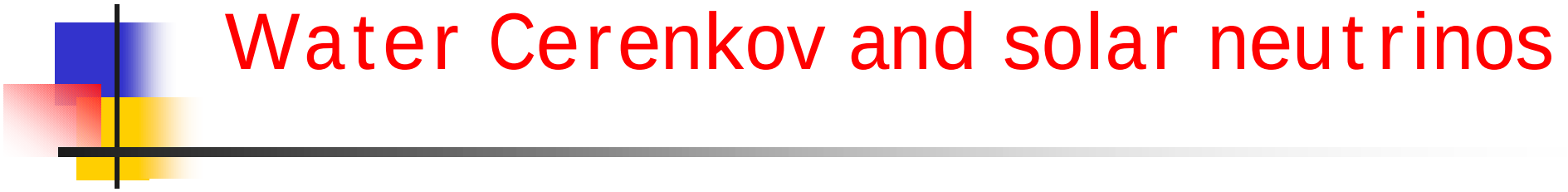

Water Cerenkov and solar neutrinos

The Super-Kamiokande detector

Solar neutrino flux and solar neutrino experiments

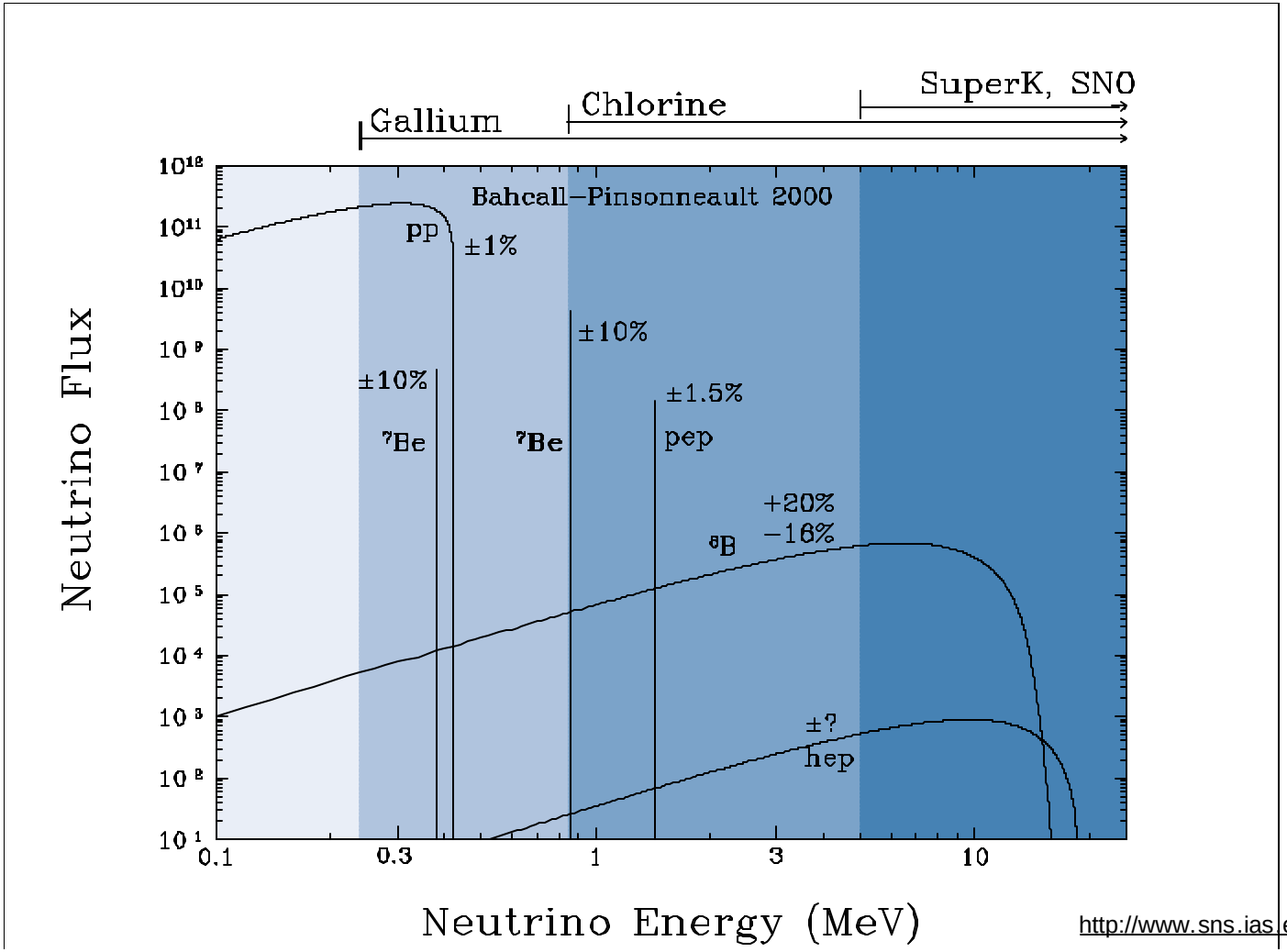

http://www.sns.ias.edu/~jnb/

How to detect solar neutrinos?

Water has p, O and e^-

~~$\nu_e + p$~~ : quantum number ($E_\nu < 14MeV$)

~~$\nu_e + {}^{16}O$~~ : energy ($E_\nu < 14MeV$)

$\nu_e(\nu_\mu \nu_\tau) + e^- \nu_e(\nu_\mu \nu_\tau) + e^-$

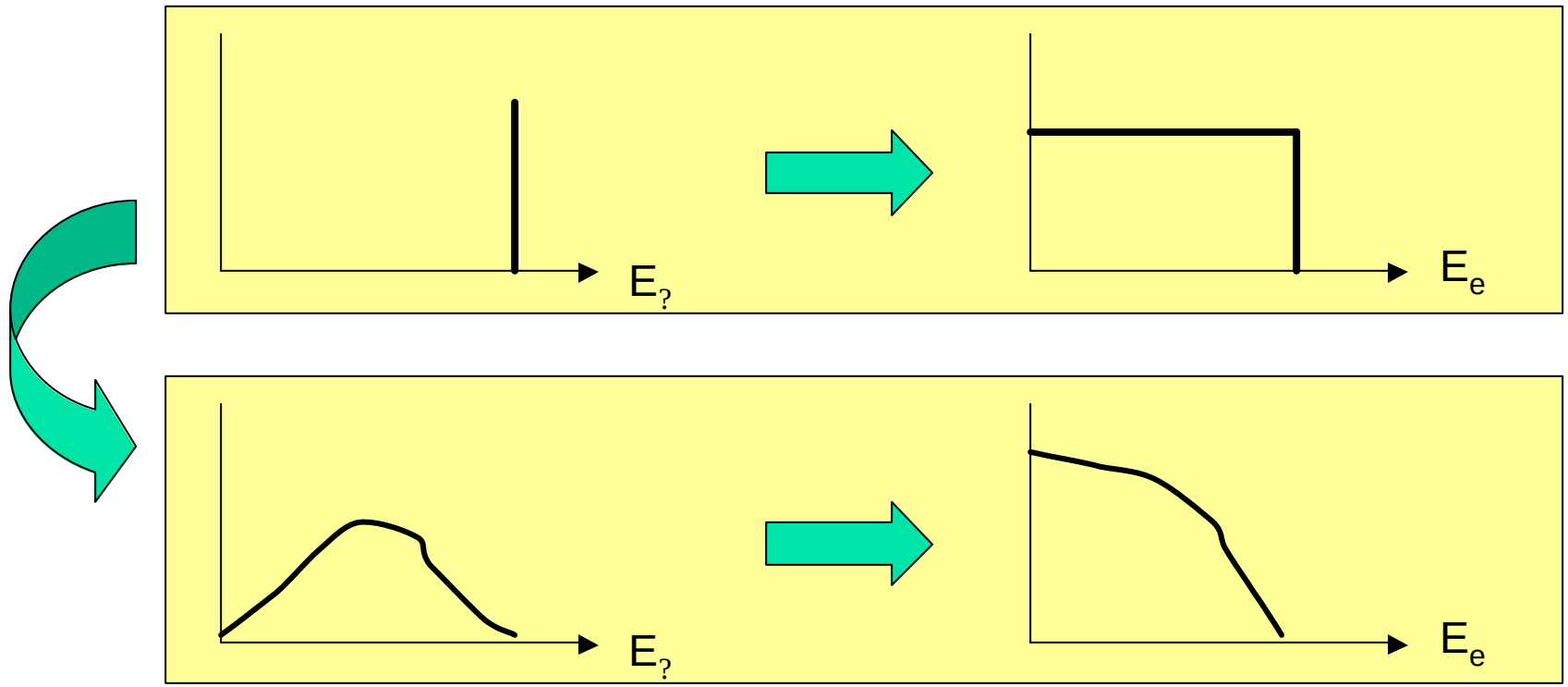

Super-Kamiokande

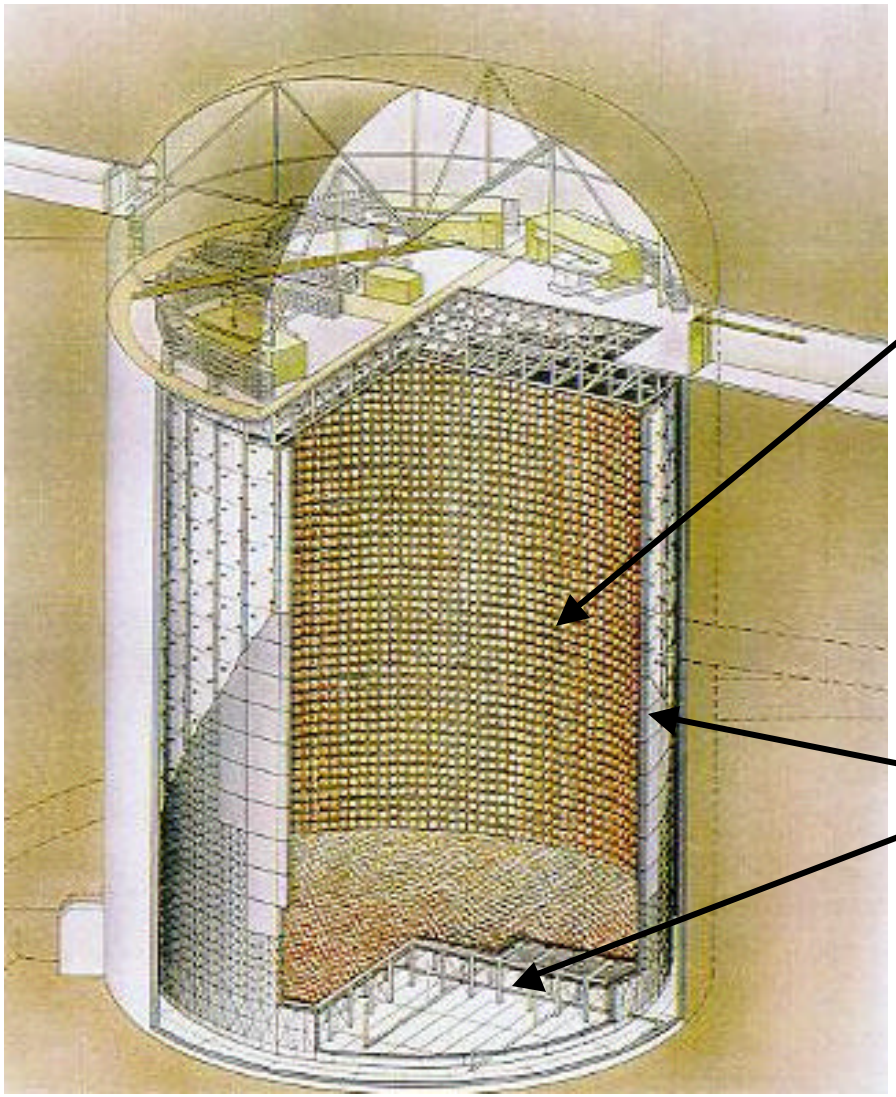

50,000 ton water Cherenkov detector

(Fid. Mass is 22,500 tons)

11,146 × (50cm ϕ PMT) : Inner detector

40% photo-cathode coverage

Number of observed Cerenkov photons ~ 6 / MeV (excluding scattered or reflected photons)

1,885 × (20cm ϕ PMT) : Outer detector

2m active detector region + 0.6m layer (no photon detection)

⇨ γ (and neutron) shield

Super-Kamiokande detector

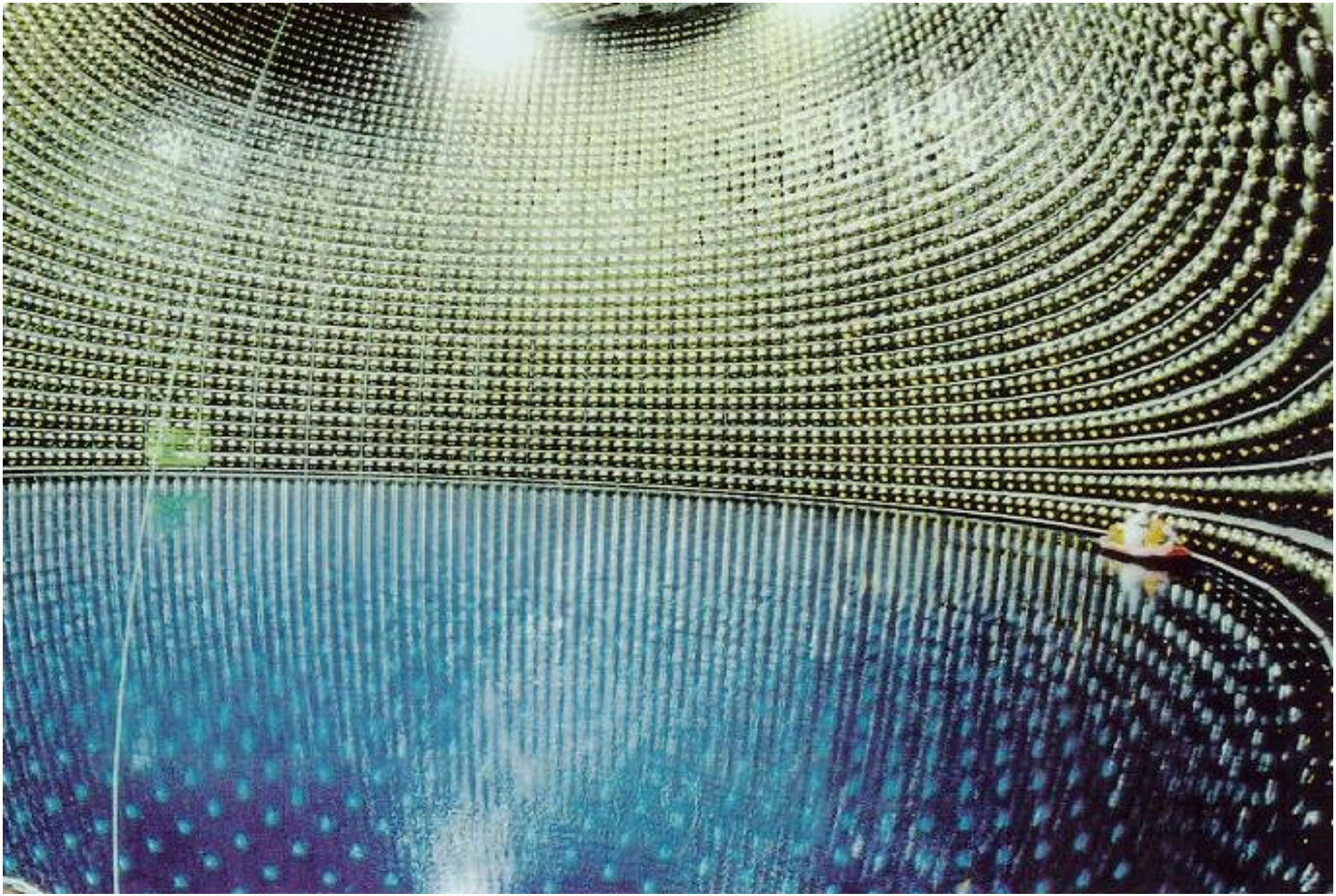

Detector calibration by an electron LINAC

Precise calibration of absolute energy scale, energy resolution, and angular resolution using electron LINAC.

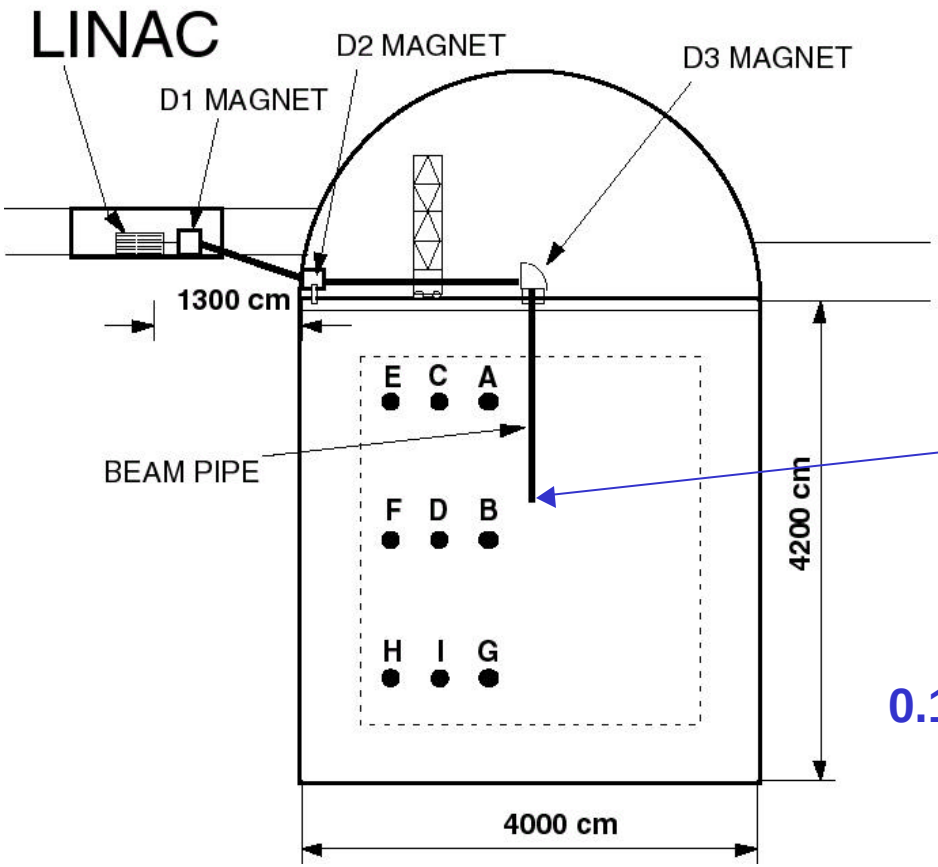

ENDCAP

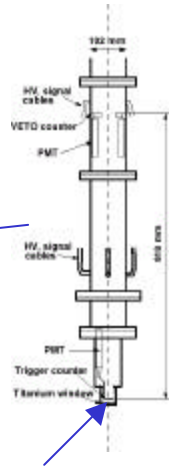

0.1mm thick Ti window

- Beam energy: 5 ~ 16 MeV/c
- Beam energy spread: < 0.5 %

Absolute energy calibration by LINAC

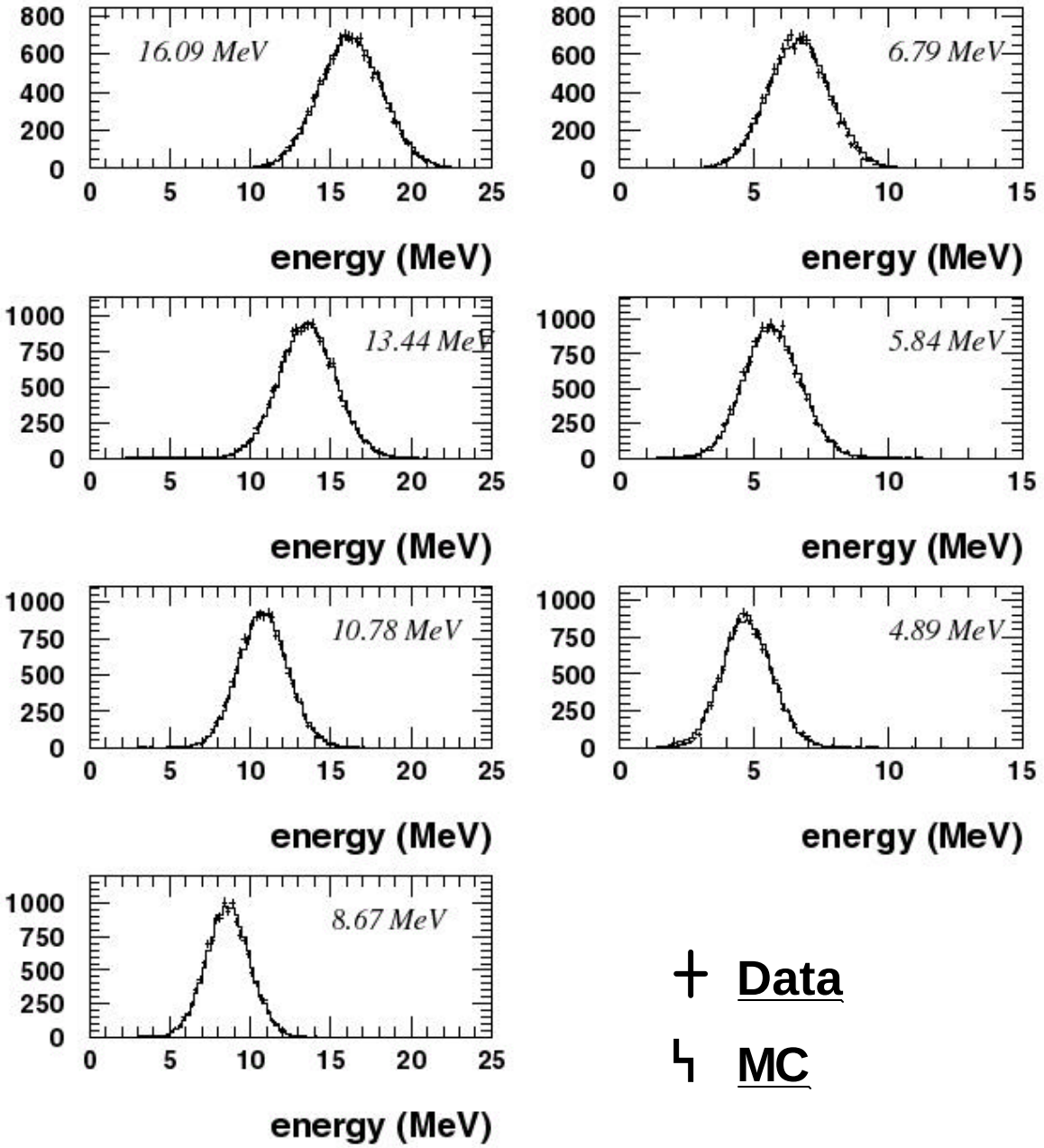

Systematic error in the absolute energy scale : 0.64 %.

^{16}N calibration

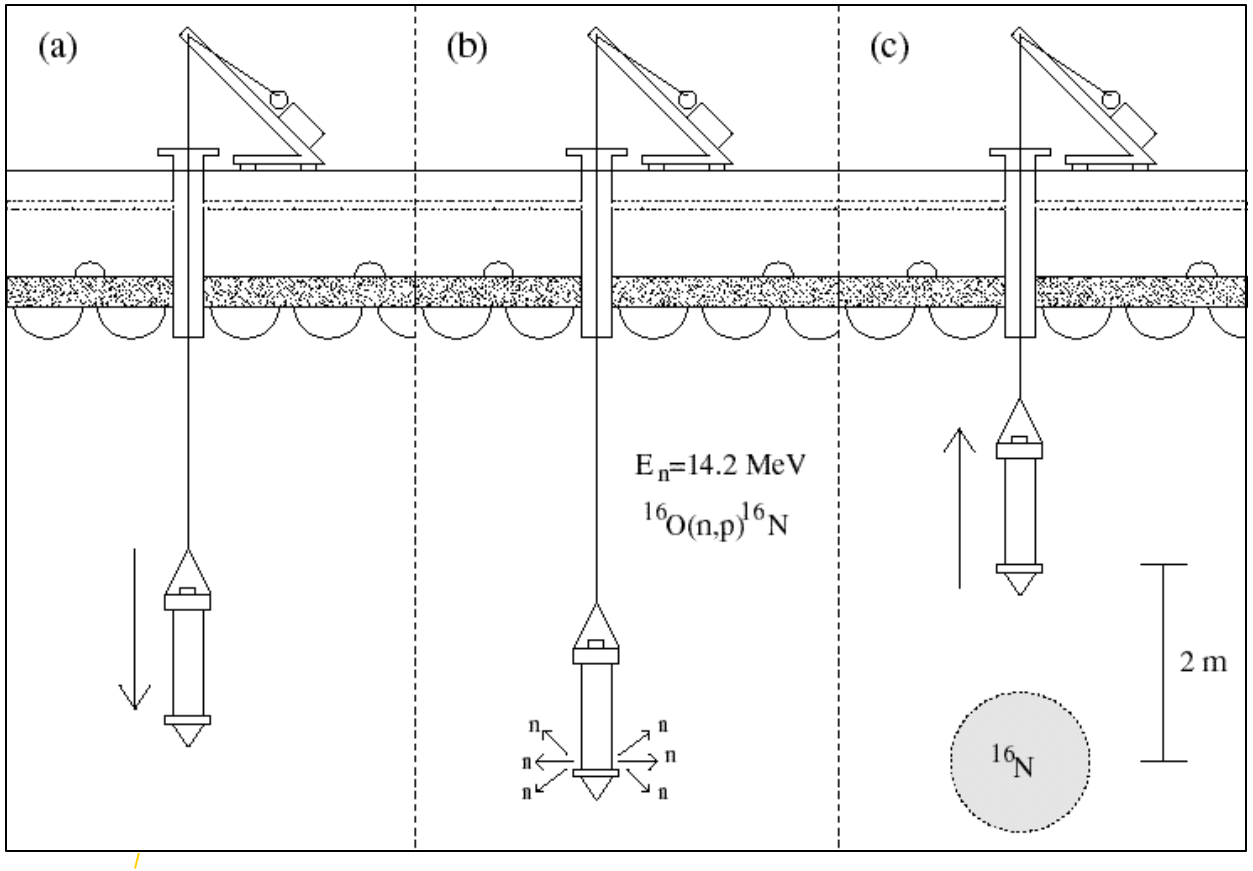

DT generator **D+T? He+n (14.2 MeV) n+^{16}O? p+^{16}N**

~10^6 n /pulse

~1% of n creates ^{16}N

^{16}N decay is precisely known.

66.2% 6.129MeVγ + 4.29MeVβ,

28.0% 10.419 MeV β, and etc.

Data taken at various positions in the detector.

Uniform direction complementary to LINAC calibration.

^{16}N calibration data

Energy spectrum

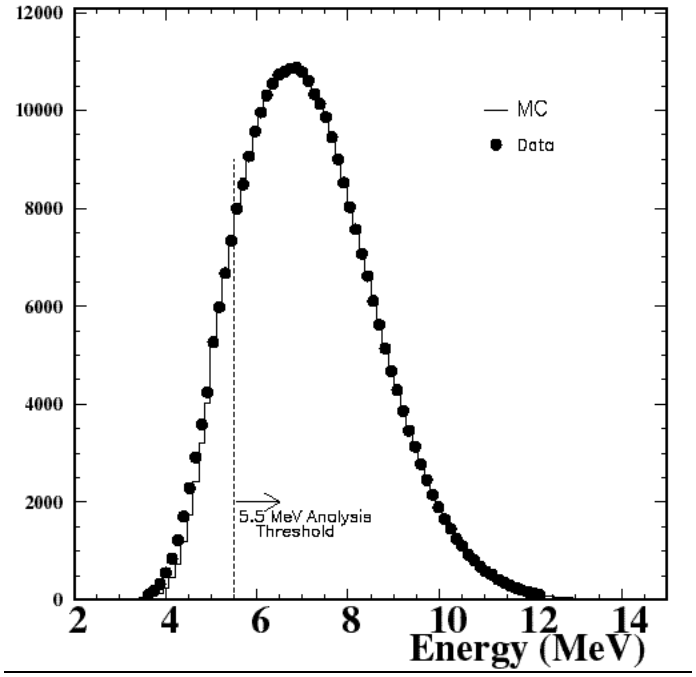

Direction dependence of the energy scale

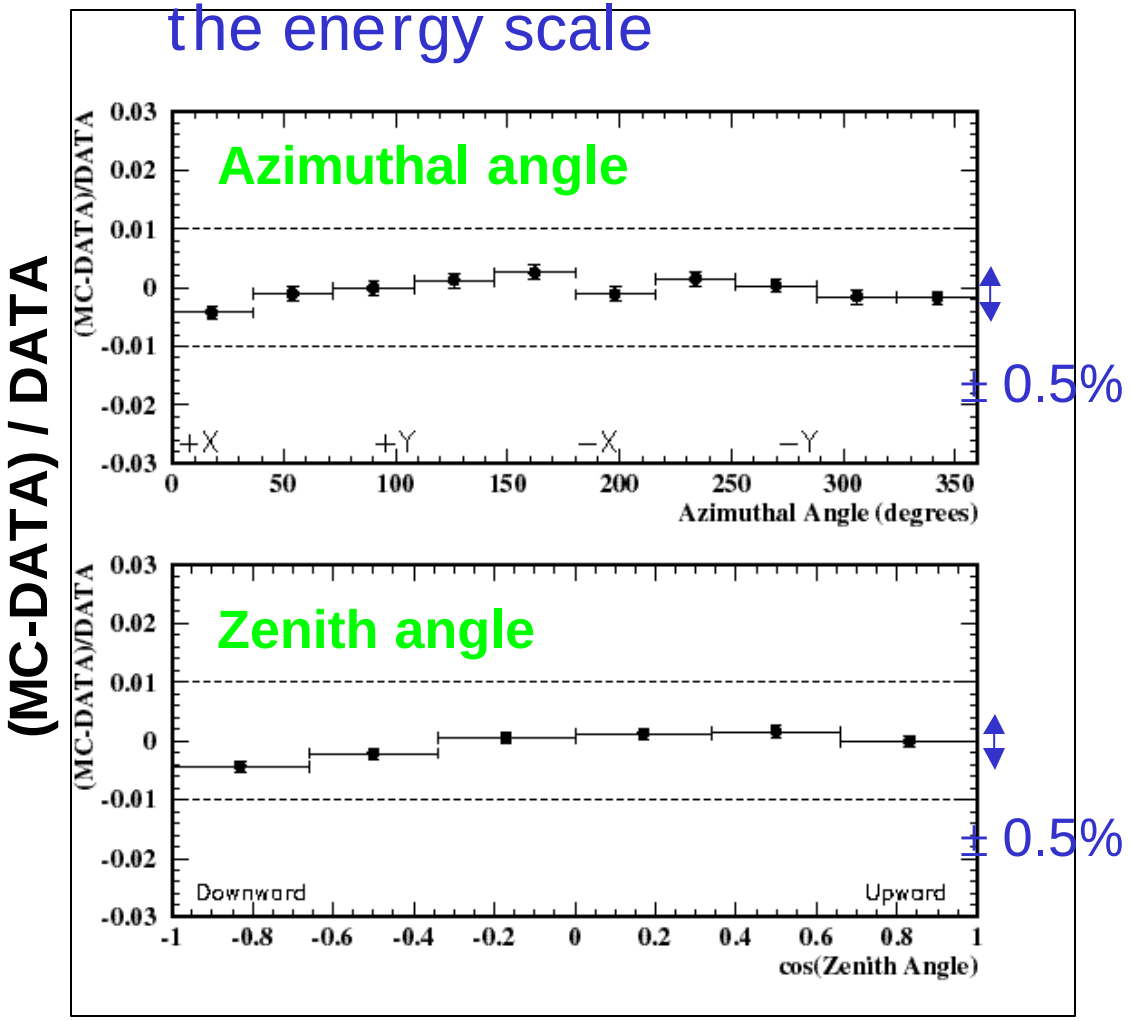

Direction and energy of solar neutrinos

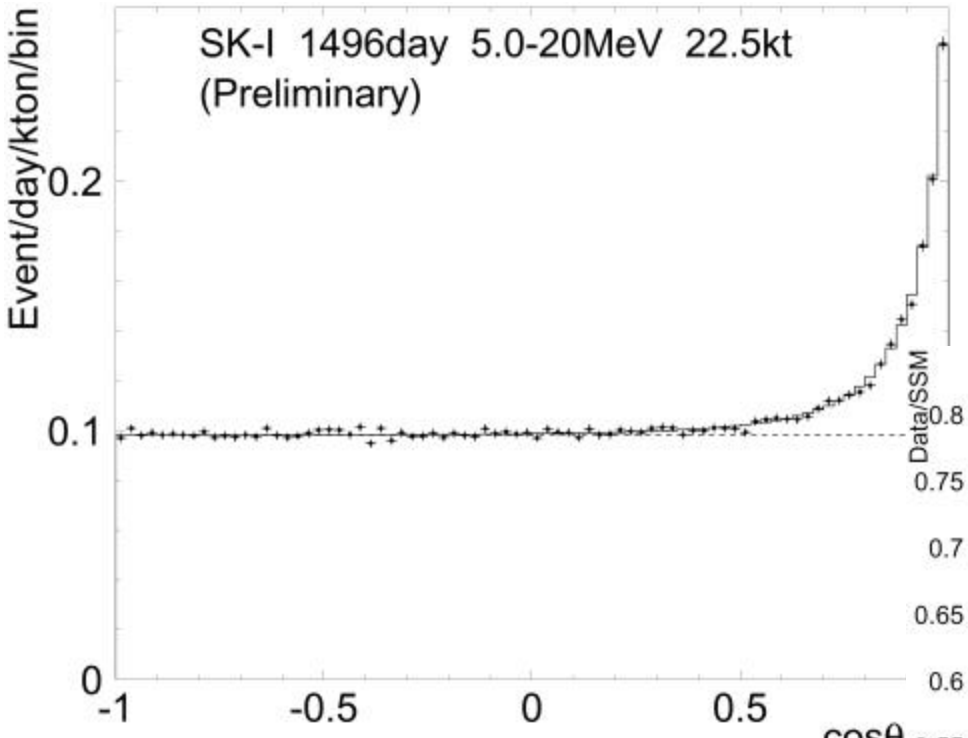

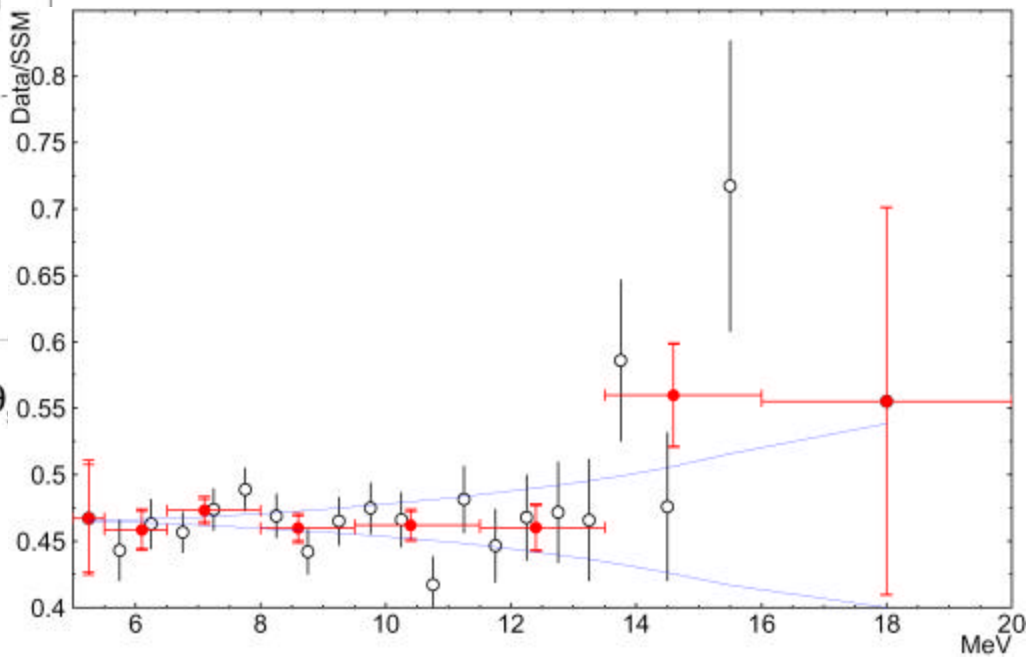

Water Cerenkov and atmospheric neutrinos

The Super-Kamiokande detector

Spectrum...

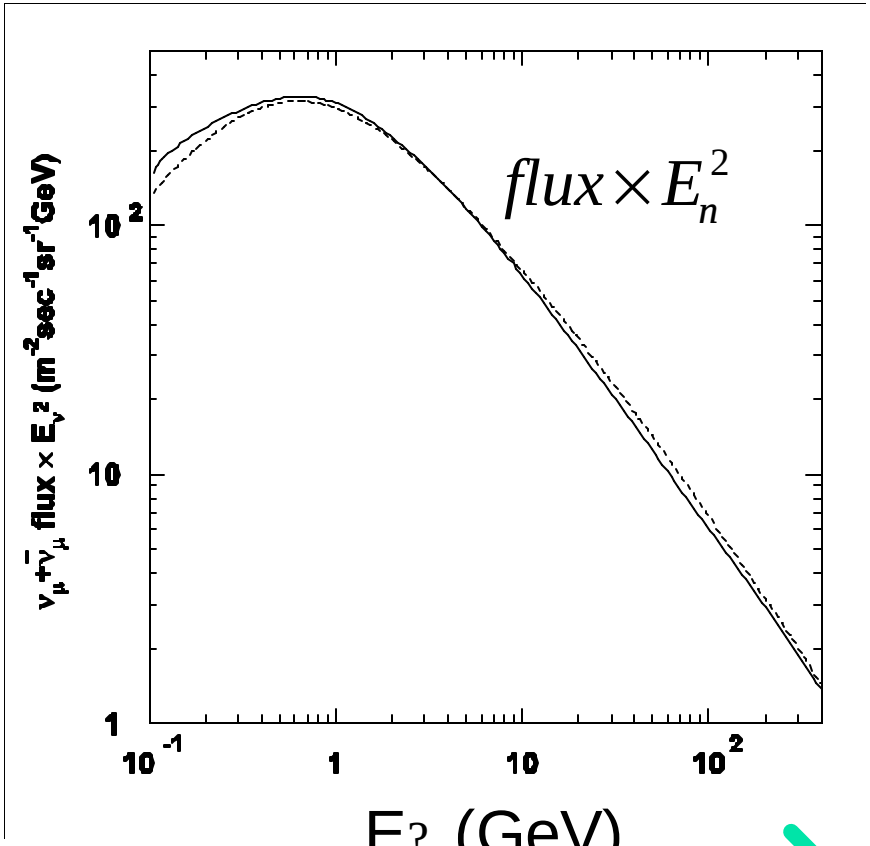
$flux \times E_n^2$
$\nu_\mu + \bar{\nu}_\mu$ flux × E_ν^2 ($m^{-2}sec^{-1}sr^{-1}GeV$)
10^2
10
1
10^{-1}
1
10
10^2
E? (GeV)

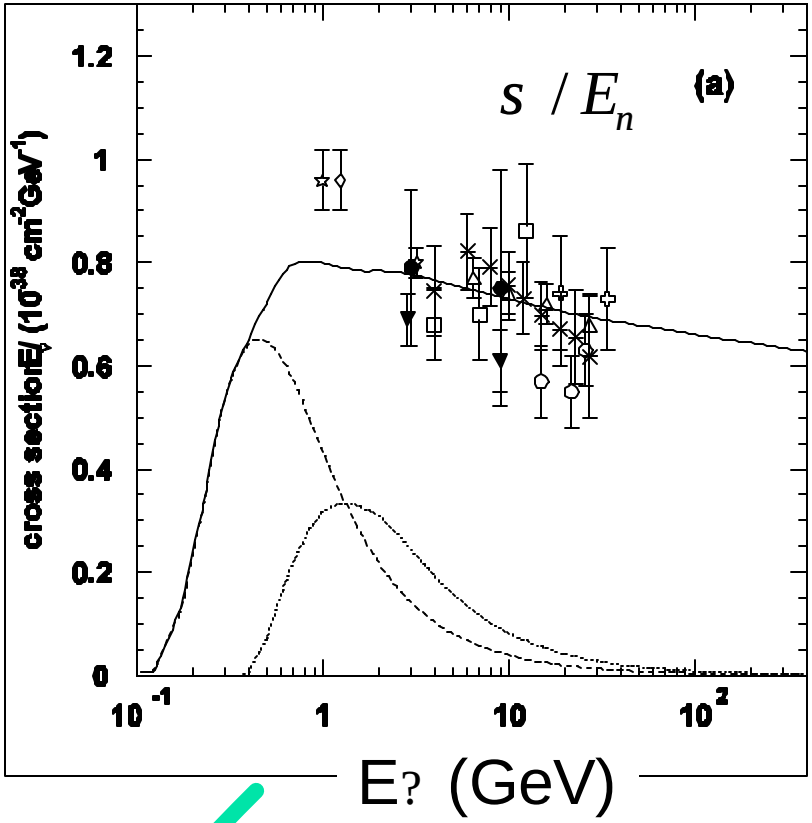
s / E_n
(a)
cross sectionE/ (10^{38} $cm^{-2}GeV^{-1}$)
1.2
1
0.8
0.6
0.4
0.2
0
10^{-1}
1
10
10^2
E? (GeV)

Various types of atmospheric neutrino events

FC (fully contained)

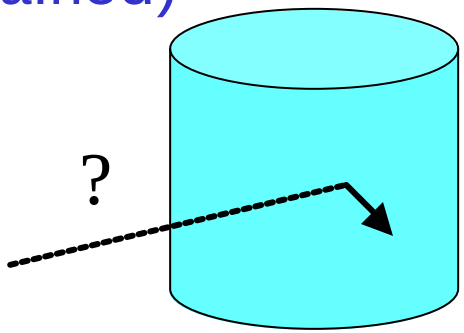

- Both CC ν_e and ν_μ (+NC)
- Need particle identification to separate ν_e and ν_μ

~ 12000 events (Super-K)
~ 360 events (Soudan2)

PC(partially contained)

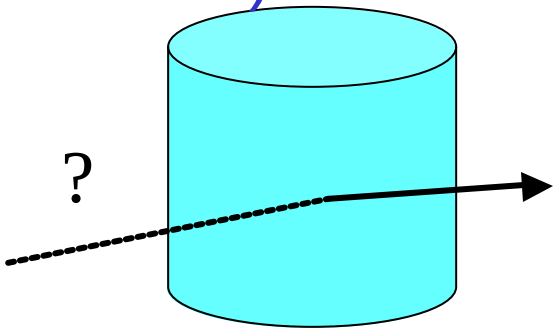

- ~ CC ν_μ

~ 900 events (Super-K)
~ 40 events (Soudan2)

Upward going muon

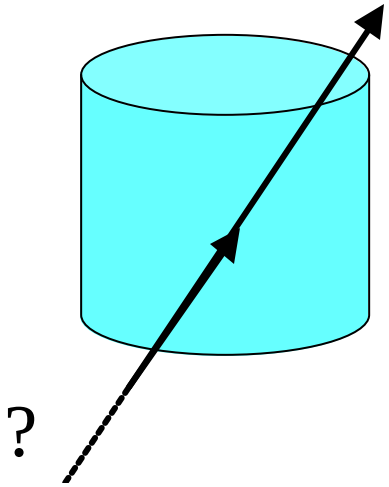

- ~ CC ν_μ

~ 1900 events (through, SK)
~ 420 events (stopping, SK)
~ 1200 events (through, MACRO)
~ 400 events (stop+PC, MACRO)

Particle identification

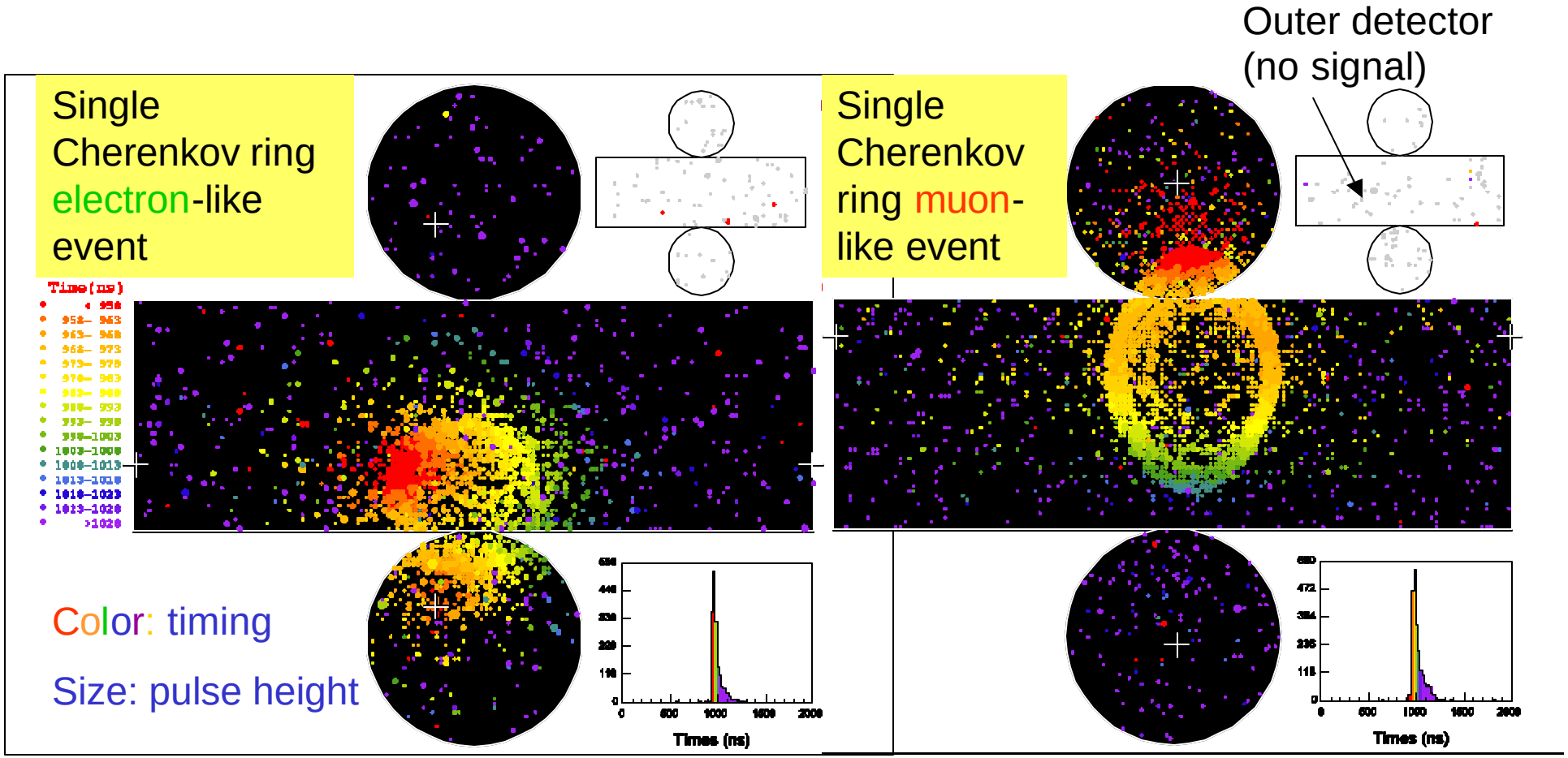

Particle ID

$$\log(L) = \sum_{q<70\deg} \left(\frac{p.e.(obs'd) - p.e._{e\ or\ m}(\exp ected)}{s_{p.e.}} \right)^2$$

Particle ID results

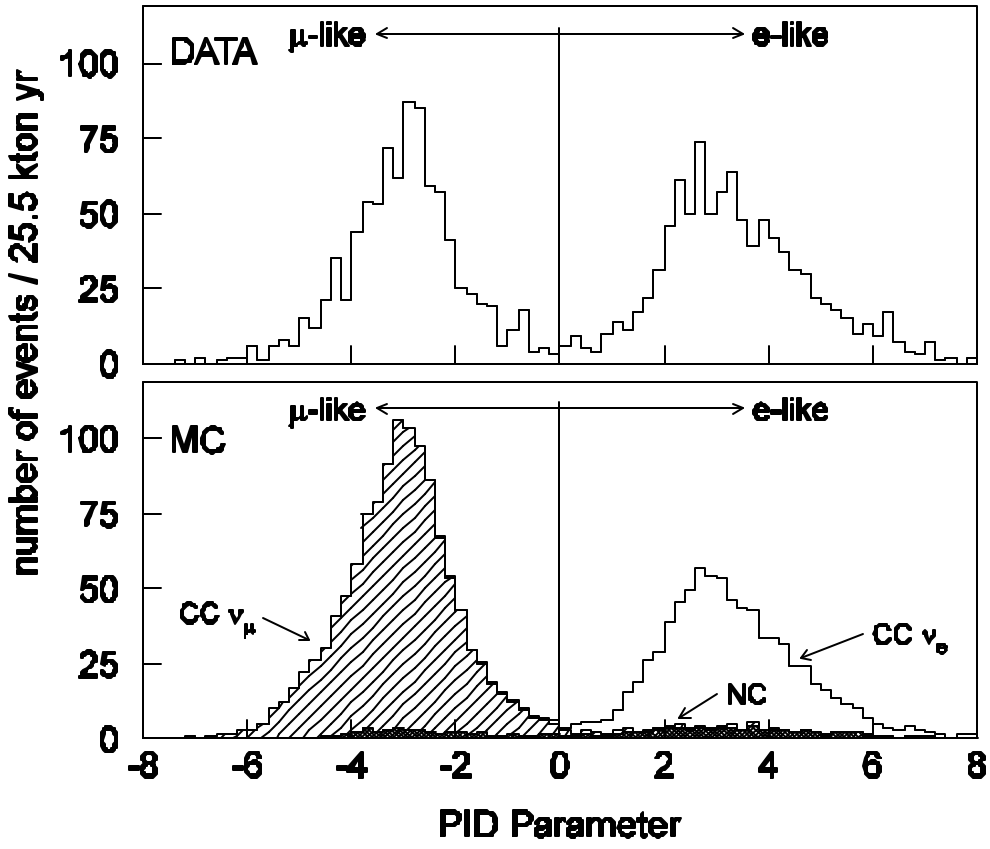

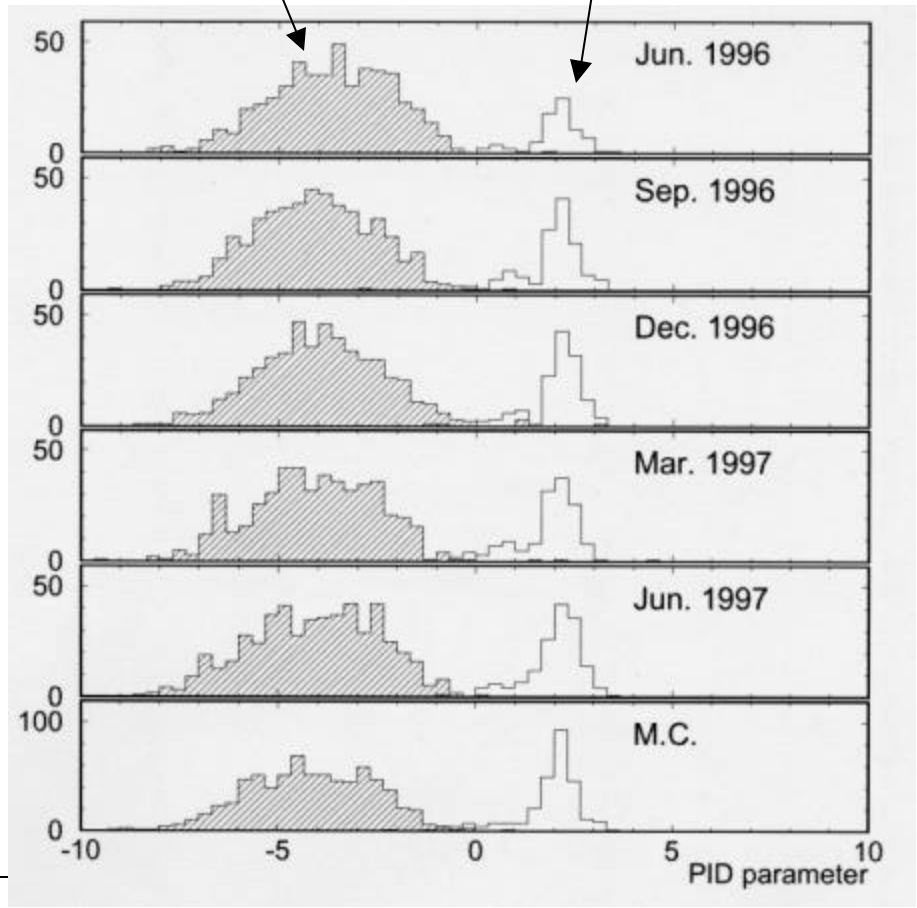

e =99%

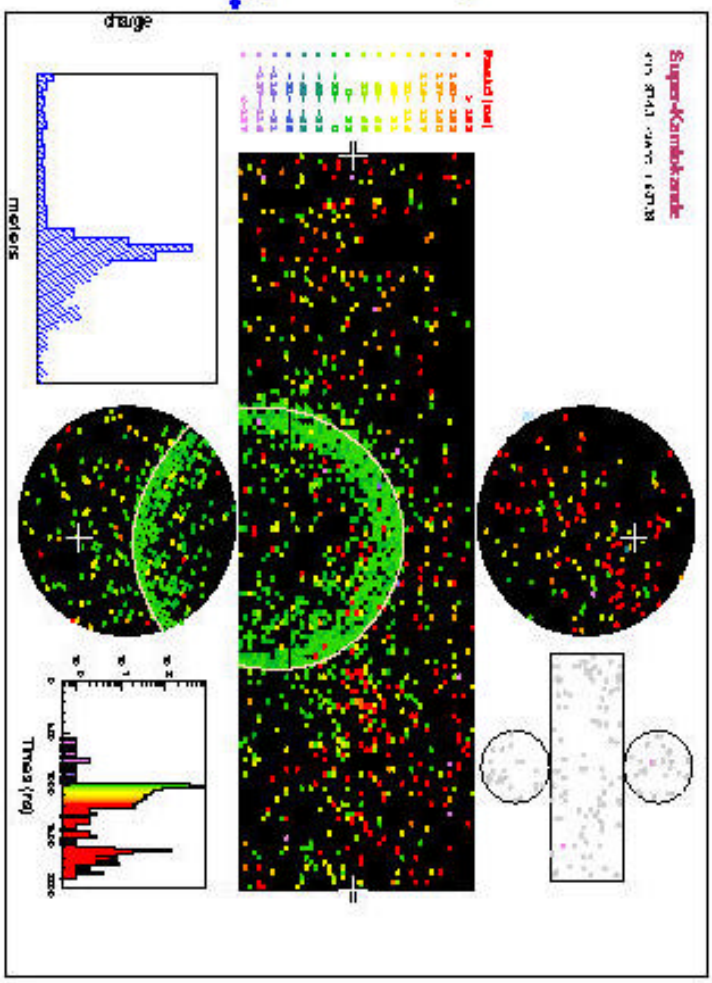
μ–like
charge
meters
Time (ns)

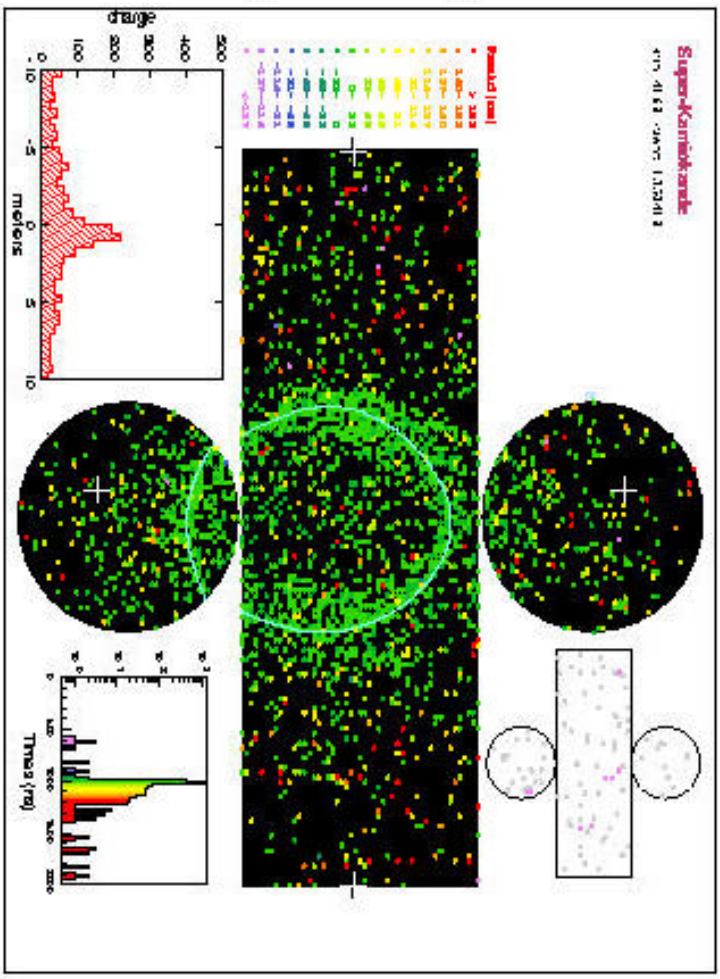
e–like
charge
meters
Time (ns)

Energy Resolution

Tested with LINAC at KEK

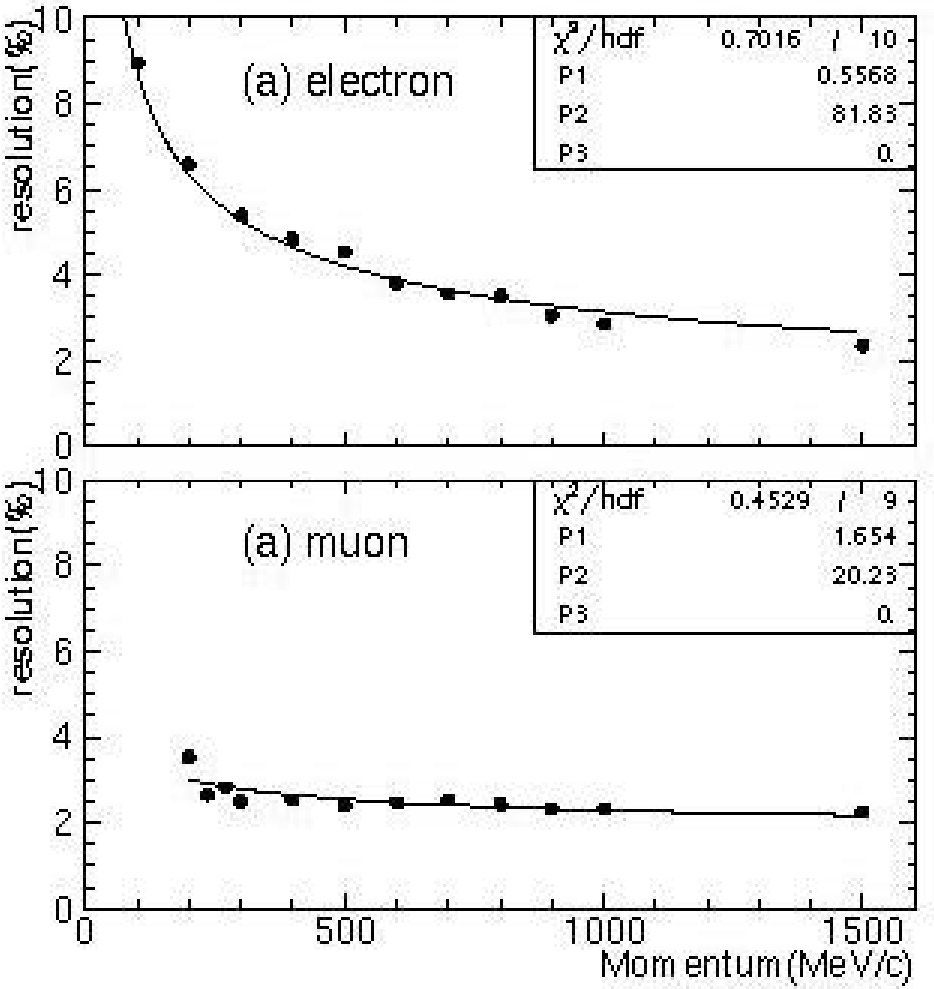

e/π^0 separation

Demonstrated in low E_ν OA beam, but very though at higher energy

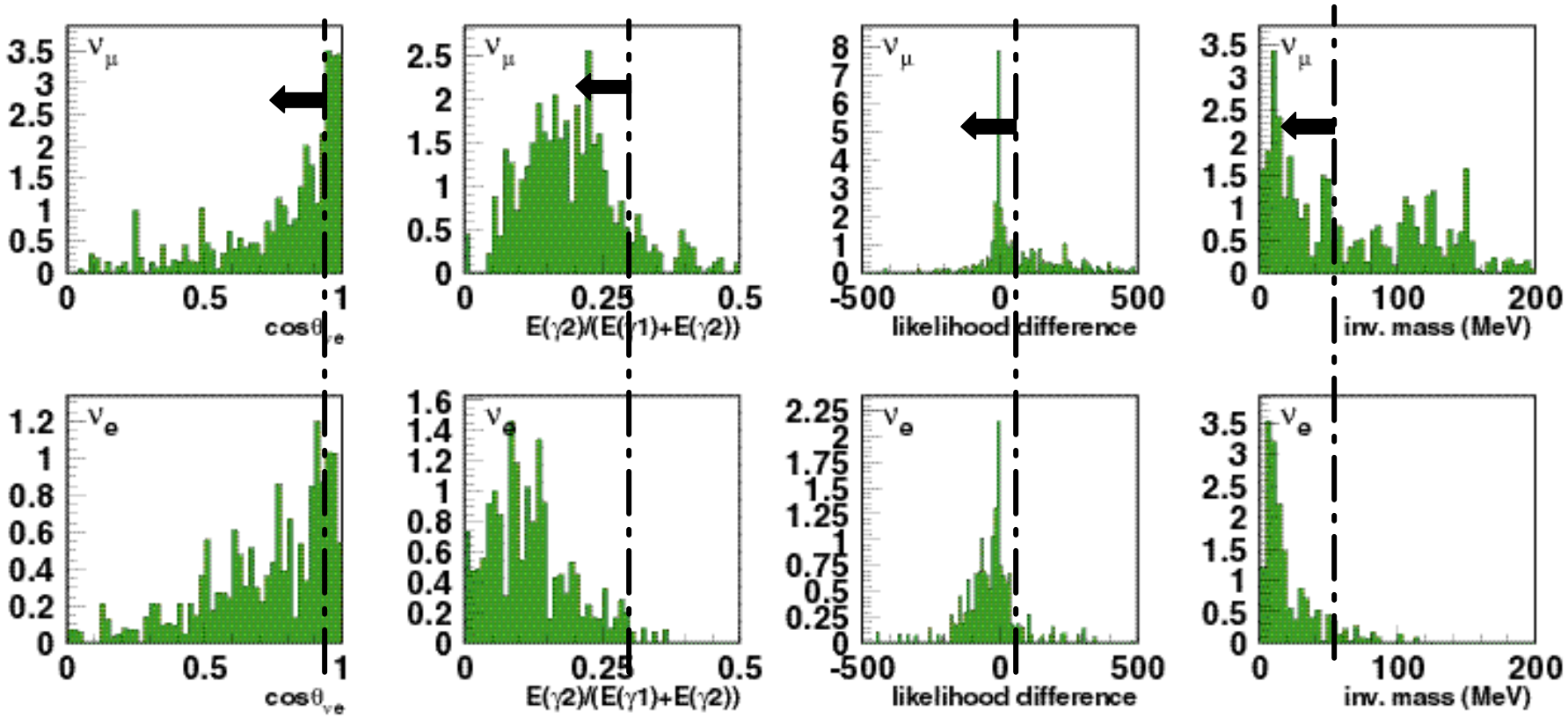

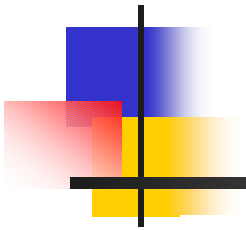

Heavy-Water Cerenkov and solar neutrinos

The SNO detector

Sudbury Neutrino Observatory

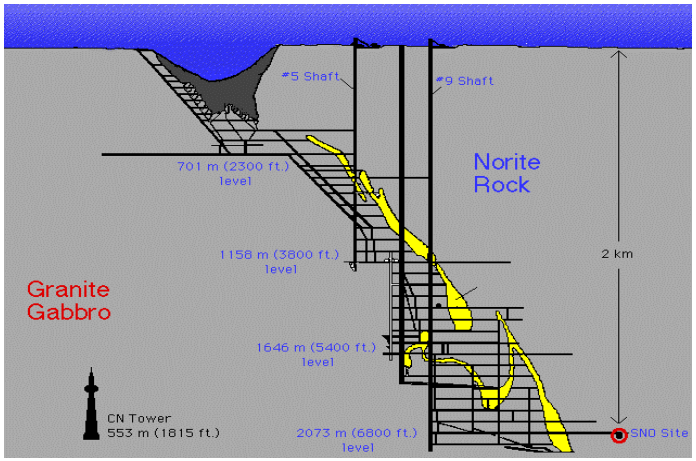

1000 tonnes D_2O

Support Structure for 9500 PMTs, 60% coverage

12 m Diameter Acrylic Vessel

1700 tonnes Inner Shielding H_2O

5300 tonnes Outer Shield H_2O

Urylon Liner and Radon Seal

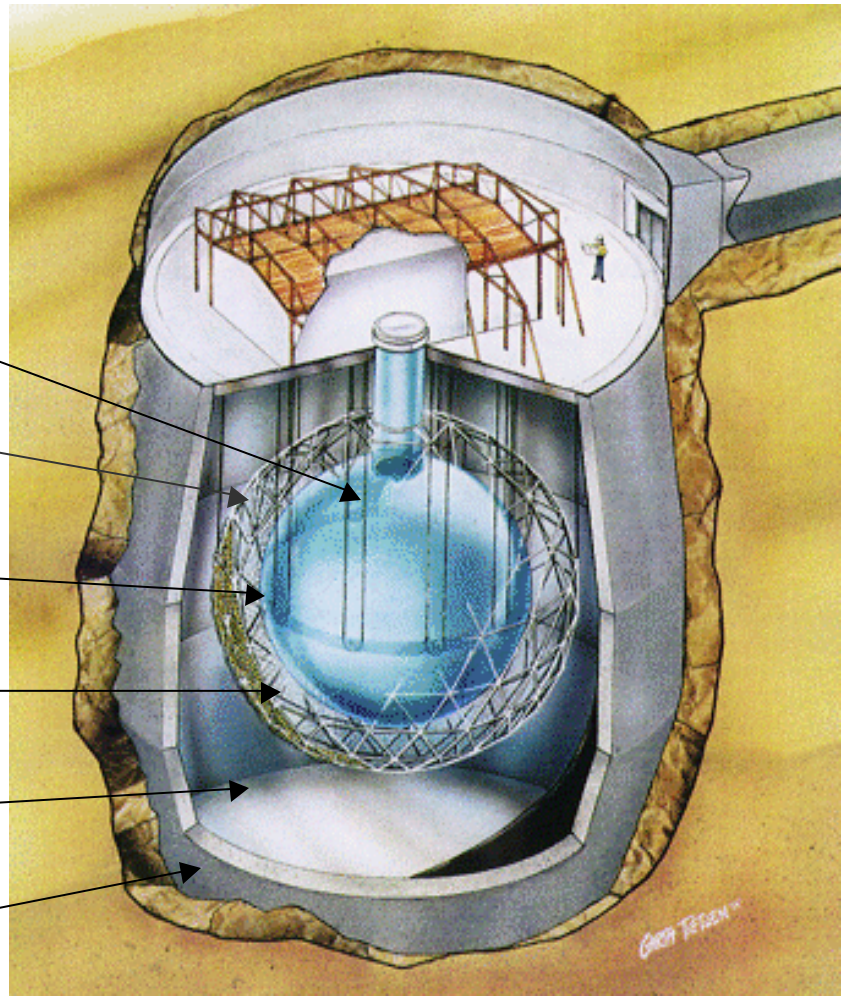

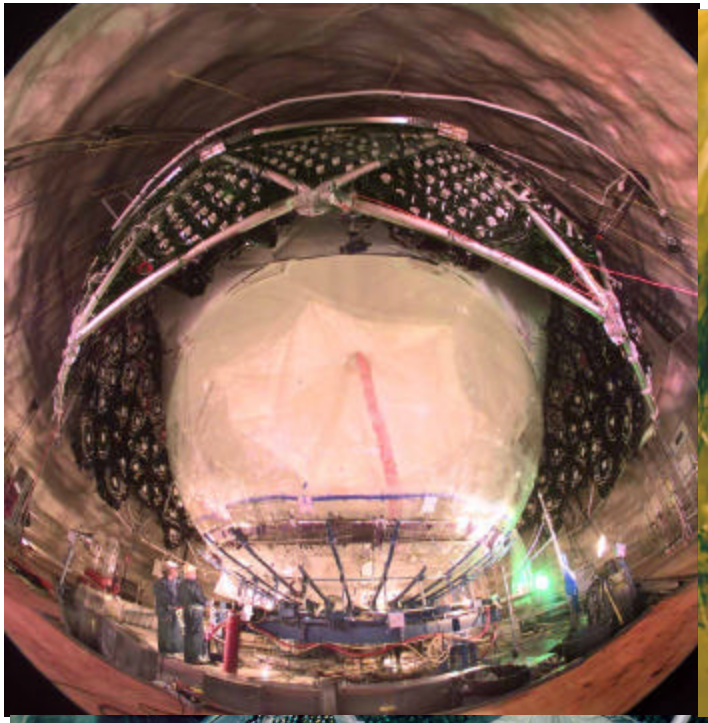

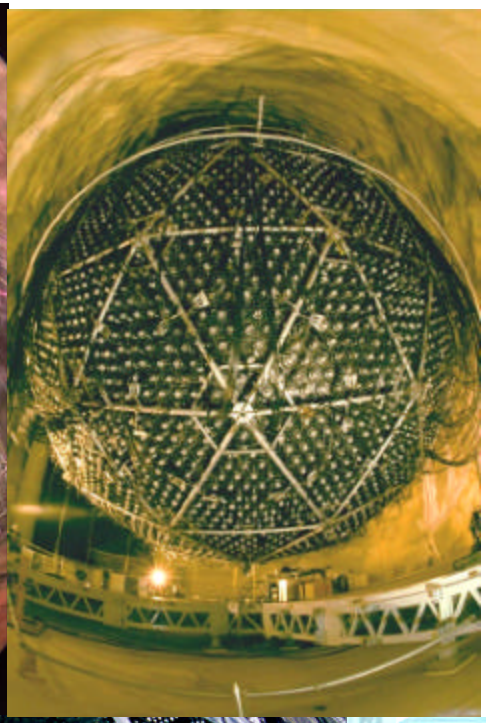

One million pieces
transported down in the
~ 10 foot square mine
cage and re-assembled under
Class 2000 air conditions.

> 60,000 Person-Showers so far

ν reactions in SNO

ES $?_x + e^- \Rightarrow ?_x + e^-$

- **Both SK, SNO**
- **Mainly sensitive to n_e, less to n_m and n_t**
- **Strong directional sensitivity**

CC $n_e + d \Rightarrow p + p + e^-$

- **Good measurement of n_e energy spectrum**
- **Weak directional sensitivity μ 1-1/3cos(q)**

- n_e ONLY

NC $n_x + d \Rightarrow p + n + n_x$

- **Measure total ^{8}B n flux from the sun.**

- Equal cross section for all n types

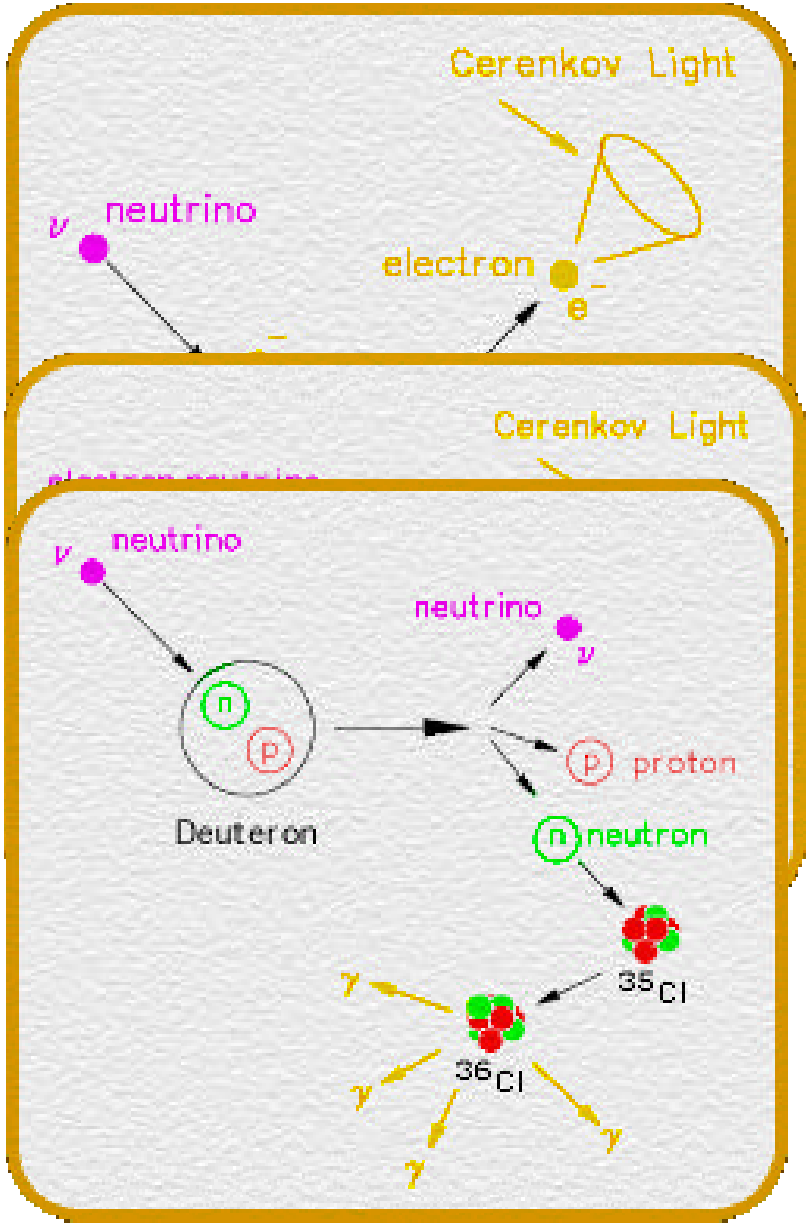

Three ways to measure the NC events

	Neutron Detection Method
Pure D_2O **Nov. 1999- May 2001** ▪ Good CC sensitivity	Capture on D $n + d \rightarrow t + \gamma \ldots \rightarrow e^-$ (E_γ = 6.3 MeV)
Added Salt in D_2O ▪ Enhanced NC sensitivity **Since June 2001**	Capture on Cl $n + {}^{35}Cl \rightarrow {}^{36}Cl + Sg \ldots \rightarrow e^-$ (E_{Sg} = 8.6 MeV)
Neutral Current Detectors ▪ ^{3}He proportional counters in the D_2O	Capture on ^{3}He $n + {}^3He \rightarrow p + t$ Event by event separation of CC and NC events

Understanding Detector Response

Monte Carlo

Cherenkov production (e^-, γ, β-γ)
Photon propagation and detection
Neutron transport and capture
Reconstruction
(position, direction, energy)

Calibrations

Pulsers	
Pulsed Laser	**337nm to 620 nm**
^{16}N	**6.13 MeV γ's**
^{3}H(p,γ)^{4}He	**19.8 MeV γ's**
^{8}Li	**<13.0 MeV β's**
^{252}Cf	**neutrons**
U/Th	**^{214}Bi & ^{208}Tl β-γ's**

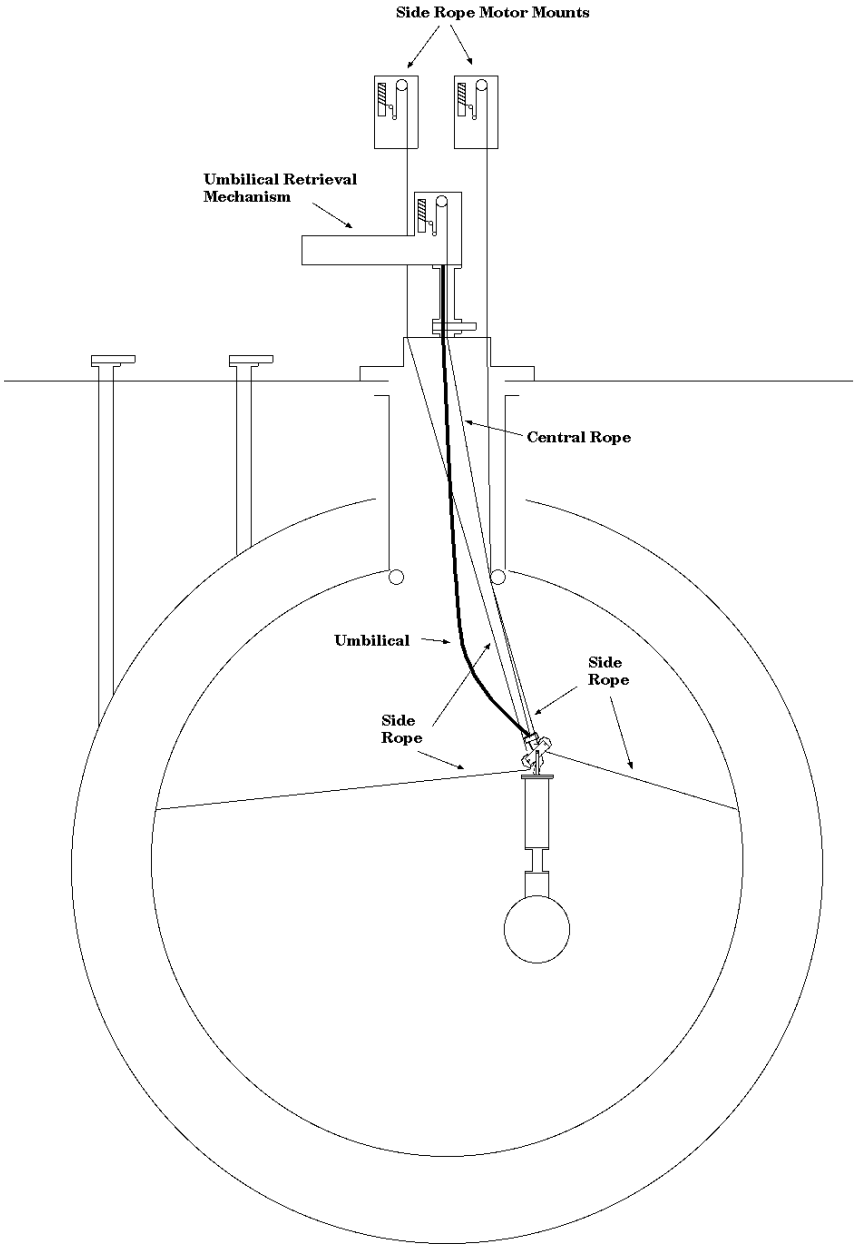

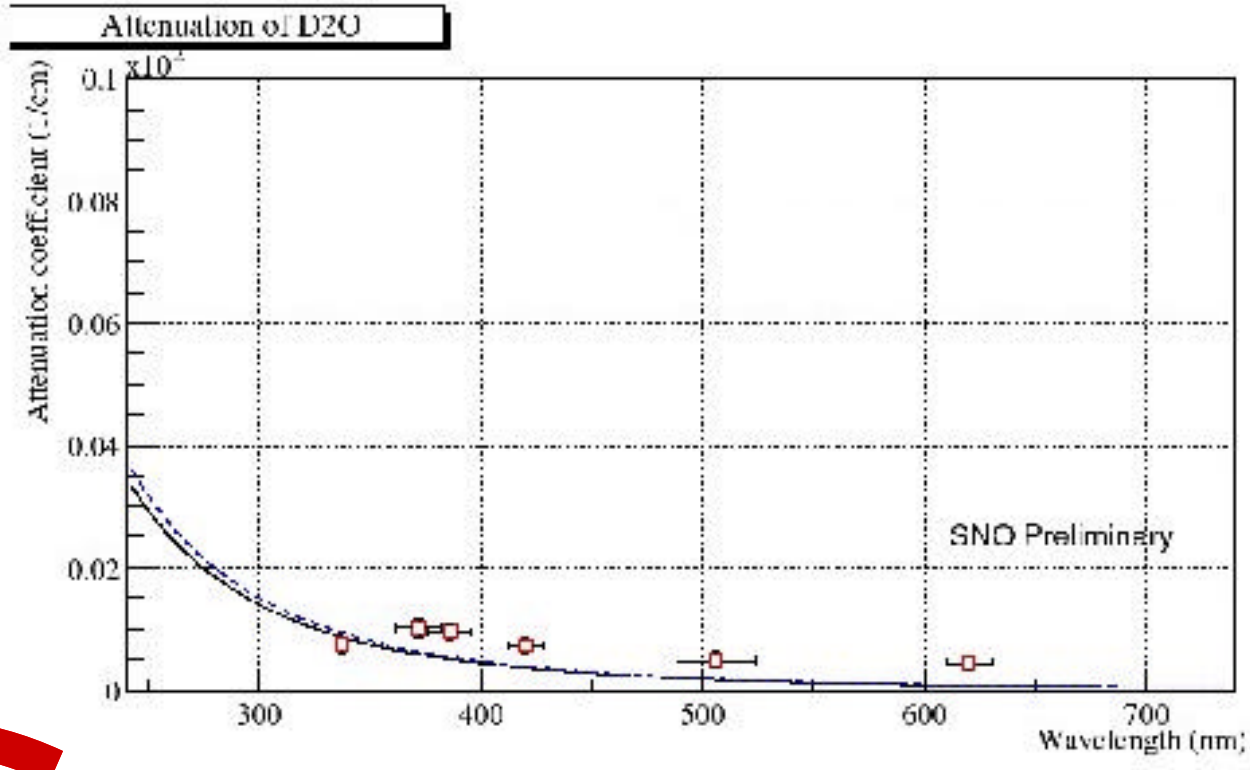

D_2O and H_2O are very clean. D_2O attenuation length ~100 m!

SNO Energy Calibrations

6.13 MeV

19.8 MeV

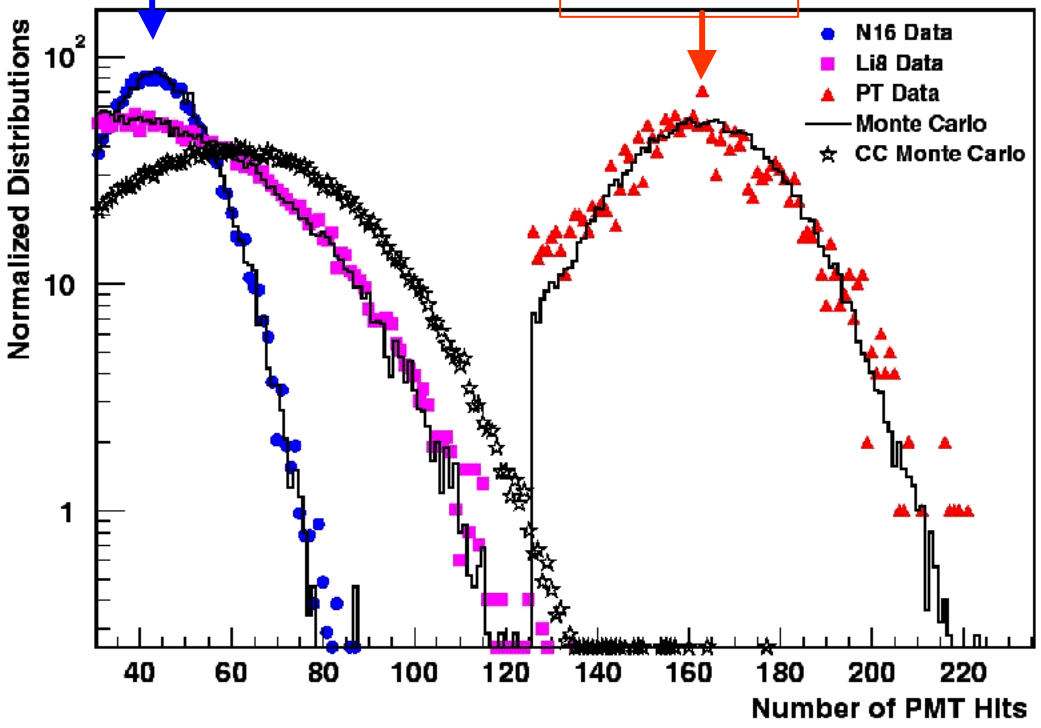

β's from ^{8}Li

γ's from ^{16}N and t(p,γ)^{4}He

^{252}Cf neutrons

n + **d** ® **t** + g **…** ® **e**$^{-}$

(E_g = 6.3 MeV)

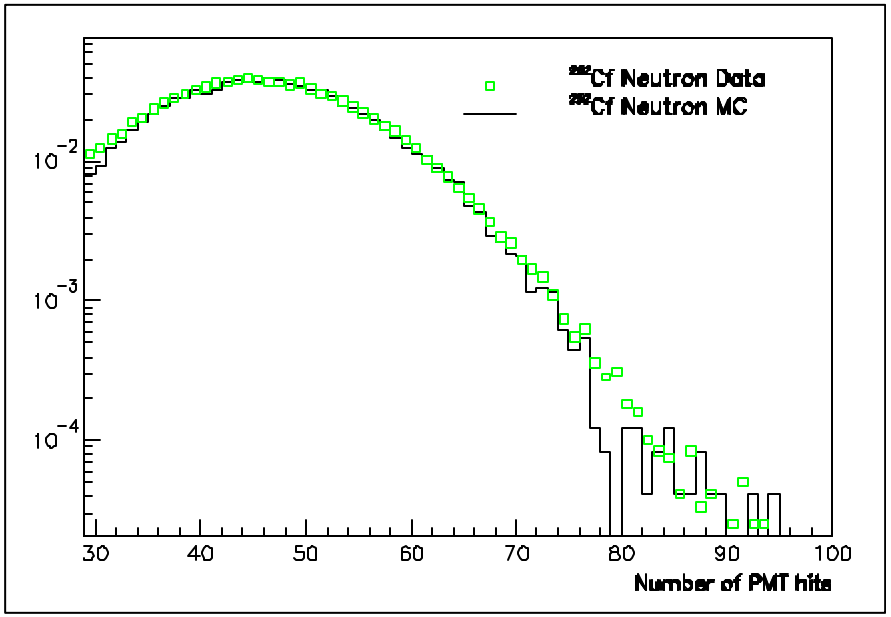

Neutron Capture Efficiency & Uncertainties

Response vs Radius

Capture Efficiency

Total **29.90 +/- 1.10 %**

With threshold & fiducial cut **14.38 +/- 0.53 %**

Flux Uncertainty

$\Delta NC/NC$

$-4.0,+3.6$ %

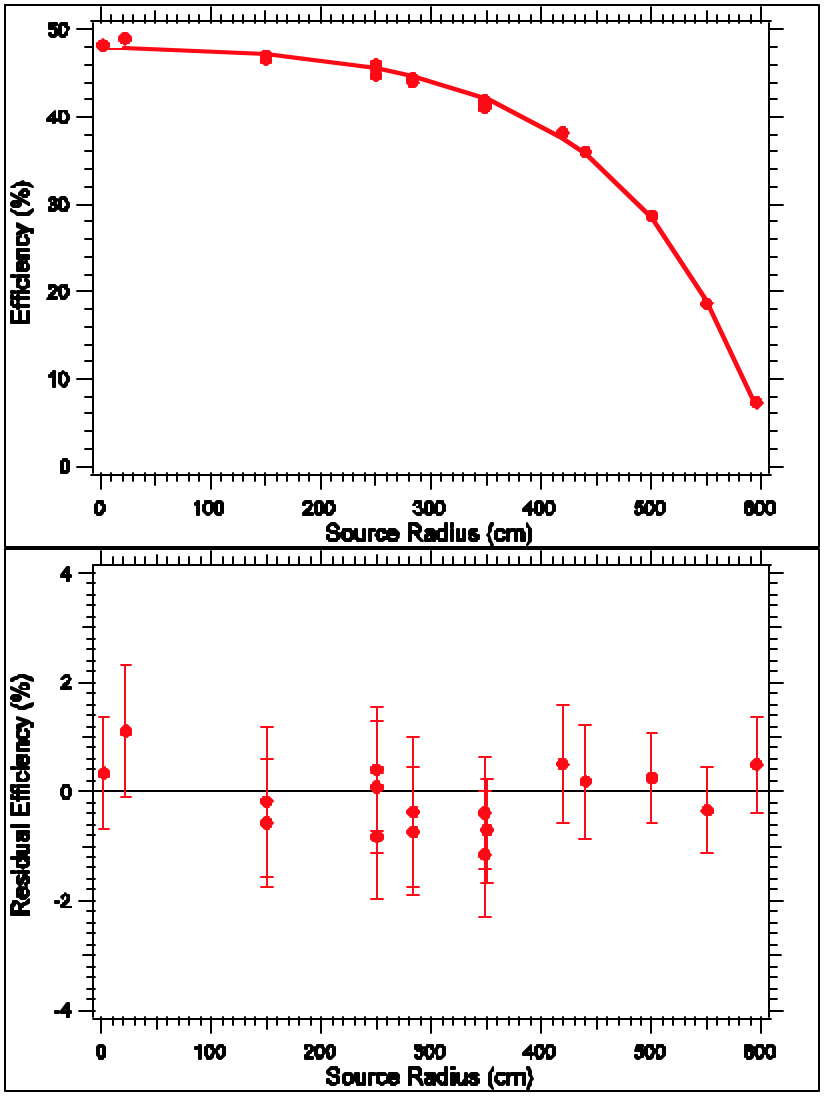

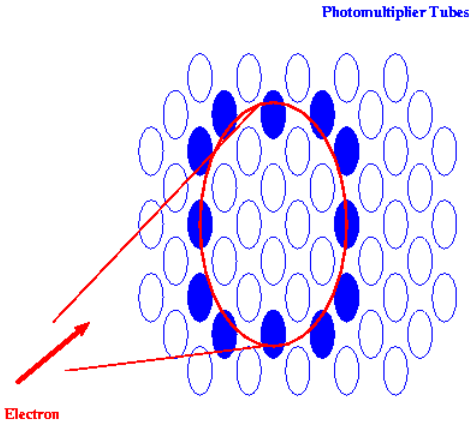

NEUTRINO EVENT DISPLAYED ON SNO COMPUTER SYSTEM

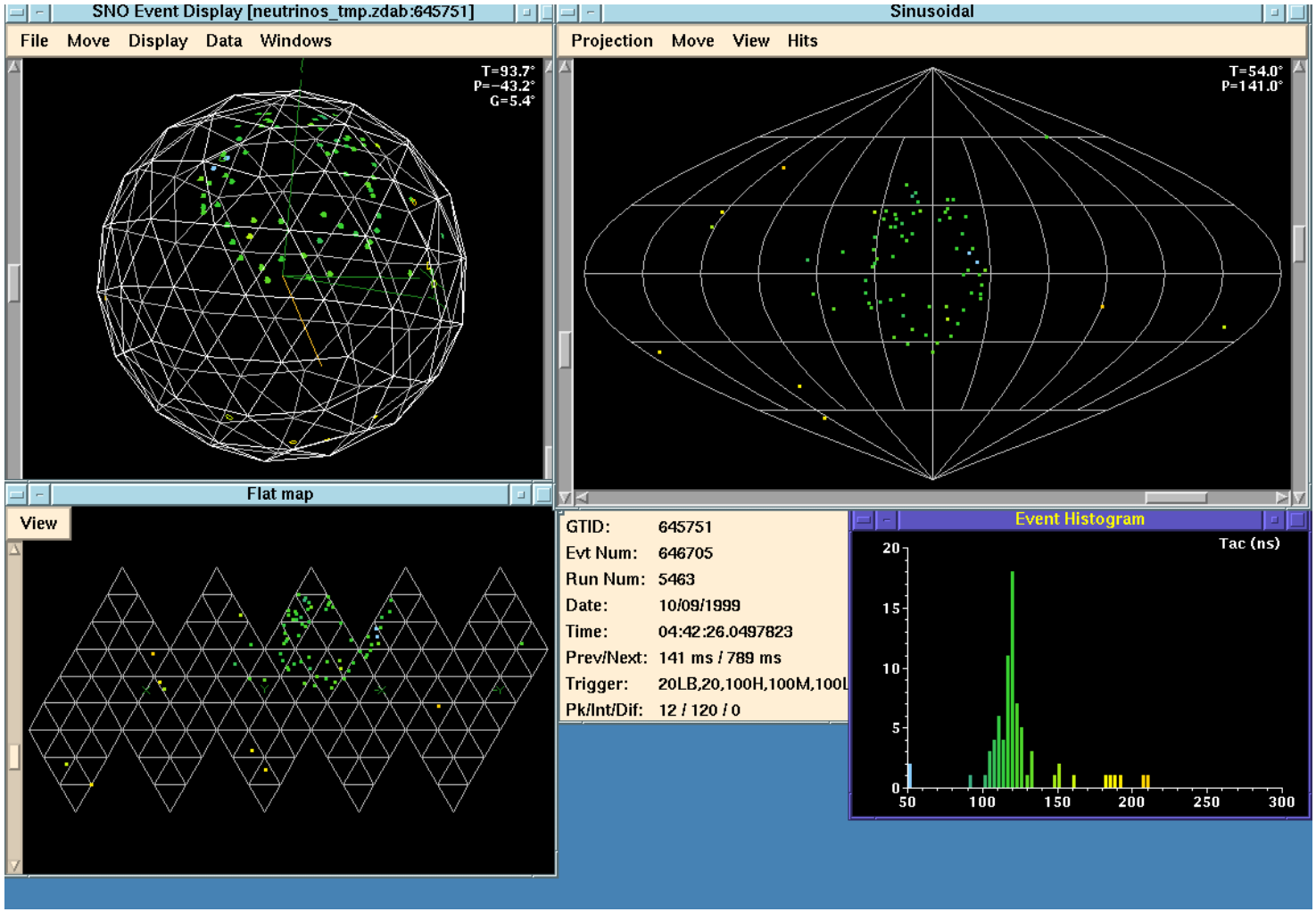

Instrumental Backgrounds

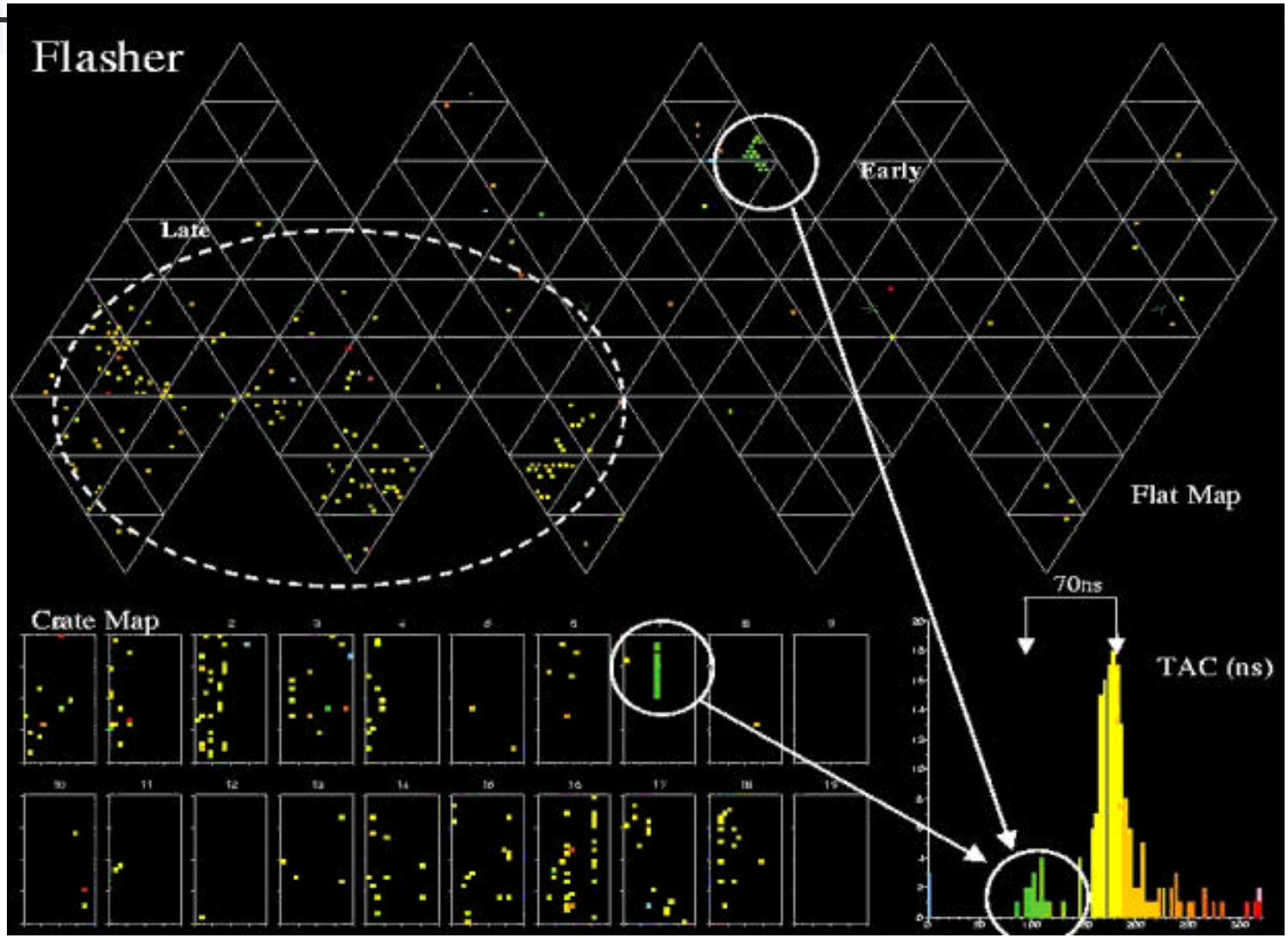

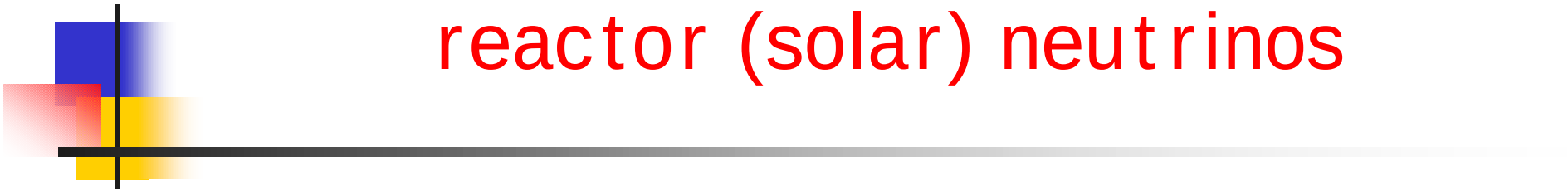

Liquid Scintillator Cerenkov and reactor (solar) neutrinos

The KamLAND detector

The KamLand detector

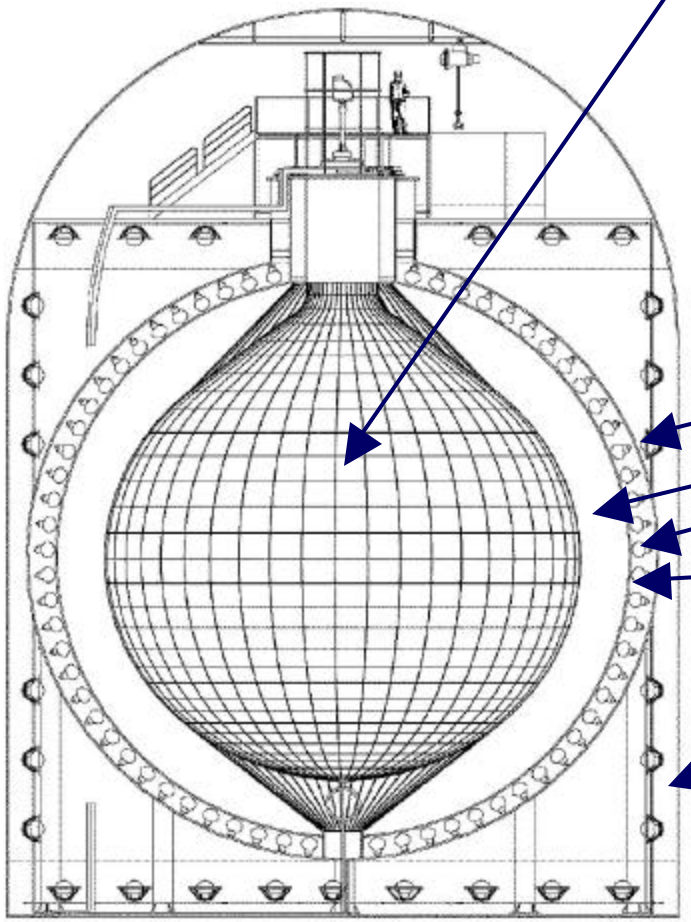

- Detector site : Old Kamiokande site (2700 m.w.e.)
- 1,000 ton Liquid Scintillator
  - 80%: dodecane, 20%: pseudocumene, 1.5 g/liter: PPO (ρ = 0.78)
  - housed in spherical balloon (13m diameter) of transparenet nylon/EVOH composite film (135μm)
  - supported by cargo net structure
- 3,000 m^3 Scintillation Light Detector
  - 18m diameter stainless steel tank filled with paraffin oil ($\Delta\rho$ = 0.04%, lighter than LS)
  - 1,325 17-inch+554 20-inch PMT's photosensitive coverage ~ 34 %
  - 3m thick acrylic wall (120 plates) : Rn barrier
- Water Cherenkov Outer Detector
  - 225 Kamiokande 20-inch PMT's

Present analysis ~ 22%

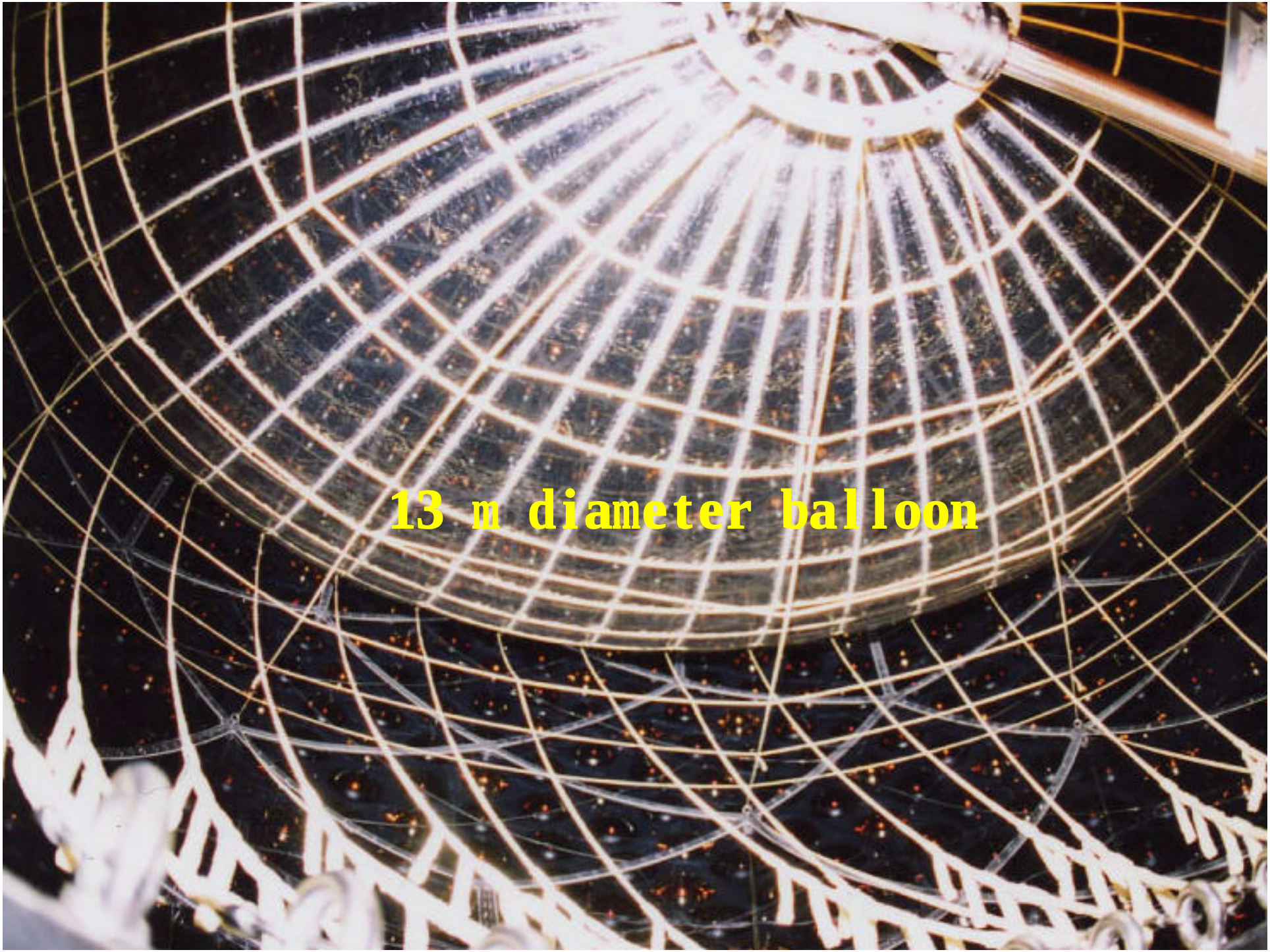
13 m diameter balloon

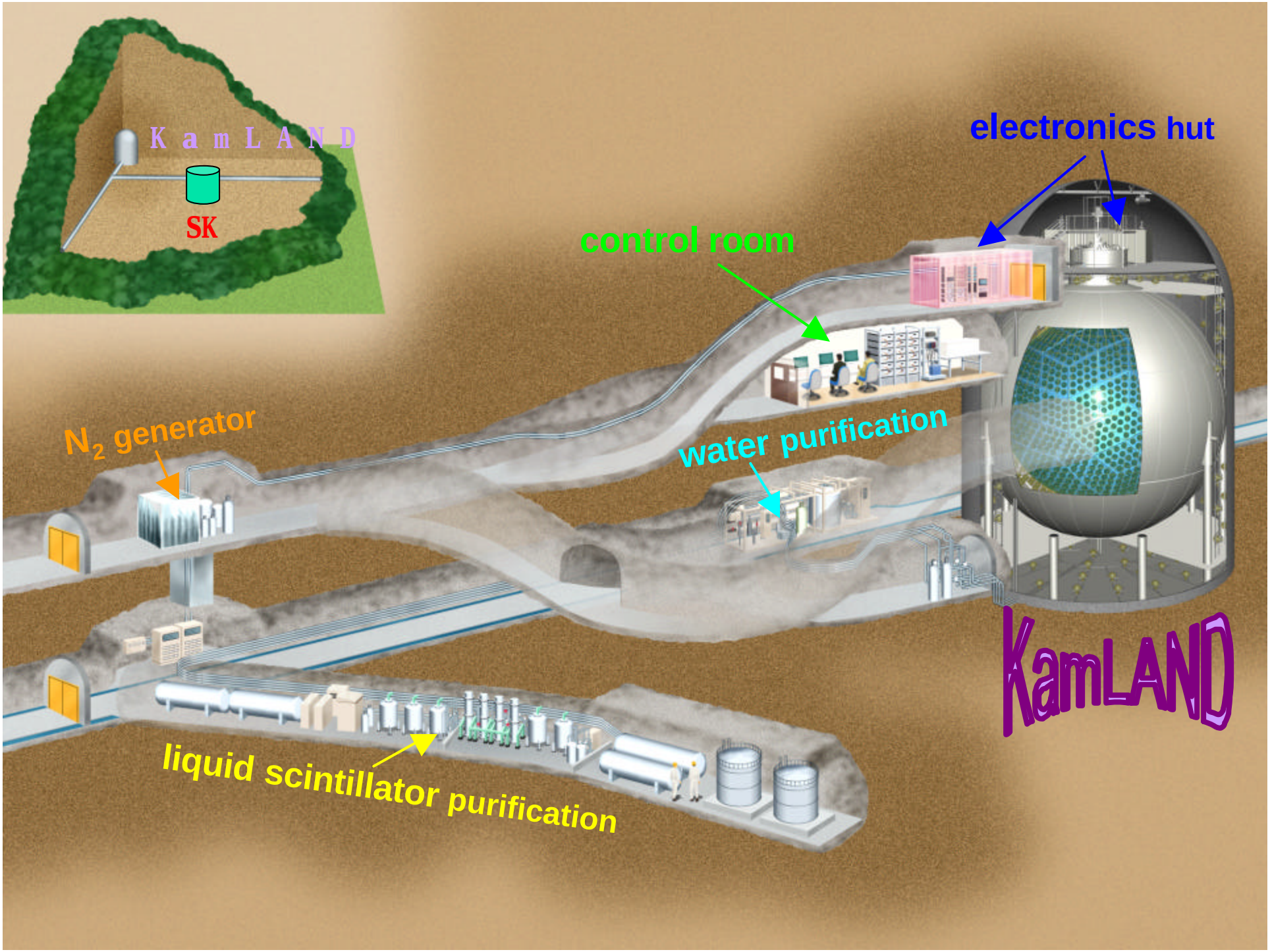
KamLAND
SK
electronics hut
control room
water purification
N_2 generator
liquid scintillator purification
KamLAND

20 % of world nuclear power

~ 70 GW

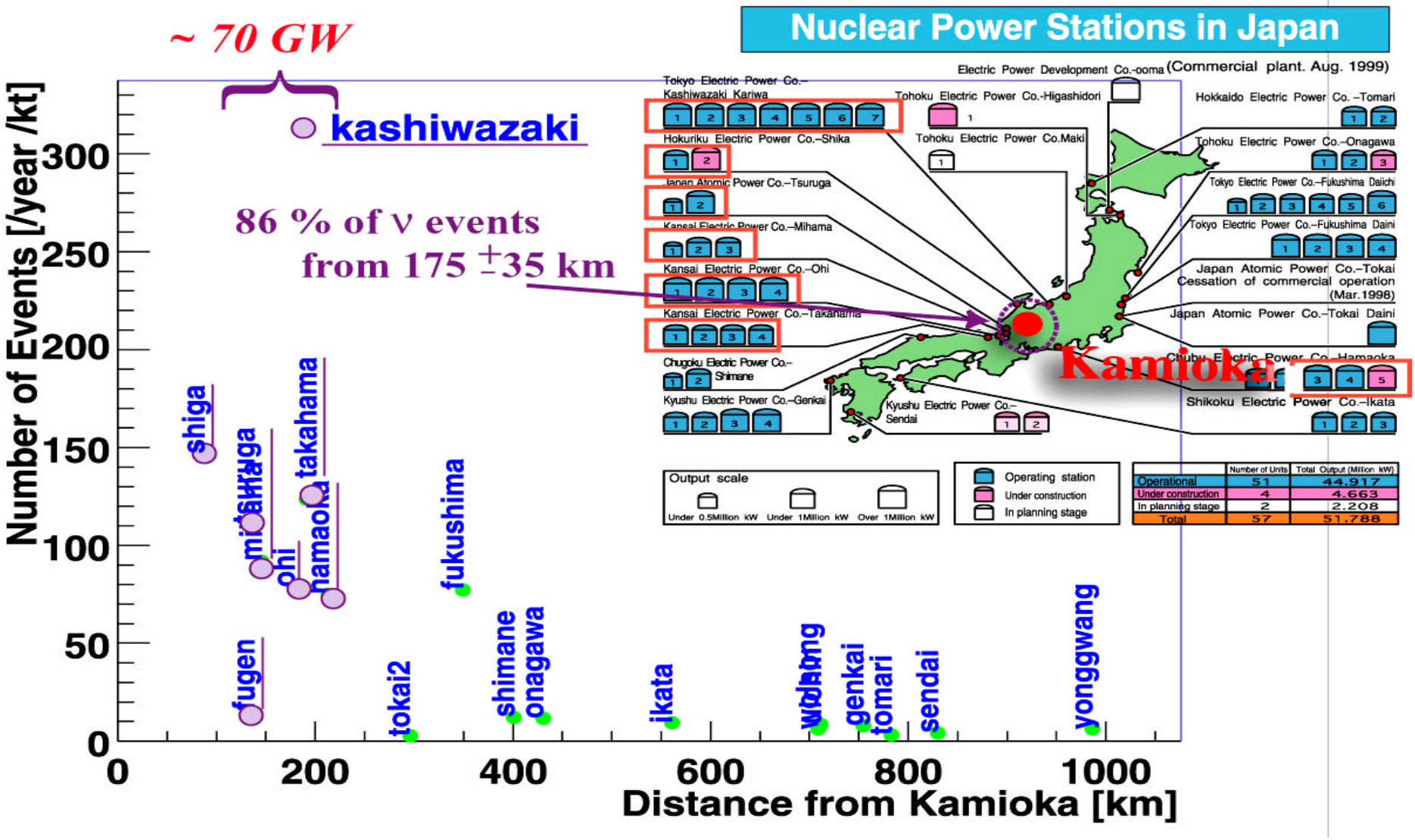

$\bar{\nu}_e$ Production : Fission Rate

- **Main Fuel Component :**

  4 main isotopes

  ^{235}U, ^{238}U, ^{239}Pu, ^{241}Pu (99.9%)

  others (^{240}Pu, ^{242}Pu, ,) (< 0.1%)

- **Time evolution of fission rate :**

  Reactor thermal power

  calculation in one of the Palo Verde reactor core

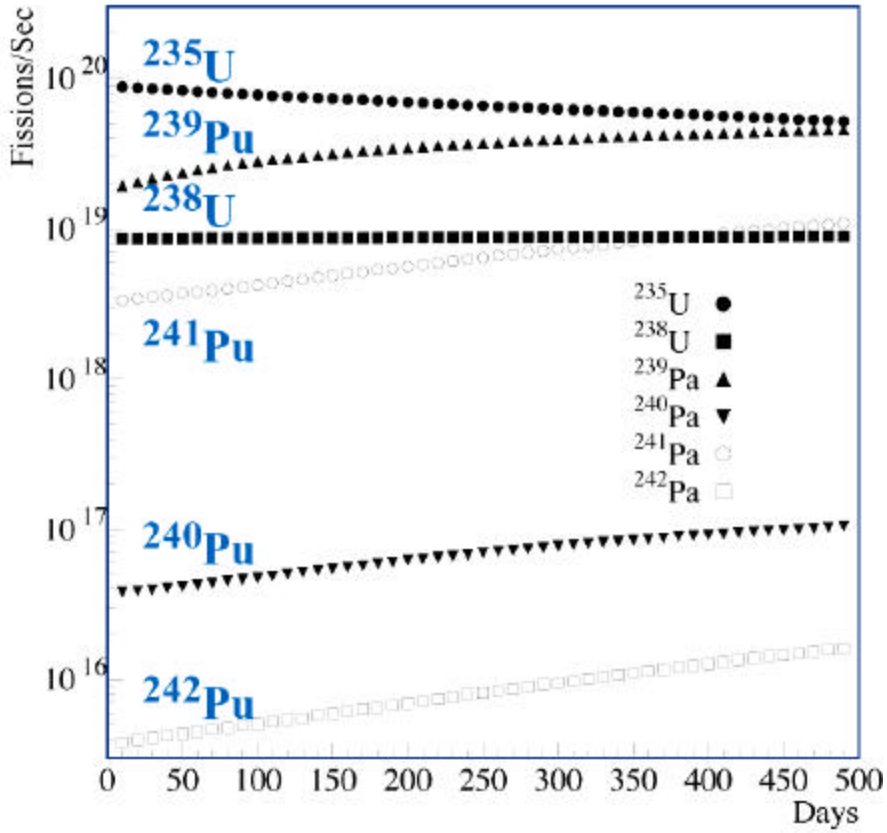

Uncertainty < 1% (neutrino yield)
: fuel-sampling & analyzing for isotopic components

→ **No need for near detector**

Reactor $\bar{\nu}_e$ Energy Spectrum

- $\bar{\nu}_e$ associated with ^{235}U, ^{239}Pu and ^{241}Pu

  measured β – spectra
  from thermal neutron fissions

  superposition of 30 hypothetical β-decay branches

  conversion $E_e \longrightarrow E_\nu$

- $\bar{\nu}_e$ associated with ^{238}U

  calculation based on
  744 unstable fission products

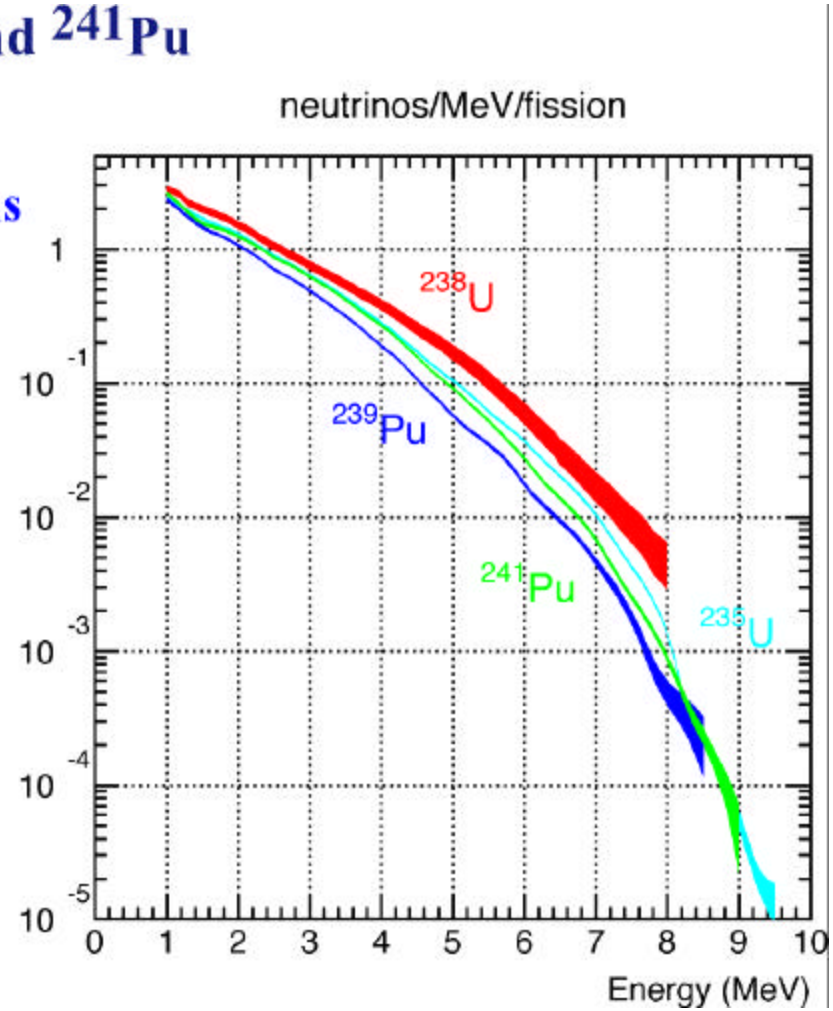

Reactor $\bar{\nu}_e$ Detection in Liquid Scintillator

reaction process : inverse- β decay ($\bar{\nu}_e + p \longrightarrow e^+ + n$)

$+ p \longrightarrow d + \gamma$

distinctive two-step signature

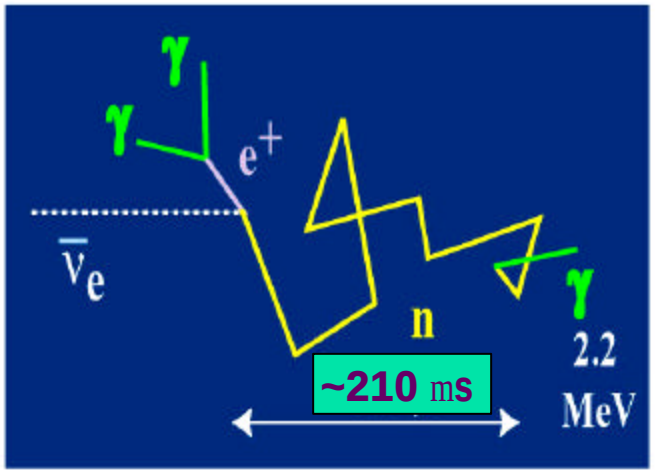

$$E_{th} = \frac{(M_n + m_e)^2 - M_p^2}{2M_p} = 1.806\ MeV$$

- **prompt part :** e^+

  $\bar{\nu}_e$ **energy measurement**

  $$E_\nu \sim (E_e + \Delta)\left[1 + \frac{E_e}{M_p}\right] + \frac{\Delta^2 - m_e^2}{M_p}$$

  $$\Delta = M_n - M_p$$

- **delayed part :** γ **(2.2 MeV)**

- **tagging : correlation of time, position and energy between prompt and delayed signal**

e^+ Prompt Energy Spectrum

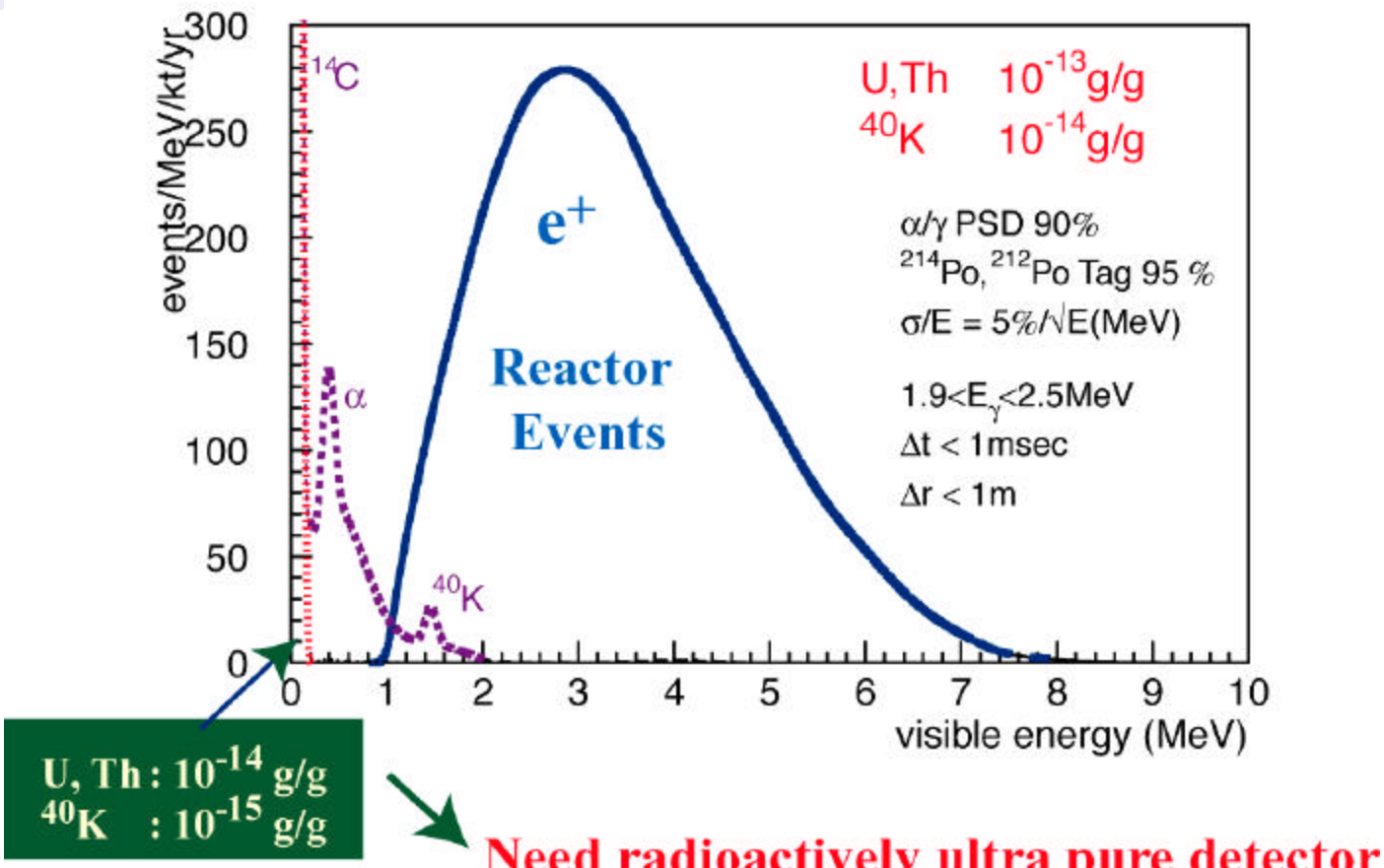

Need radioactively ultra pure detector

So… what does an event look like ?

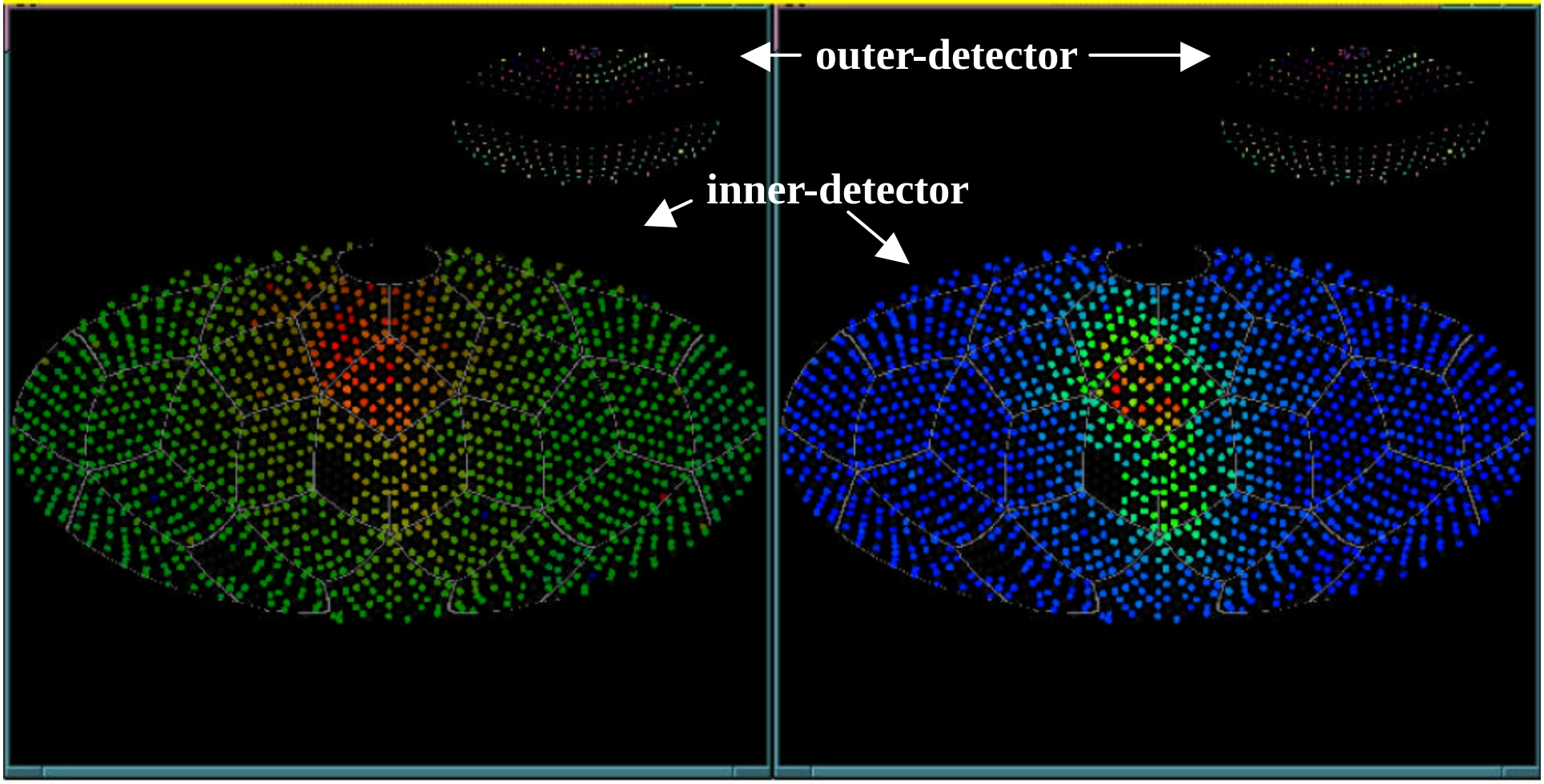

Time: Red soon, Blue late

Charge: Red alot,
Blue little

Position Reconstruction Uncertainty

^{68}Ge : 1.012 MeV (g + g) ^{65}Zn : 1.116 MeV (g)
^{60}Co : 2.506 MeV (g + g) AmBe : 2.20 , 4.40, 7.6 MeV (g)

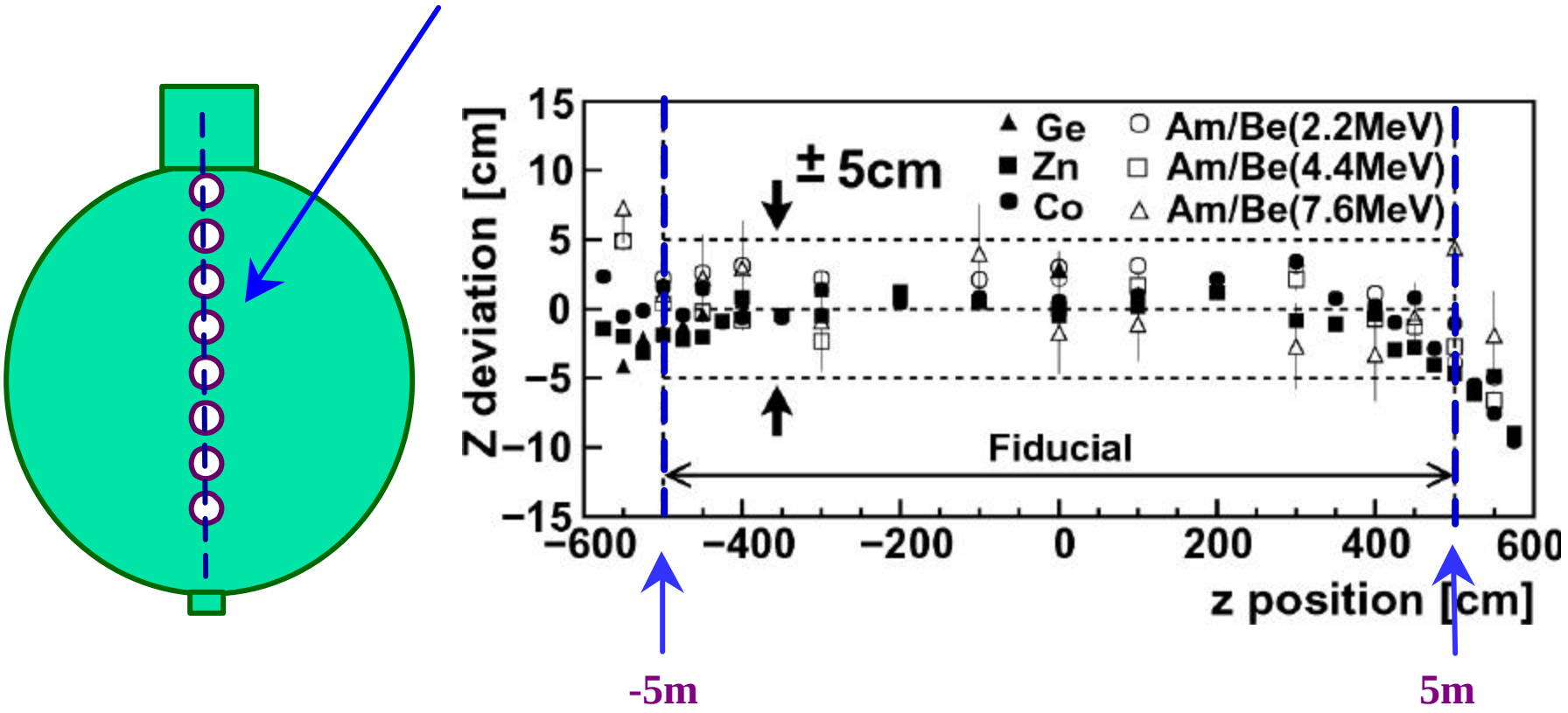

Energy Resolution & Determination

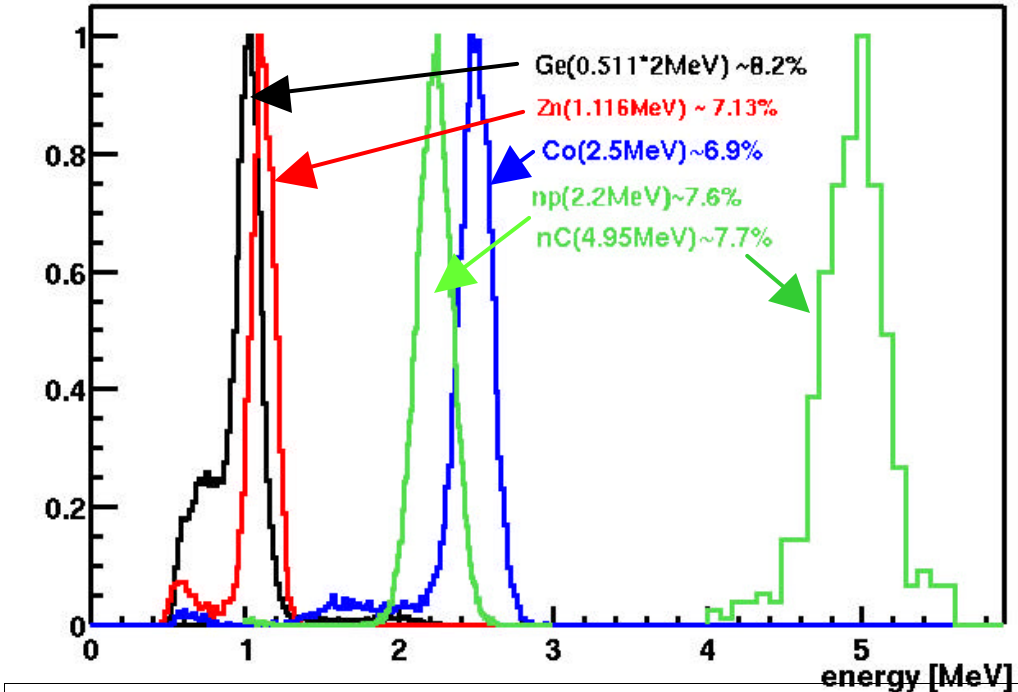

$\sigma_E/E \sim 7.5\% / \sqrt{E}$

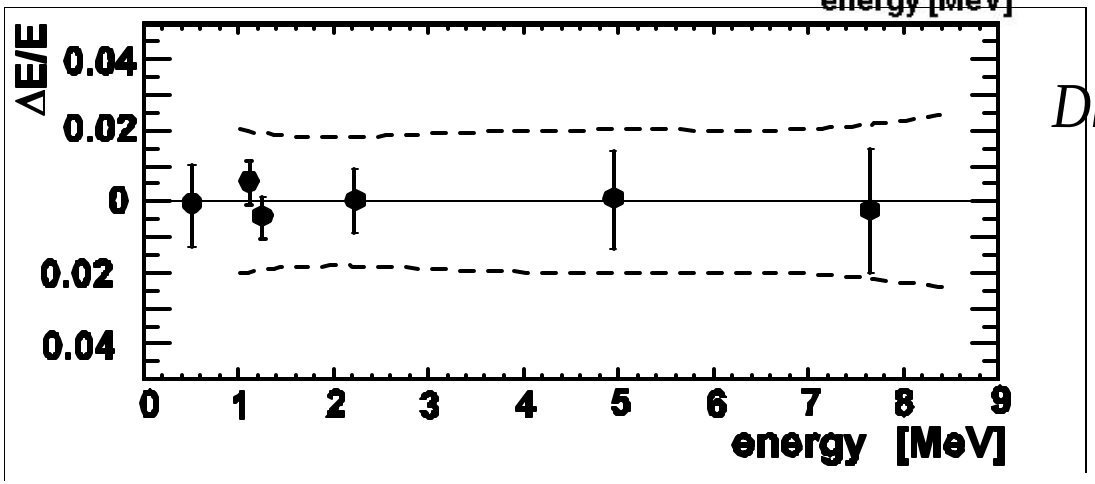

$\Delta E_{syst} = 1.9\%$ at 2.6 MeV

→ 2.1 % for $\bar{n}_e$

Radioactivity inside Liquid Scintillator

^{238}U : $^{214}Bi \xrightarrow{\beta+\gamma} {}^{214}Po \xrightarrow{\alpha} {}^{210}Pb$

$E = 3.27\ MeV$, $\tau = 28.7\ min.$

$E = 7.69\ MeV$, $\tau = 237\ \mu s$

event selection

$\Delta R < 100\ cm$

$5\ \mu s < \Delta t < 1000\ \mu s$

$E_{prompt} > 1.3\ MeV$

$0.3 < E_{delayed} < 1\ MeV$

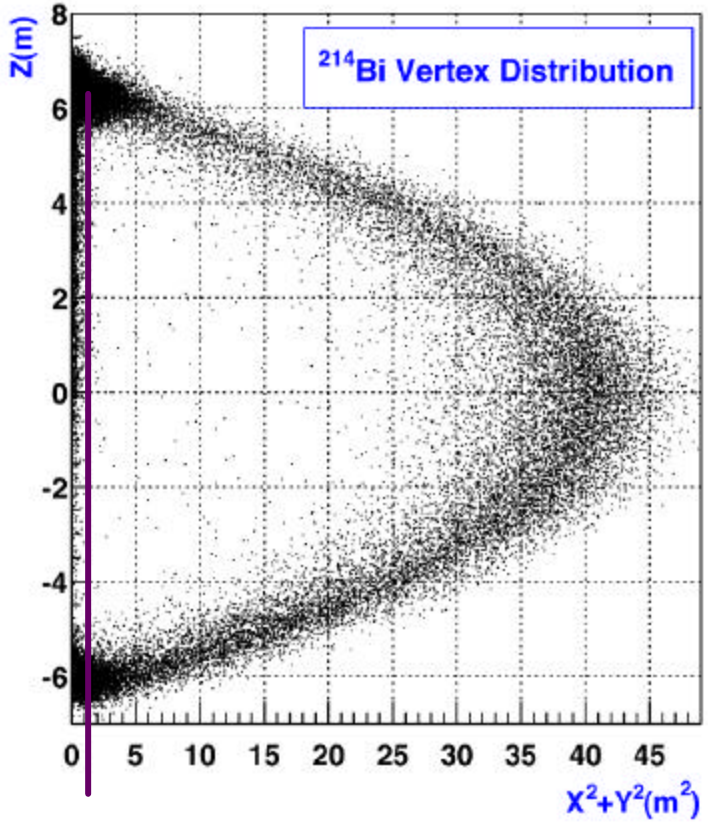

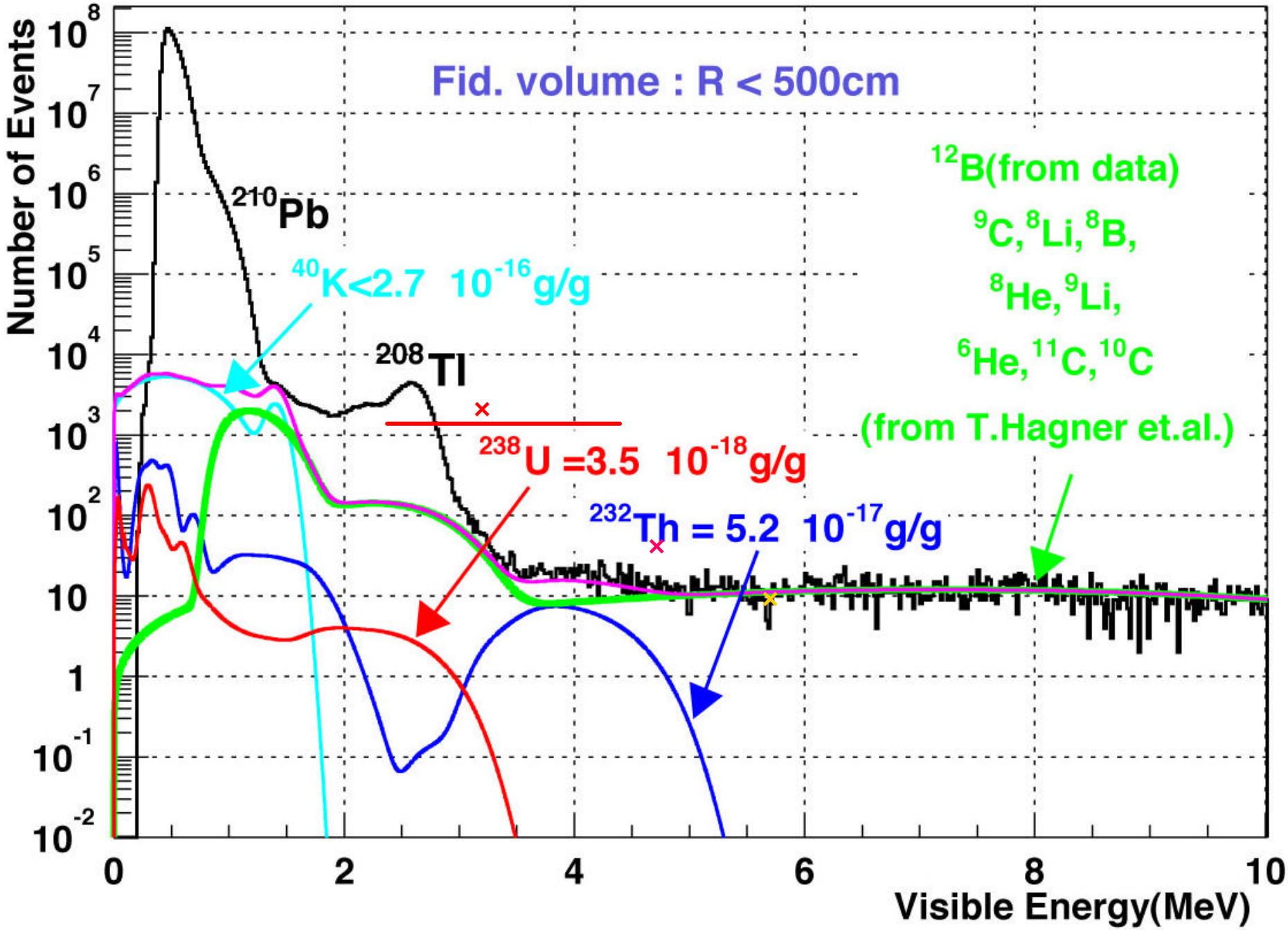
Fid. volume : R < 500cm
Number of Events
Visible Energy(MeV)
^{210}Pb
^{208}Tl
^{40}K<2.7 10^{-16}g/g
^{238}U =3.5 10^{-18}g/g
^{232}Th = 5.2 10^{-17}g/g
^{12}B(from data)
^{9}C,^{8}Li,^{8}B,
^{8}He,^{9}Li,
^{6}He,^{11}C,^{10}C
(from T.Hagner et.al.)

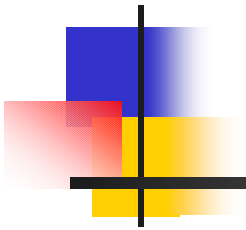

Liquid Argon TPC for neutrino physics

The ICARUS experiment

Liquid Argon

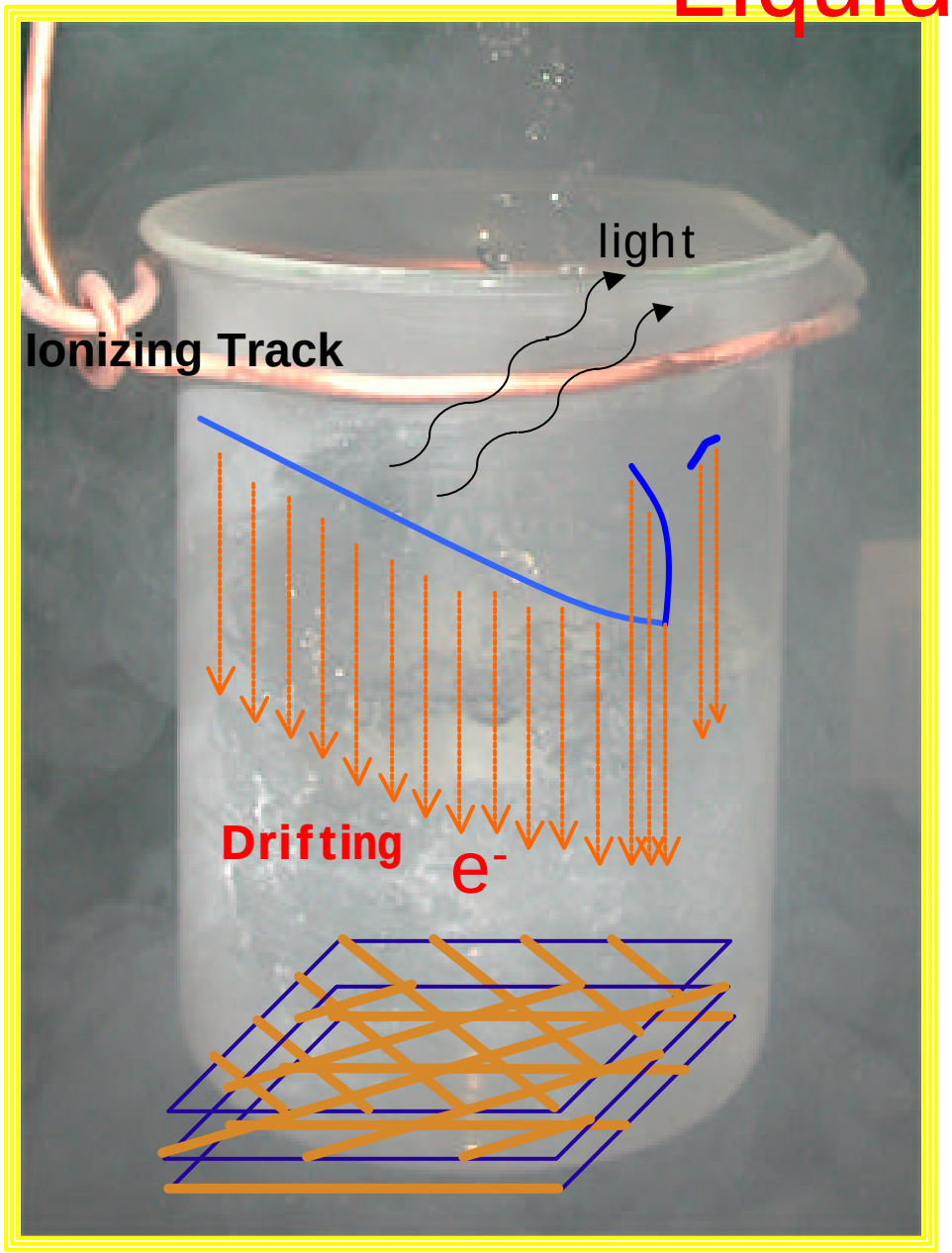

Density 1.4 g/cm³
Radiation length 14 cm
Interaction length 80 cm
dE/dx(mip) = 2.1 MeV/cm
T=88K @ 1 bar

✓About 12000 electron-ion pairs per mm of mip track are produced. About 40% recombine in our nominal drift field. When the left-over charges drift, they induce a signal on the wires

✓Since the mobility of electrons is much higher than that of ions, only electrons contribute to the observed signal.

✓Electrons can drift over macroscopic distances if argon pure

✓Multiple non-destructing readout wire plans can be assembled for multi-views

Half module of ICARUS

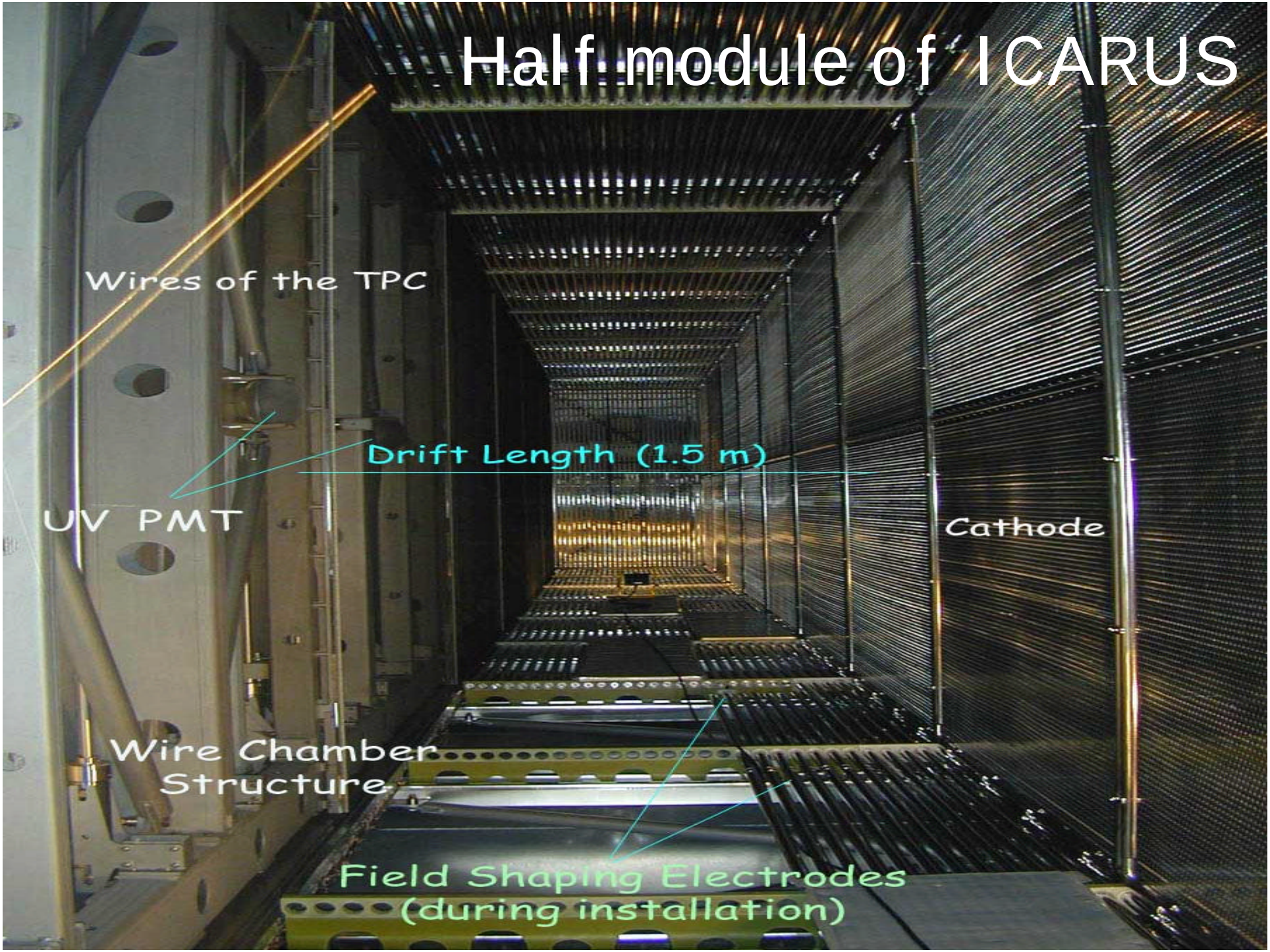

Raw Data to Reconstructed Event

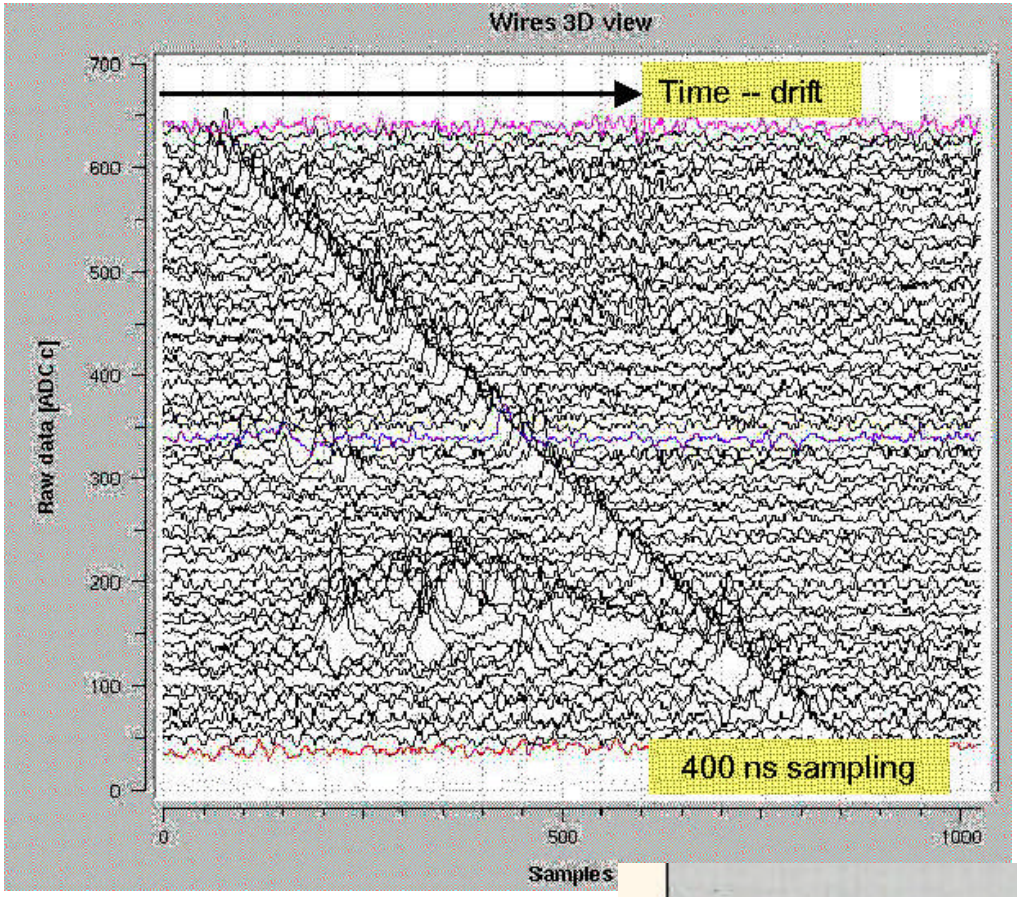

Because electrons can drift a long time (>1m!) in very pure liquid argon, this can be used to create an "electronic bubble chamber"

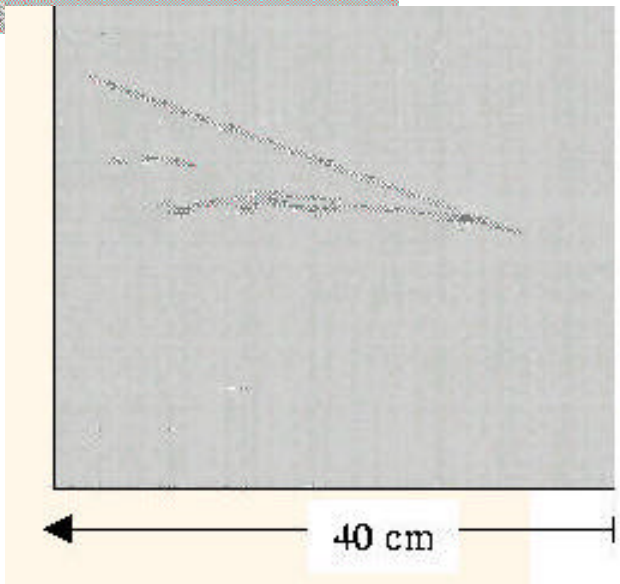

3D reconstruction

- The 3D reconstruction is based on the fact that the drift time coordinate (y-coordinate) is shared among all three views.
- The matching between the views is redundantly done at the “hit”-level

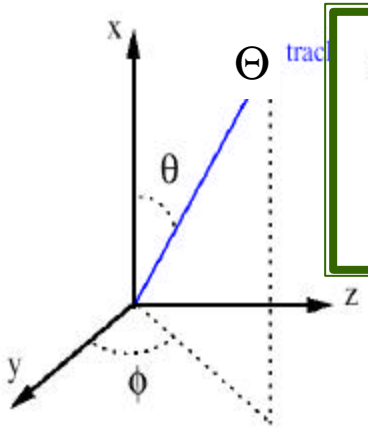

$$x_{1,2} = \frac{p}{2\cos\theta}(w_1 - w_2 + w_0)$$
$$x_3 = p\,w_3$$
$$y = \frac{s\,v}{f}$$

$$z_{1,2} = \frac{p}{2\sin\theta}(w_1 + w_2 - w_0)$$
$$z_{2,3} = \frac{p}{\tan\theta}\left(w_3 + \frac{w_2 - w_0}{\cos\theta}\right)$$
$$z_{1,3} = \frac{p}{\tan\theta}\left(\frac{w_1}{\cos\theta} - w_3\right)$$

p = 2.99 mm
θ = 60º
ω_0 = 528
f = 2.5 MHz

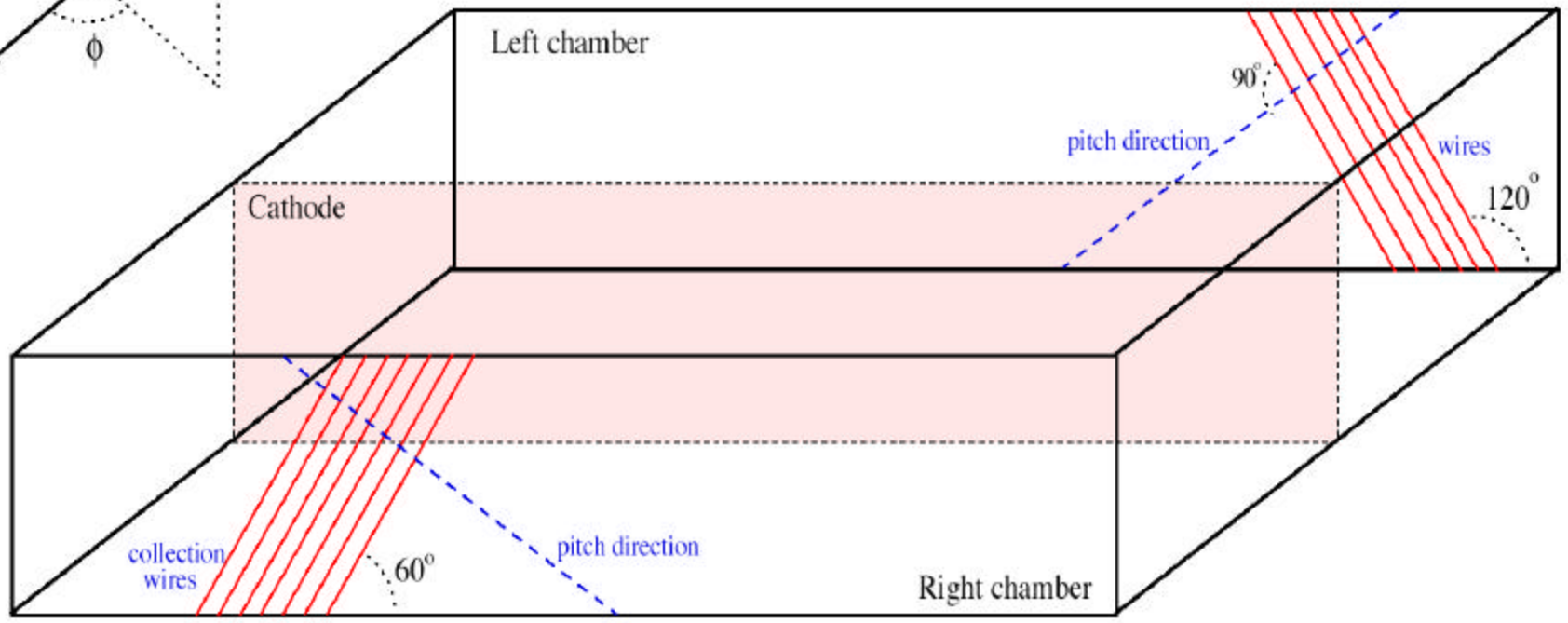

dE/dx in materials

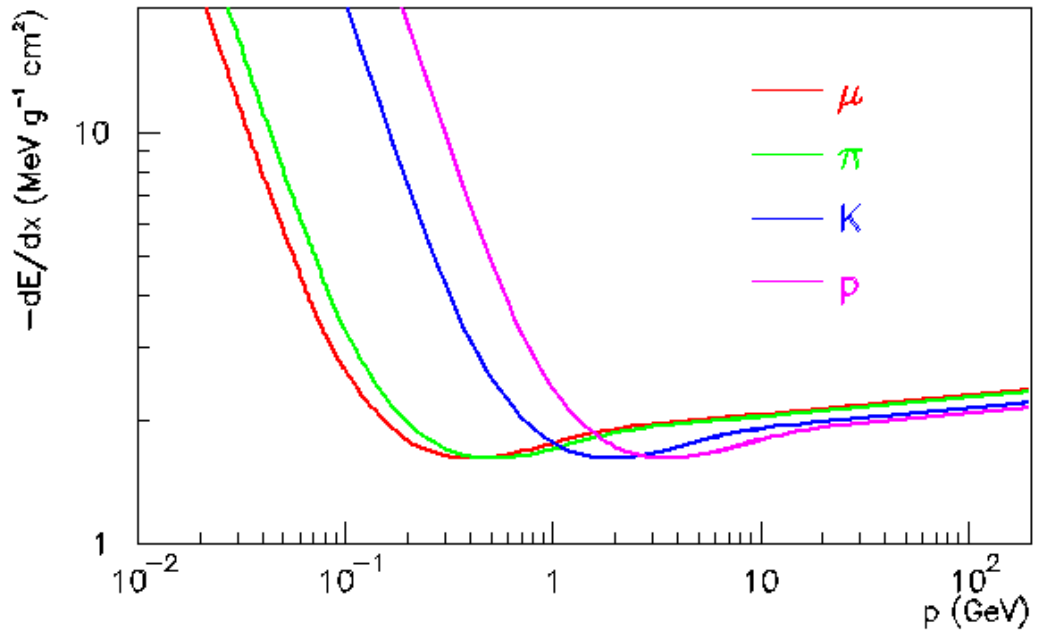

- Bethe-Block Equation
- x in units of g/cm^2
- Energy Loss Only f(β)
- Can be used for Particle ID in range of momentum

$$\frac{dE}{dx} \propto z^2 \frac{Z}{A} \frac{1}{b^2} \left[\frac{1}{2} \frac{\ln 2m_e c^2 b^2 g^2 T_{\max}}{I^2} - b^2 - \frac{d}{2} \right]$$

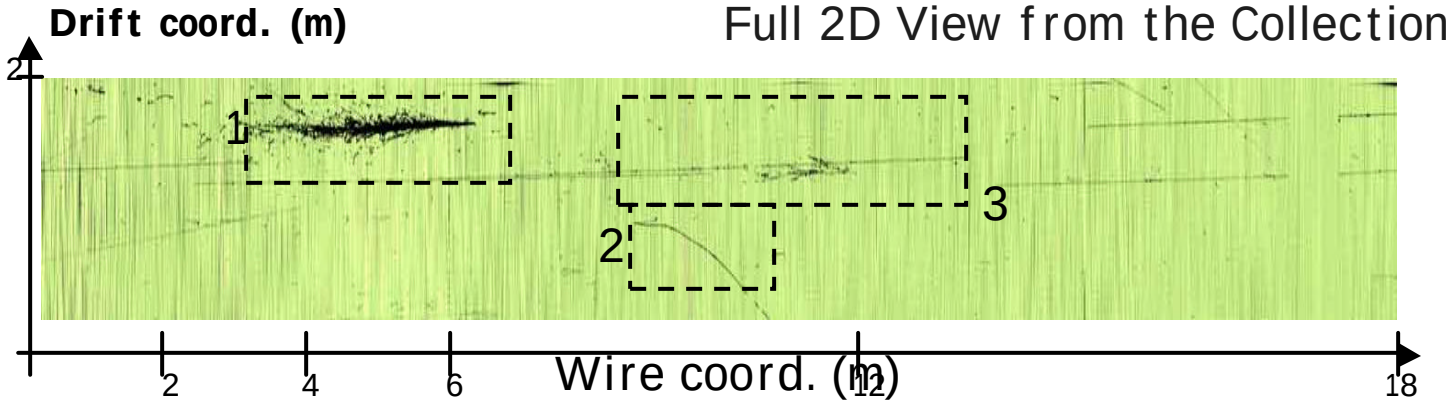

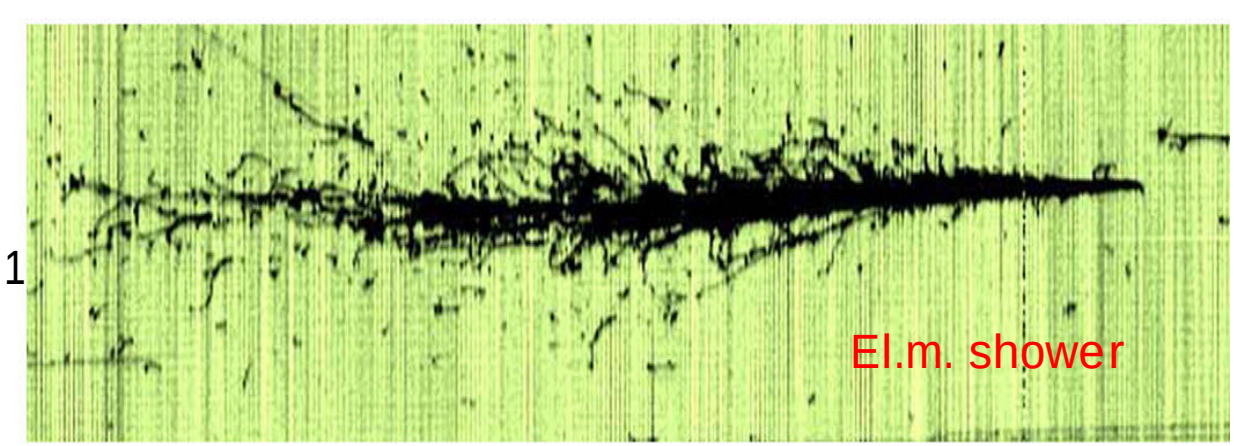

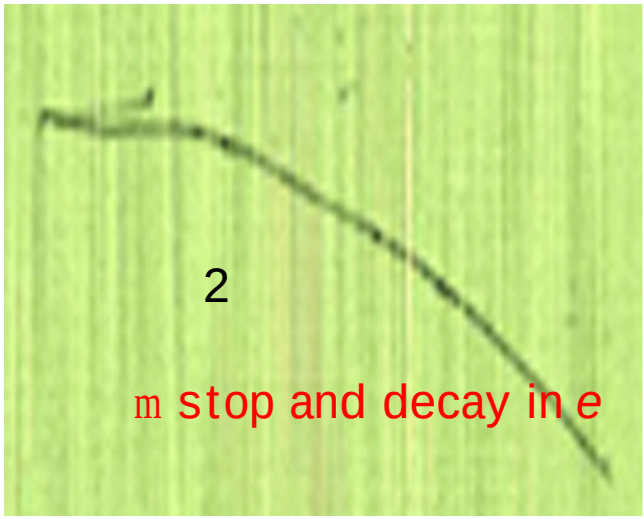

Zoom views

Detail of a long (14 m) m track with d-ray spots

T600 test @ Pv: Run 201 - Evt 12

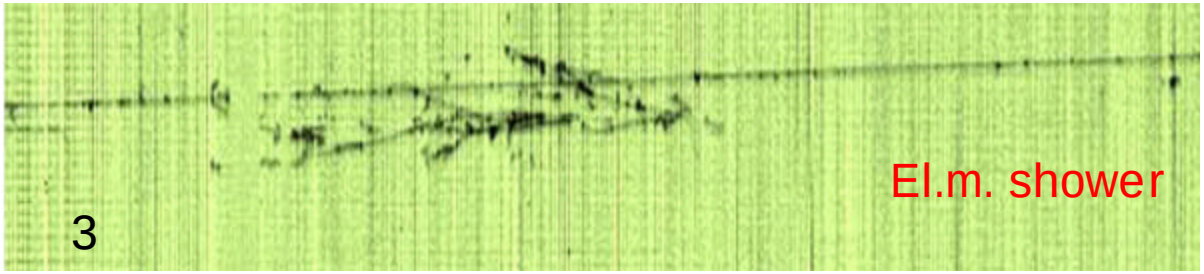

Events with hadrons

- Trk. 1 - m.i.p.
  E_{dep}= 31 MeV
  L_{trk}~ 18 cm
- Trk. 2 – heavily i.p.
  E_{dep}= 191 MeV
  L_{trk}~ 53 cm
- Trk. 3 - m.i.p.
  E_{dep}= 105 MeV
  L_{trk}~ 60 cm
- Trk. 4 - heavily i.p.
  E_{dep}= 42 MeV
  L_{trk}~ 16 cm
- Trk. 5 - m.i.p.
  E_{dep}= 111 MeV
  L_{trk}~ 60 cm

2D view

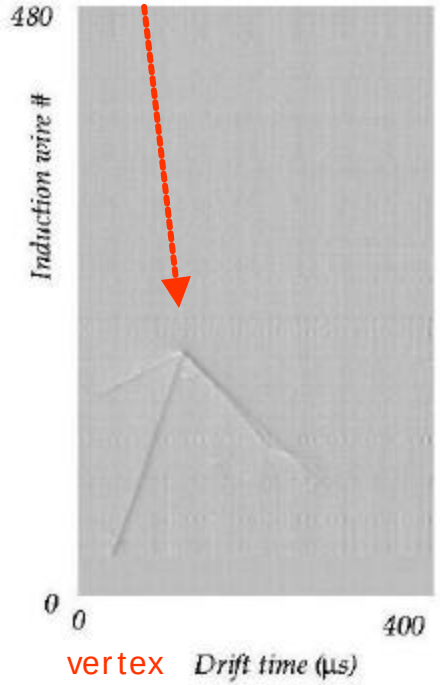

2D view

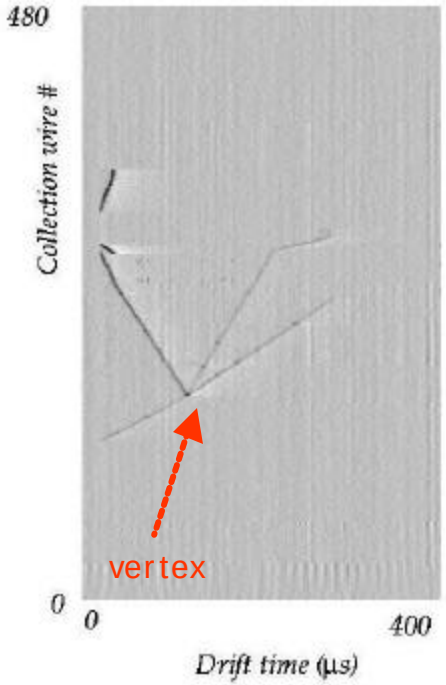

Preliminary analysis

Fully reconstructed stopping muon event

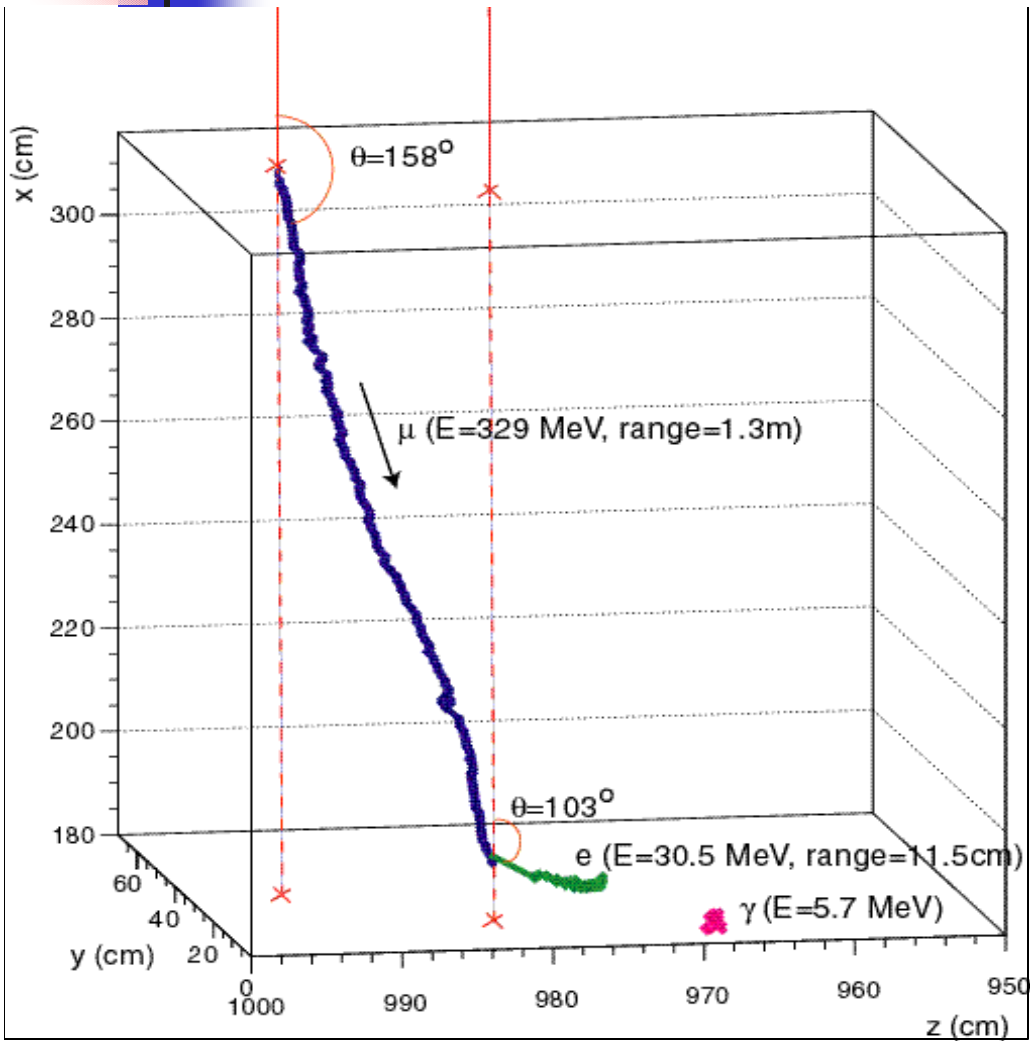

Y-Z plane projection (longitudinal cut)

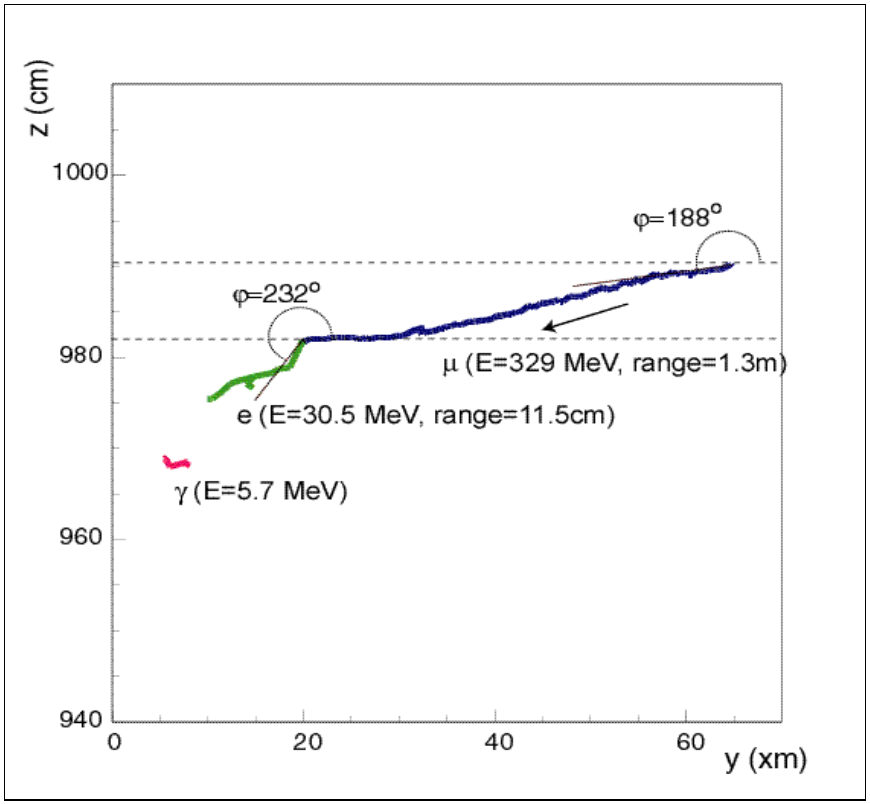

Muon momentum reconstruction by multiple scattering

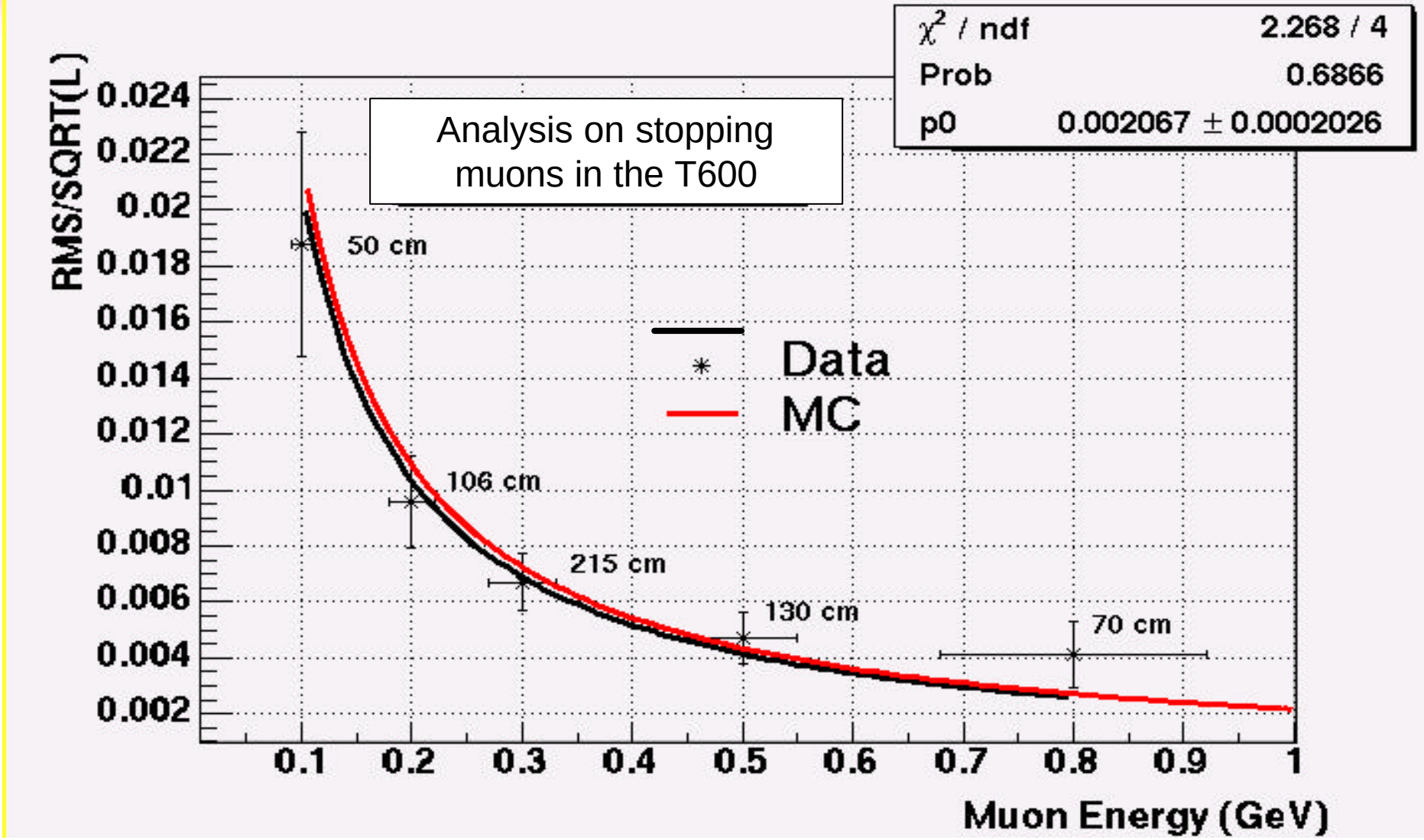

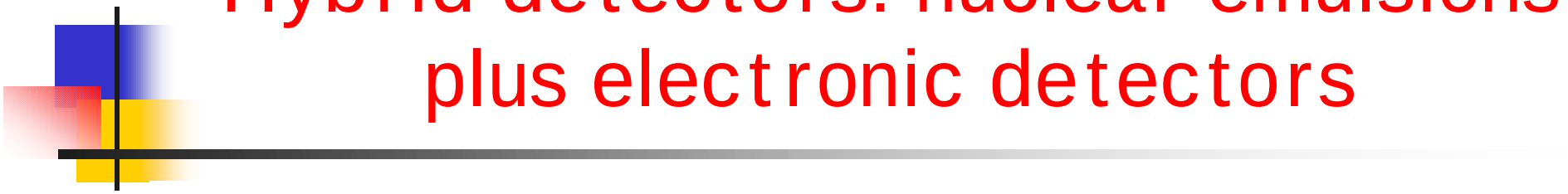

Hybrid detectors: nuclear emulsions plus electronic detectors

The CHORUS/DONUT/OPERA experiments

CHORUS detector

E.Eskut et al., Nucl. Instr. Meth. A 401 (1997) 7-44

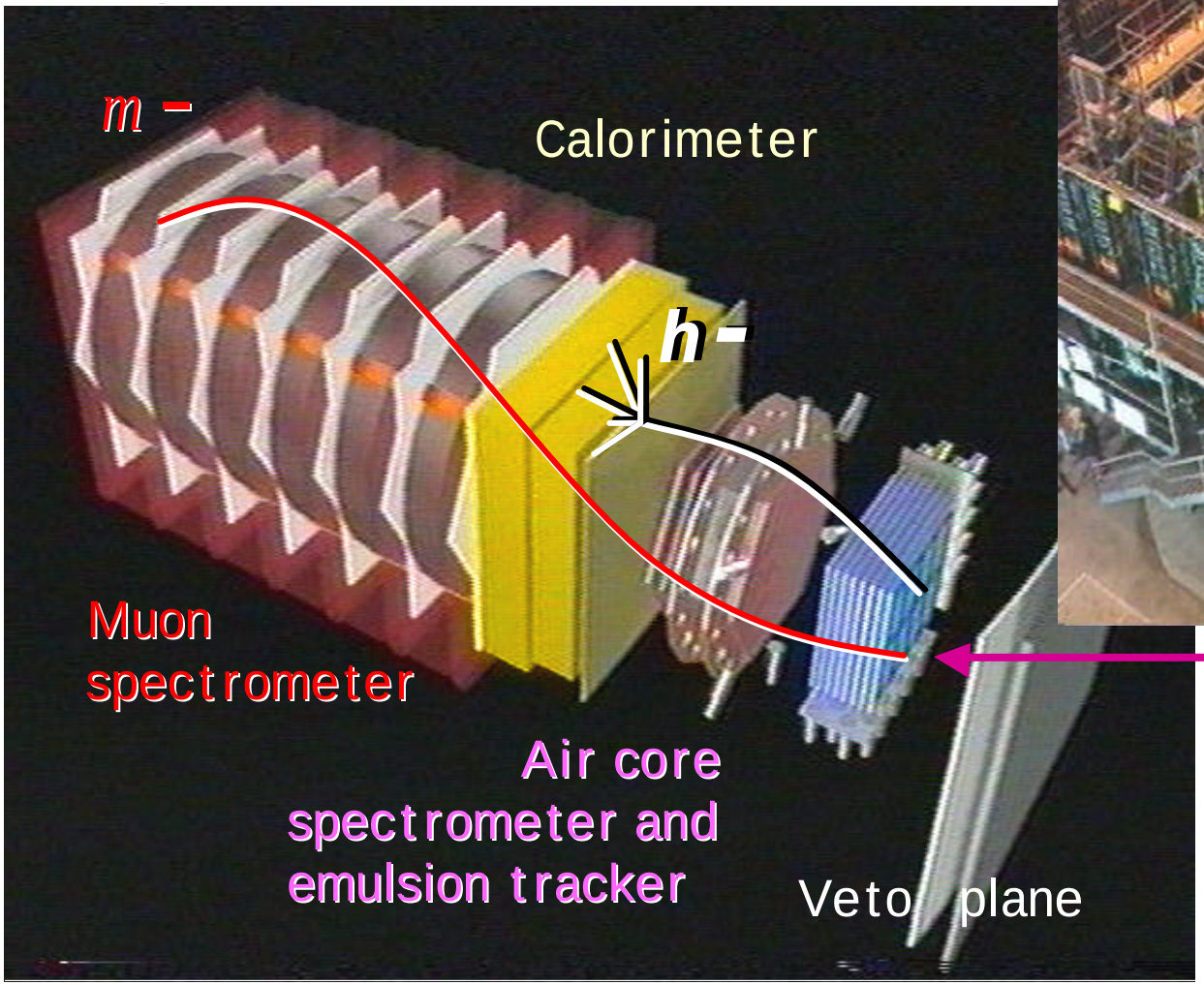

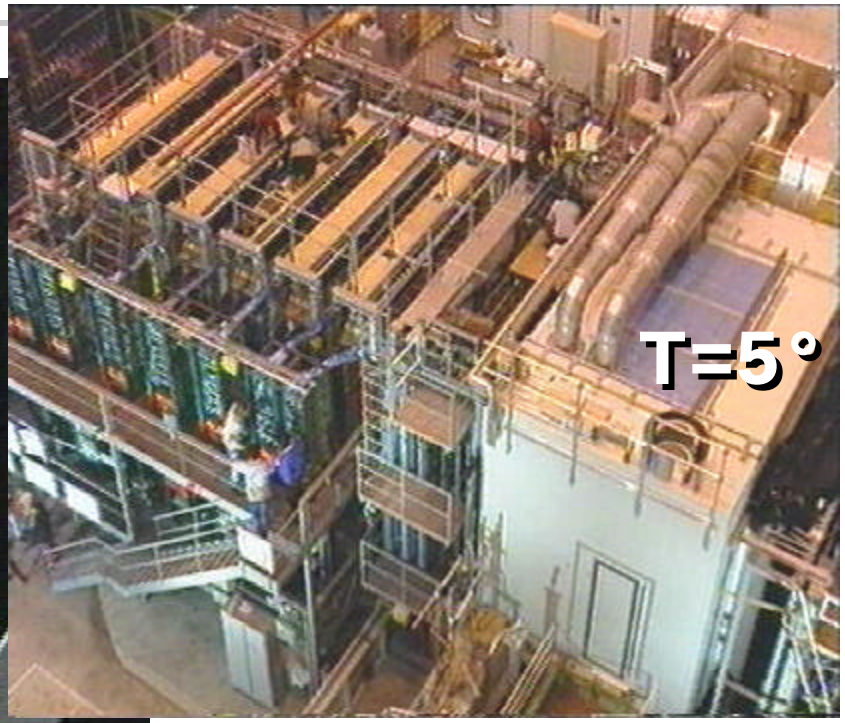

770 kg emulsion target and scintillating fibre tracker

Moving the focal plane down to the ν interaction vertex

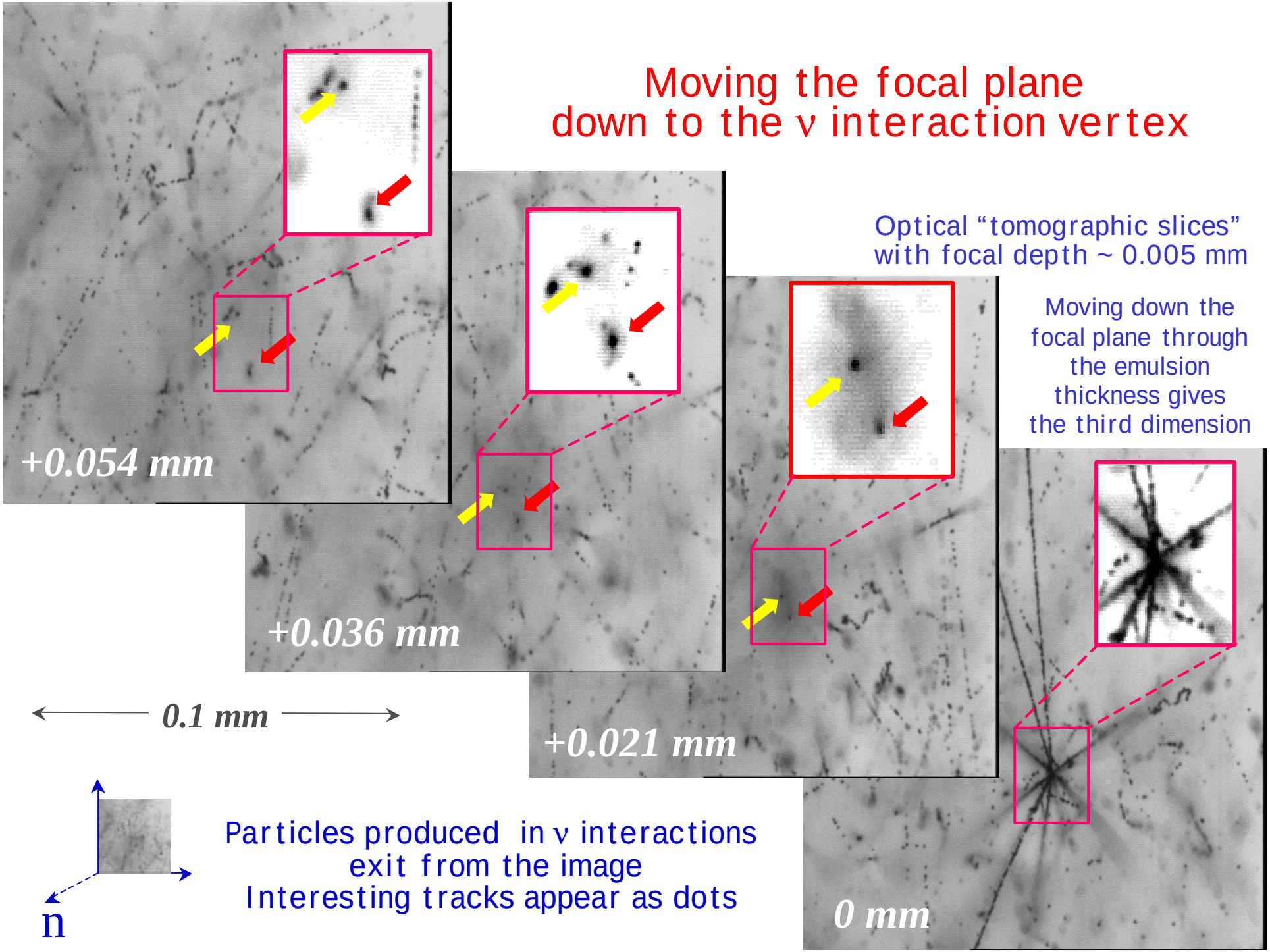

Optical "tomographic slices" with focal depth ~ 0.005 mm

Moving down the focal plane through the emulsion thickness gives the third dimension

Particles produced in ν interactions exit from the image
Interesting tracks appear as dots

Automatic Scanning

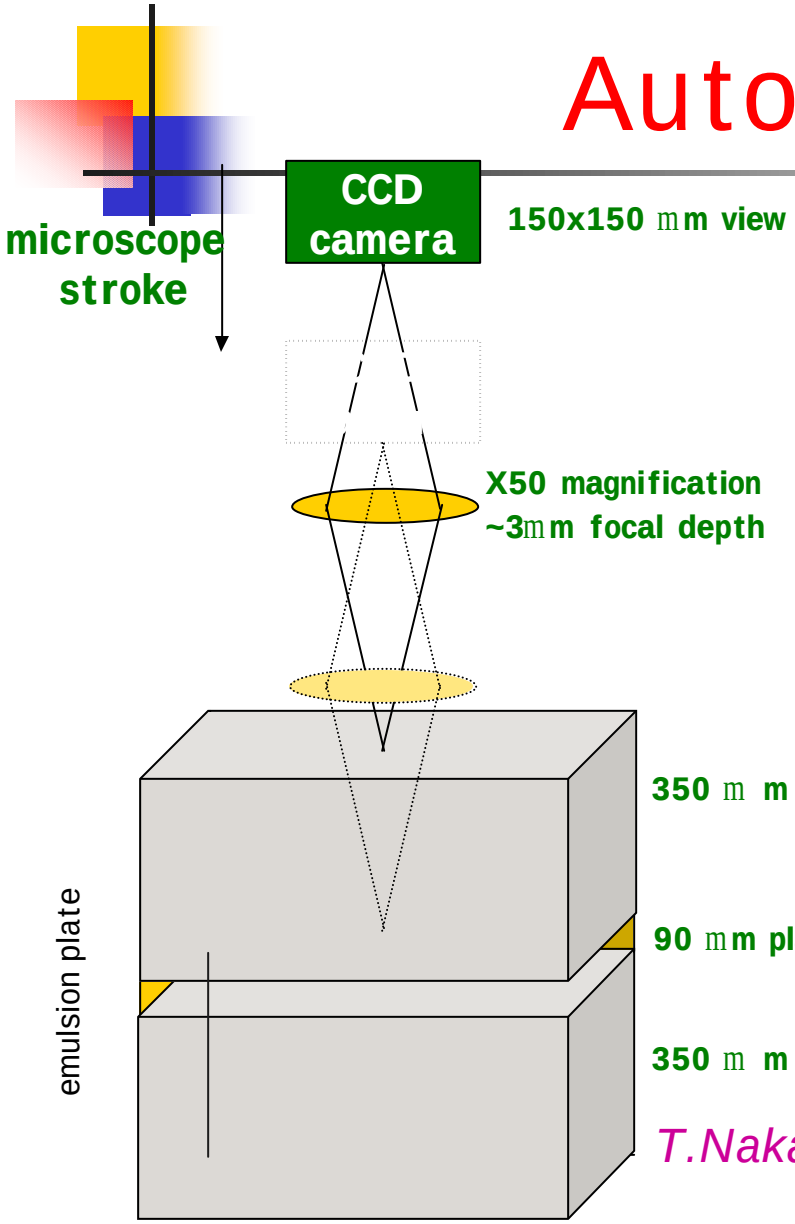

tomographic image

Tracks reconstructed by a hardware video processor
frame
to frame emulsion grains coincidence

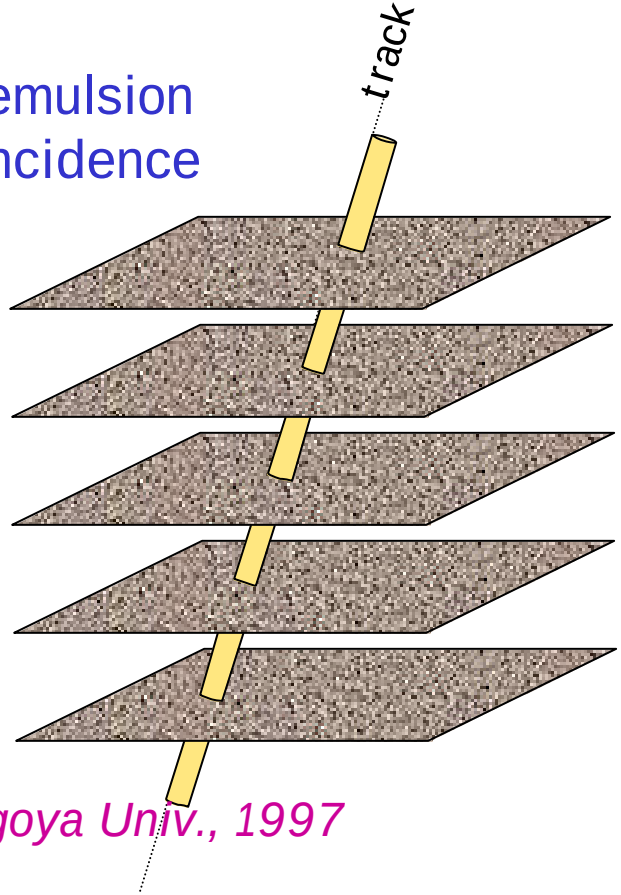

T.Nakano, Ph.D. Thesis, Nagoya Univ., 1997

Netscan analysis in CHORUS

- All track segments ($\theta < 0.4$ rad) in
- Fiducial volume: 1.5 x 1.5 mm^2 x 8 plates
- Offline analysis of emulsion data

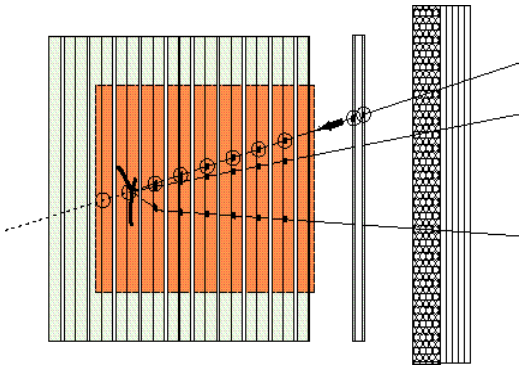

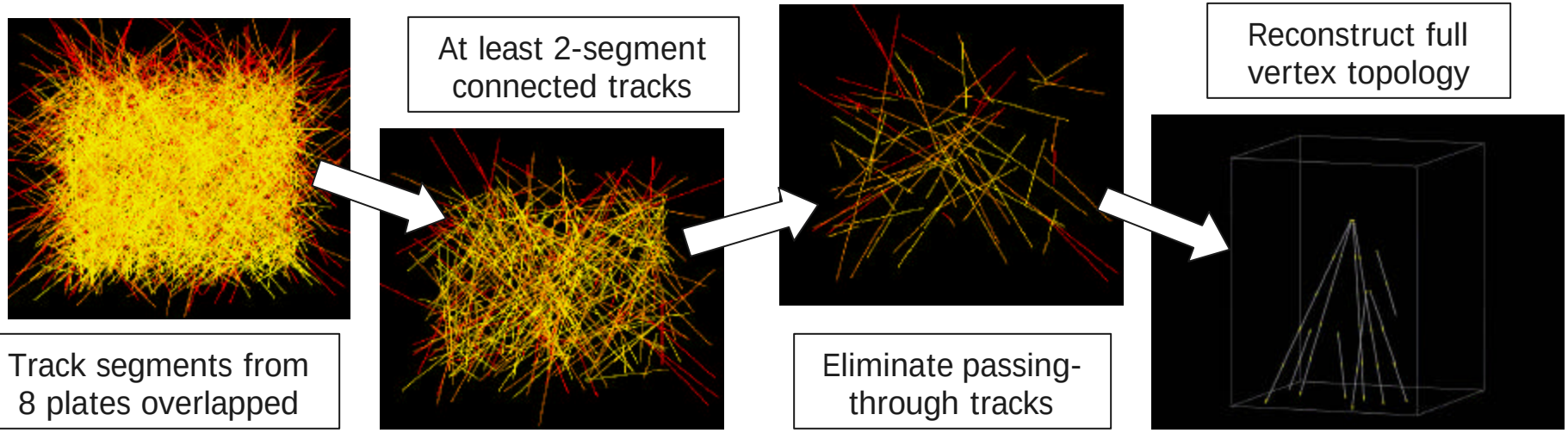

The Emulsion Cloud Chamber (ECC)

- Emulsions for tracking, passive material as target → < mm space res. → mass
  - Established technique
    - charmed "X-particle" first observed in cosmic rays (1971)
    - DONUT/FNAL beam-dump experiment: ν_τ observed (2000)

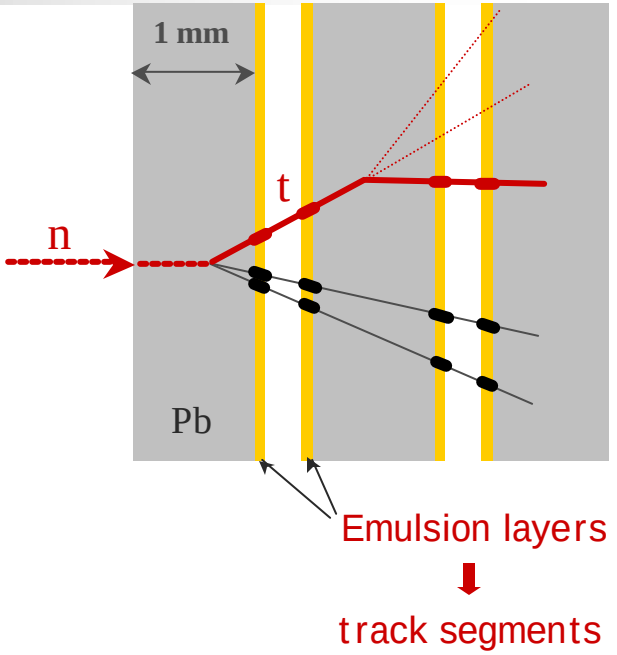

$\Delta m^2 = O(10^{-3}\ eV^2) \Rightarrow M_{target} \sim 2$ kton

modular structure ("bricks"): basic performance is preserved
large detector → sensitivity, complexity
required: "industrial" emulsions, fast automatic scanning

Experience with emulsions and/or ν_τ searches : E531, CHORUS, NOMAD and DONUT

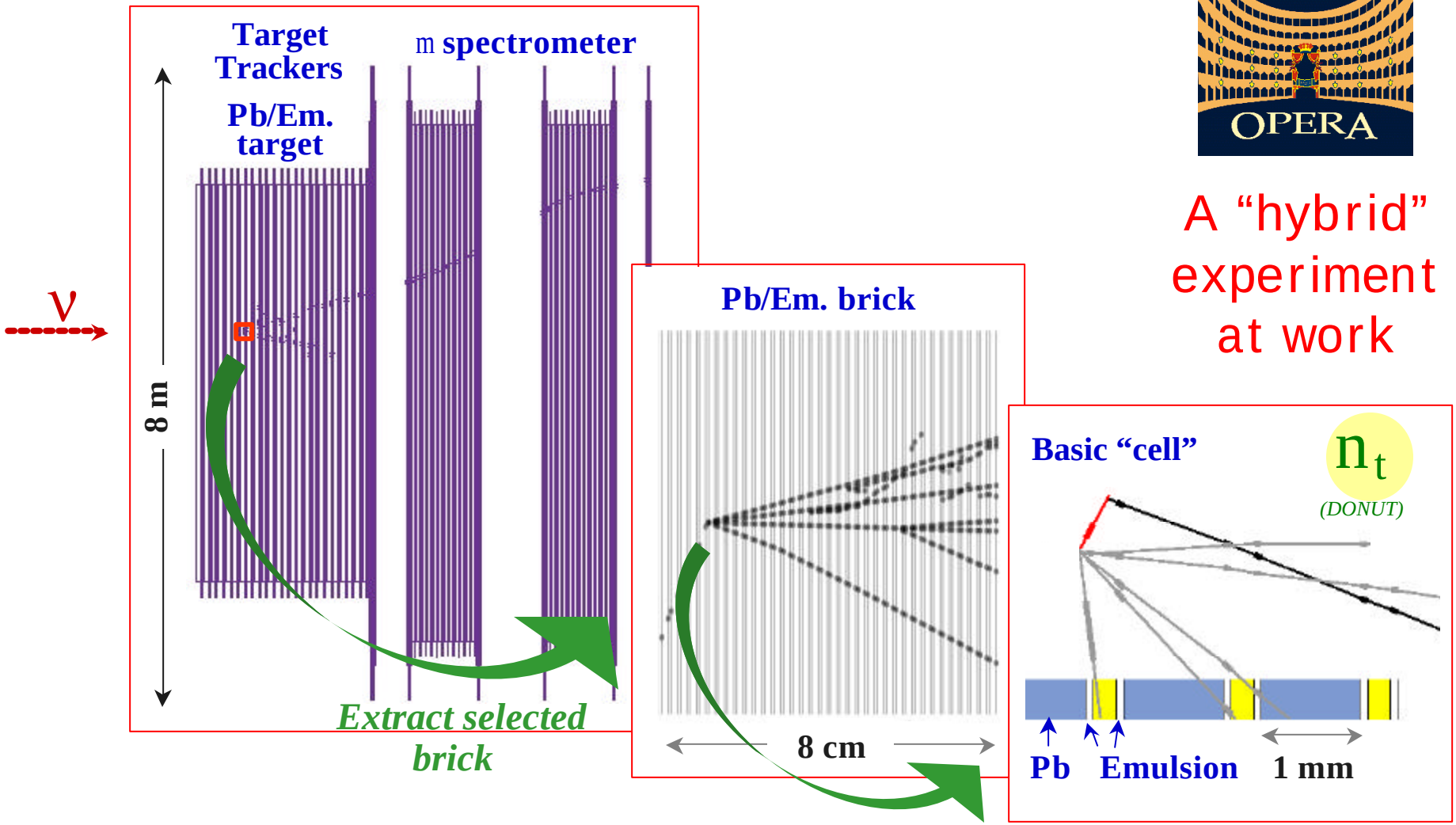

A "hybrid" experiment at work

Electronic detectors

→ select n interaction brick

→ m ID, charge and p

Emulsion analysis

® vertex search

→ decay search

→ e/g ID, kinematics

Intrinsic space resolution in tracking with emulsion

Cross sectional view of an emulsion layer

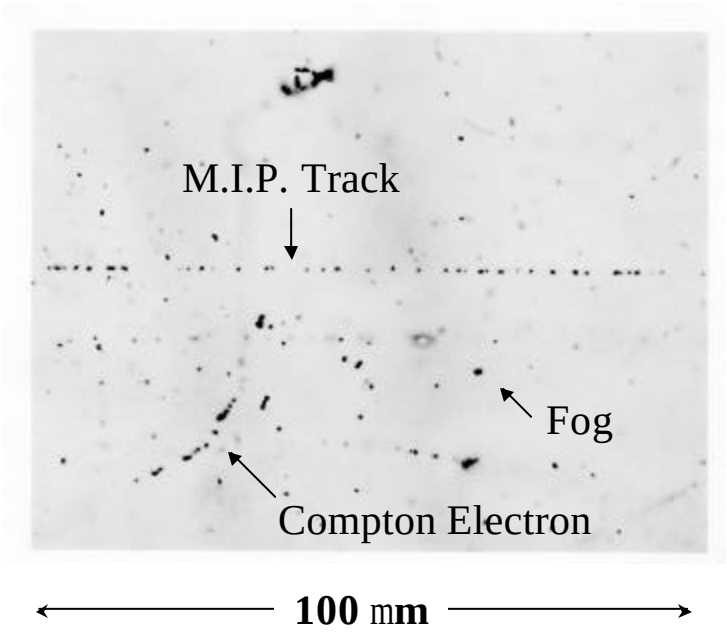

~ 30 grains / 100 mm
grain diameter ~ 0.6 mm

Ag grain after development

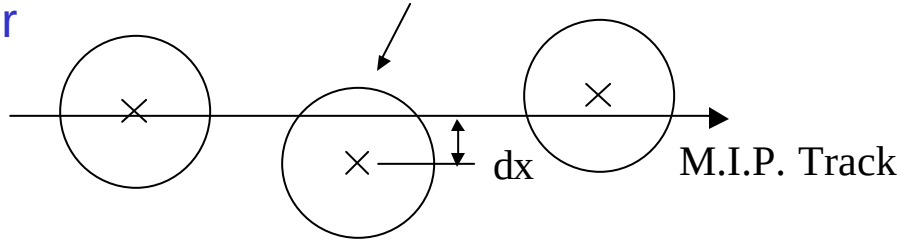

intrinsic tracking accuracy

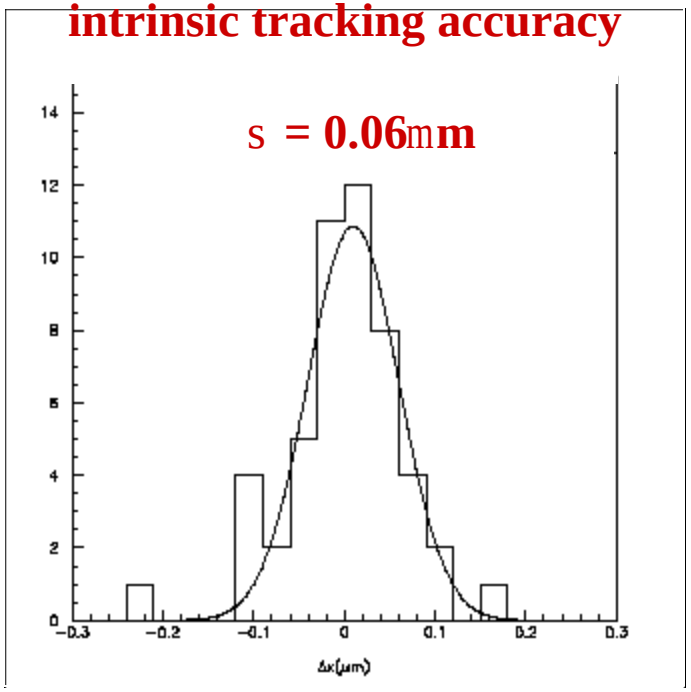

Angular resolution with Track Selector readout

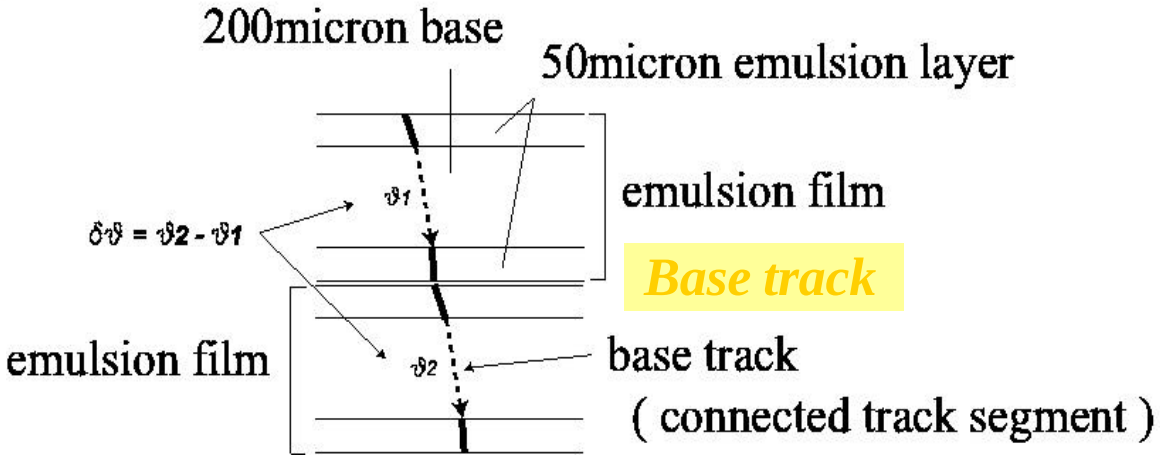

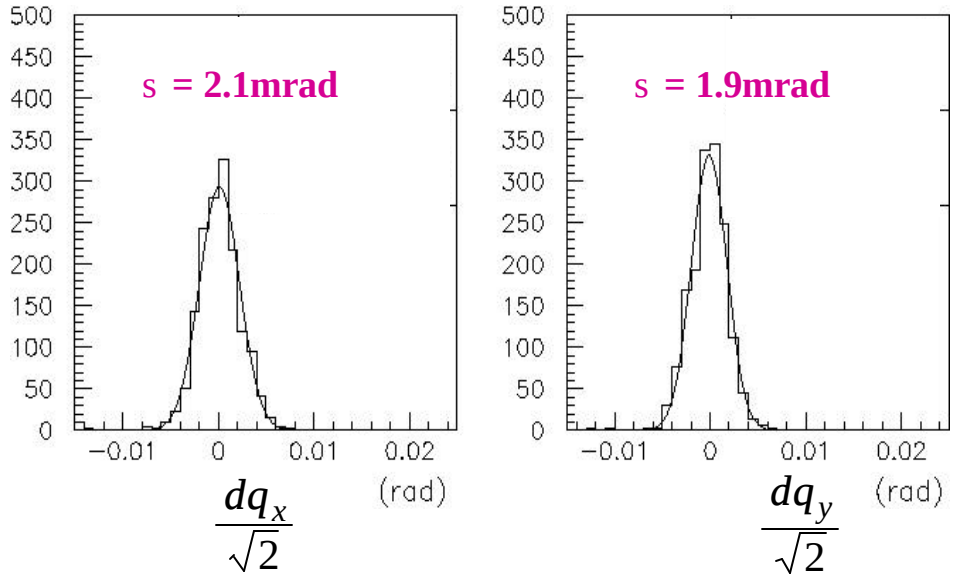

Base track resolution

(limited by digitisation error in image processing)

σ (angle) = 2.1 mrad

σ (position) = 0.21 μm

Precision measurements for small samples

resolution close to the intrinsic resolution

DONUT: $\tau \rightarrow e$ candidate

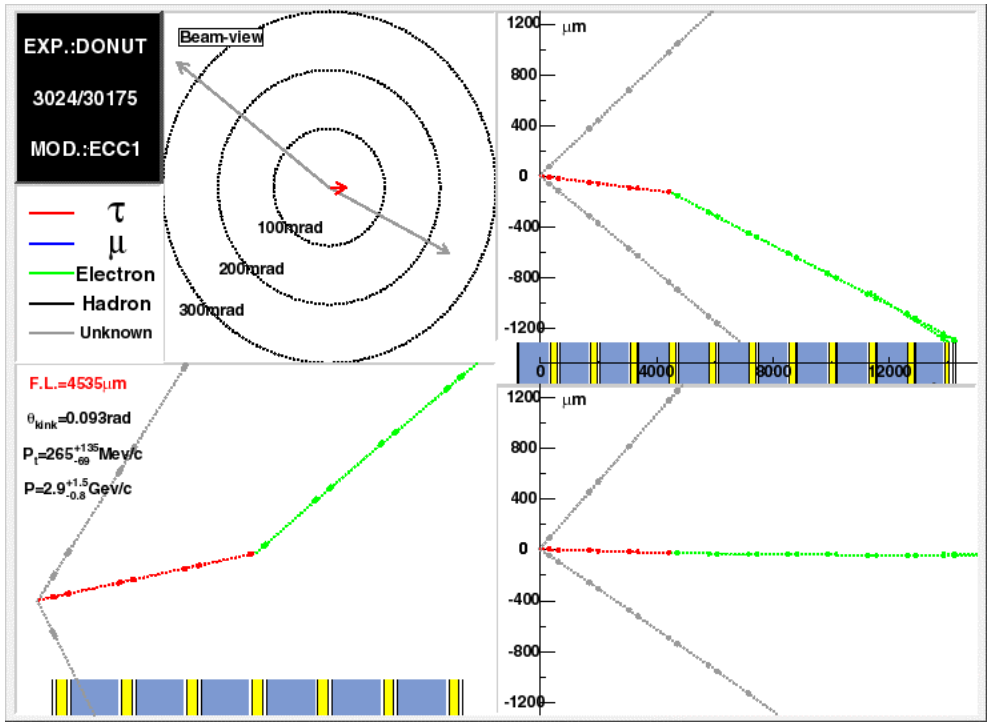

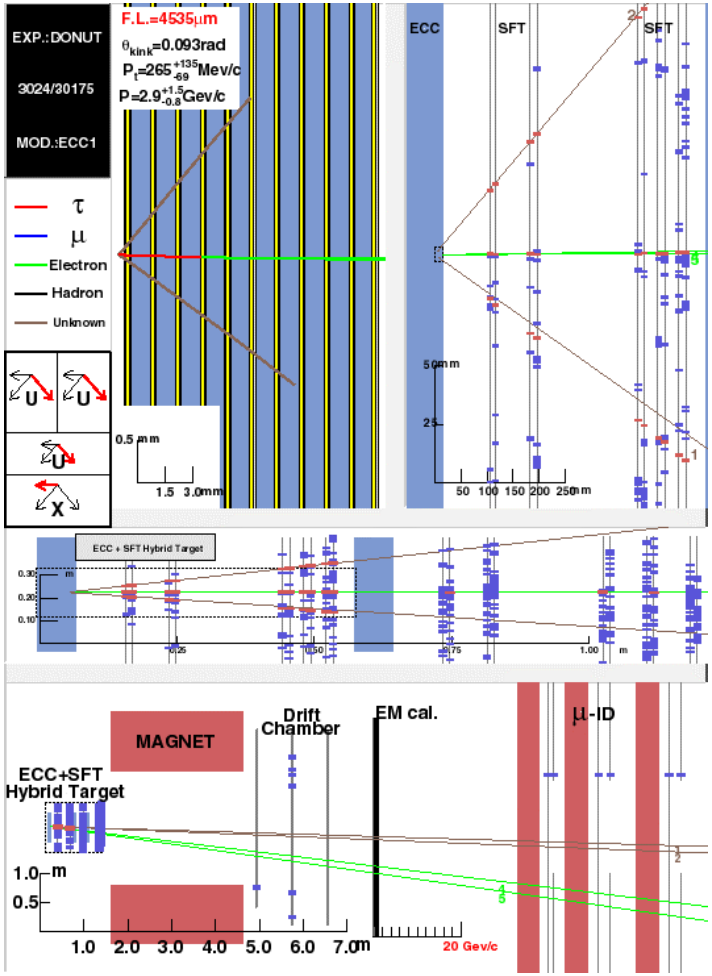

Momentum measurement from Multiple Coulomb Scattering

(allows additional b.g. rejection by kinematic criteria)

Angular method

{ Not relying on alignment of emulsion films
Relying on parallelism of Pb plates and emulsion films

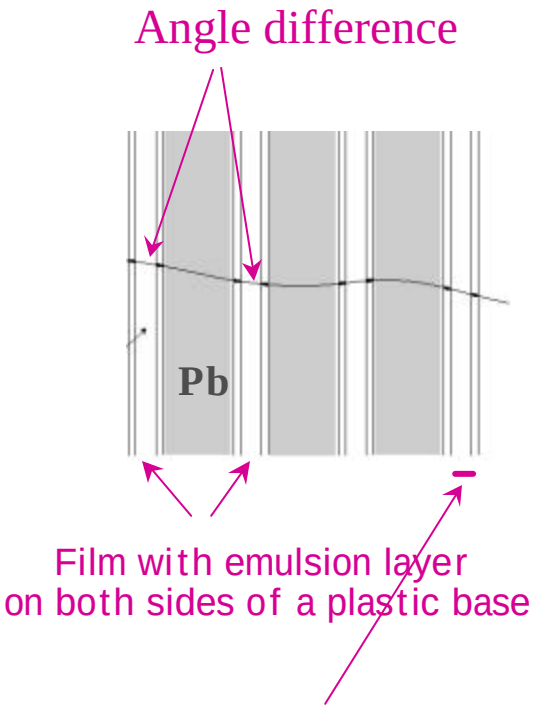

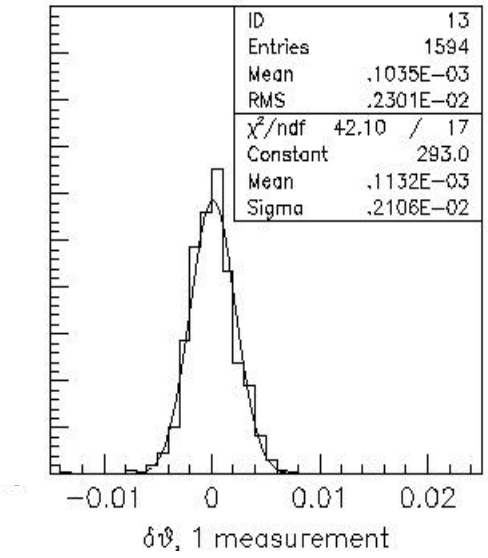

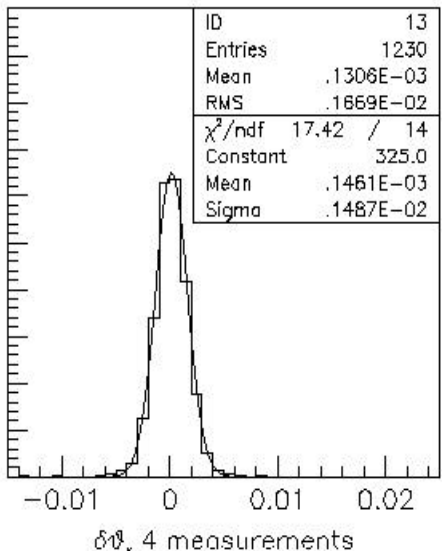

With intrinsic resolution 10.0 GeV/c

(max p measured with $\Delta p/p < 0.2$ after $5X_0$)

Global kinematics for $\tau \rightarrow h$

(for events with a τ decay candidate)

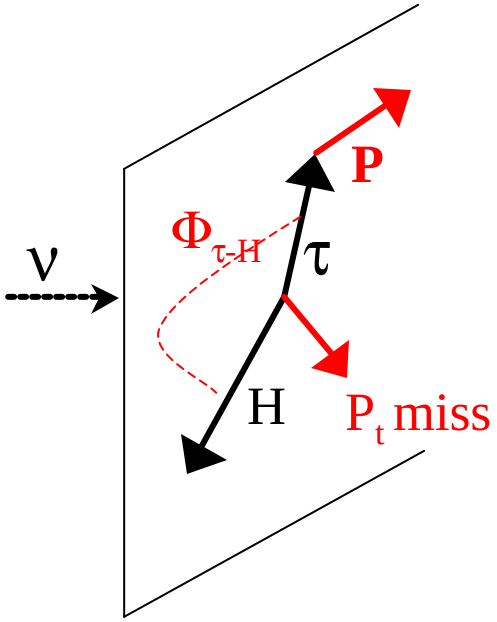

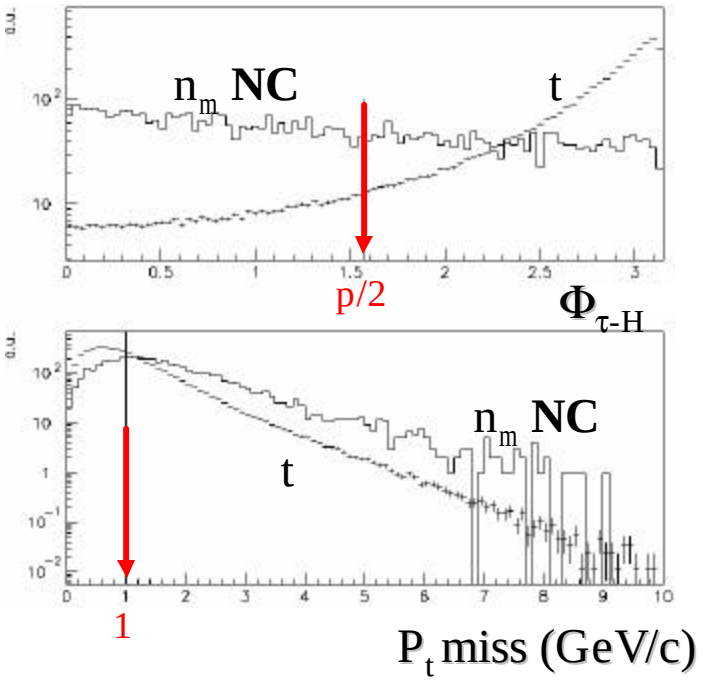

This is just an example: it works also (event better) for ν_eCC interactions

Electron identification and energy measurement (1)

- Electron identification close the Pb critical energy
- Performance estimated by reproducing the full chain:
  - Fuji-emulsions stored for about 2 months
  - Emulsion refreshing at the Nagoya University
  - Transportation of packed emulsions to CERN
  - Test exposure at the PS beam (mixture of e and π , C upstream of the ECC)
  - Emulsion developed soon after the beam exposure
  - Scanning and analysis

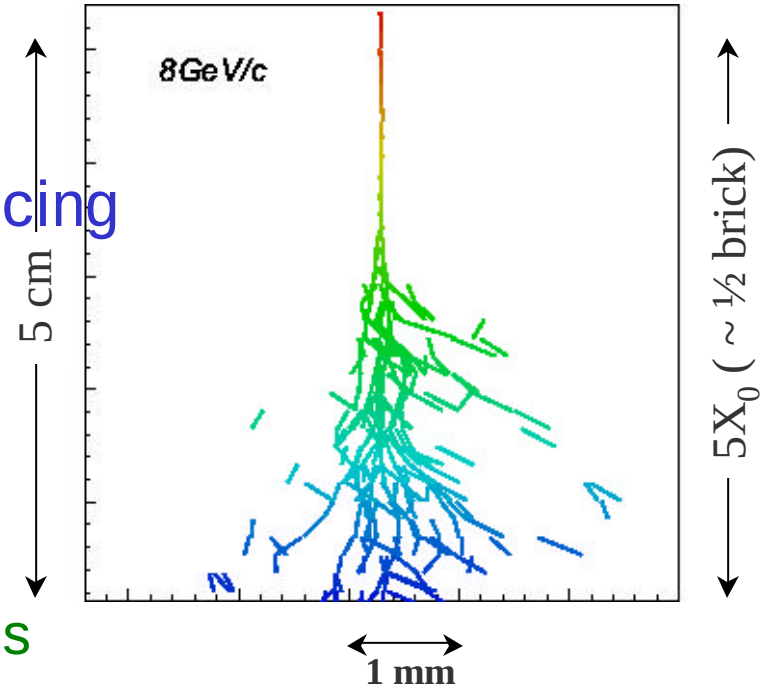

Electron identification and energy measurement (2)

Identification

- Method based on shower identification and on MCS of the track
- e/π ratio is measured with Cerenkov and ECC (good agreement)
  - ECC 1.42±0.17 Cerenkov 1.46±0.11 at 2GeV
  - ECC 0.41±0.05 Cerenkov 0.32±0.03 at 4GeV
- ε_e = 88 (91) % at 2 (4) GeV (in agreement with MC)

Energy

- Measured by counting the number of track segments into a cone along the electron track
- Multiple Coulomb Scattering before showering
- Resolution ~ 20%

γ/π^0 reconstruction

- γs assigned to primary or to decay vertex depending on Impact Parameter

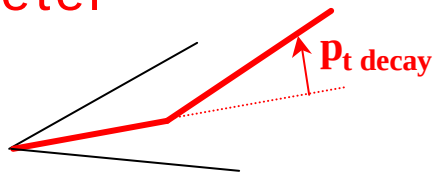

- γs assigned to the decay vertex
  - improved $p_{t\ decay}$ resolution (charged+neutral)
  - looser cut and higher efficiency
- γs assigned to the primary vertex
  - improved missing p_t resolution

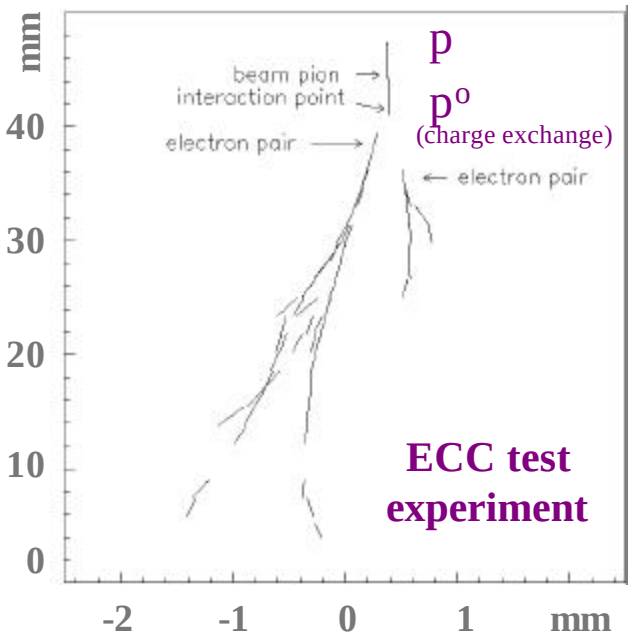

π^0 mass reconstruction also possible (Δm ~30%), but not used in the following analysis

Pointing accuracy to the vertex of e-pairs from γ conversions

Studied in CHORUS and DONUT by NetScan

(½ X_0 depth in ECC)

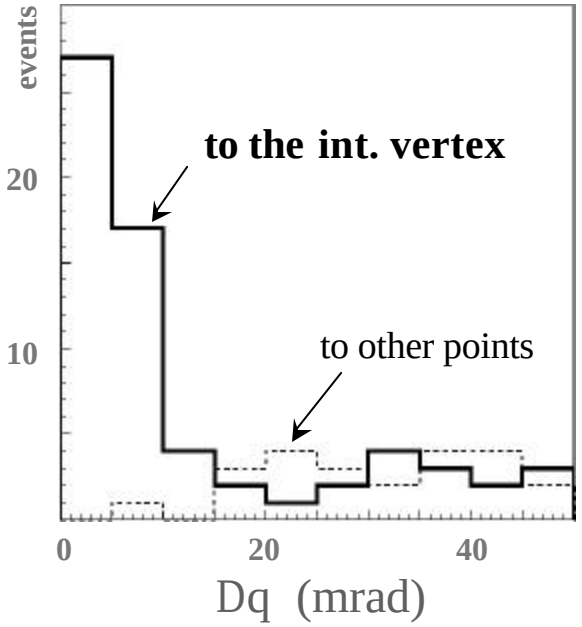

CHORUS

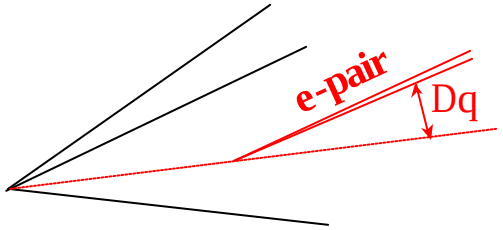

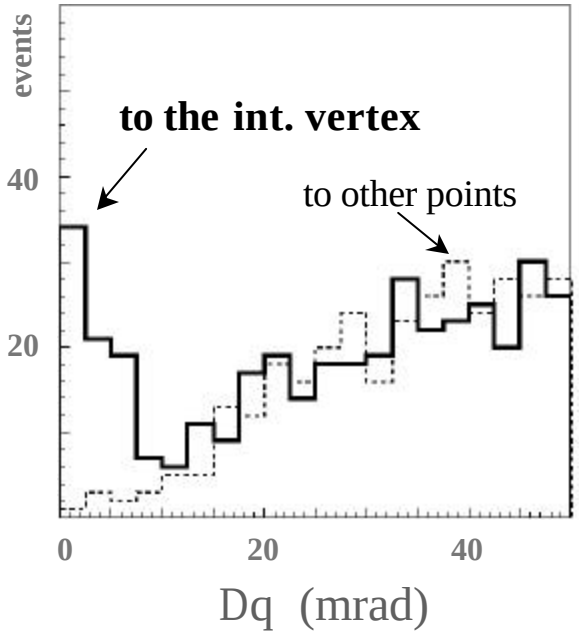

DONUT

(ECC Fe-emulsion)

Important for increasing the sensitivity to $t \to h\, n p^0$

Averaged dE/dX (under study)

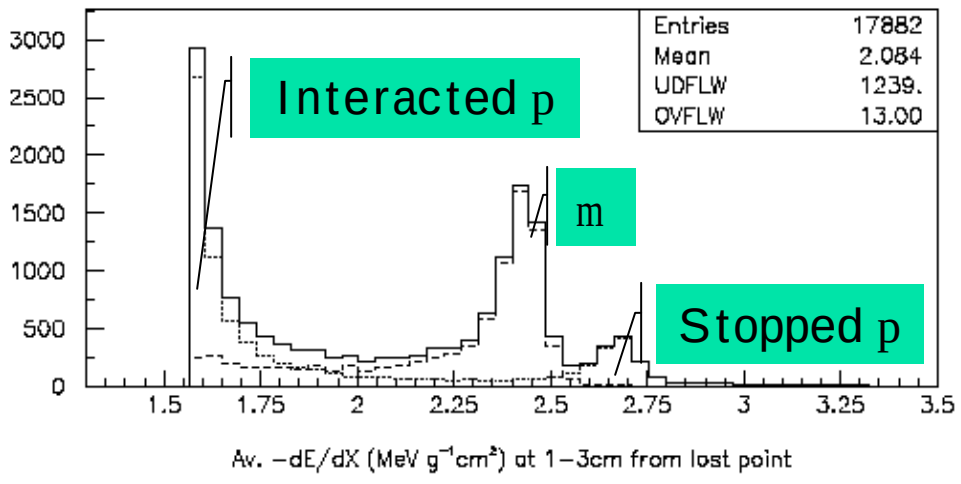

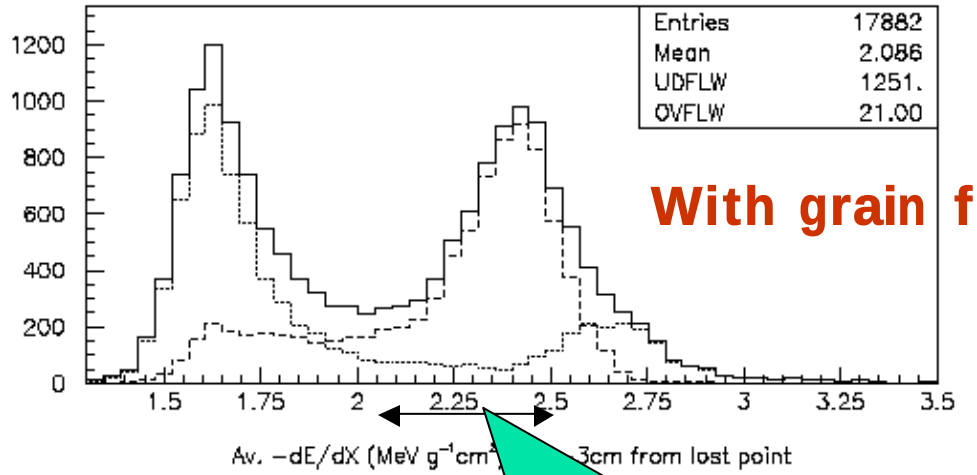

With grain fluctuation

Identified as m

dE/dX calibration and particle ID

In general, we can measure dE/dX and pβ in ECC, this information gives particle ID.

- Half brick ECC were exposed by KEK π2 secondary beam, mixture of pion and proton.
- Beam momentum **1.2**, 1.0, 0.8 and 0.6 GeV/c.
- First look for 1.2 GeV/c has done.
  - For pion pβ=1.188GeV/c
  - For proton pβ=0.948GeV/c

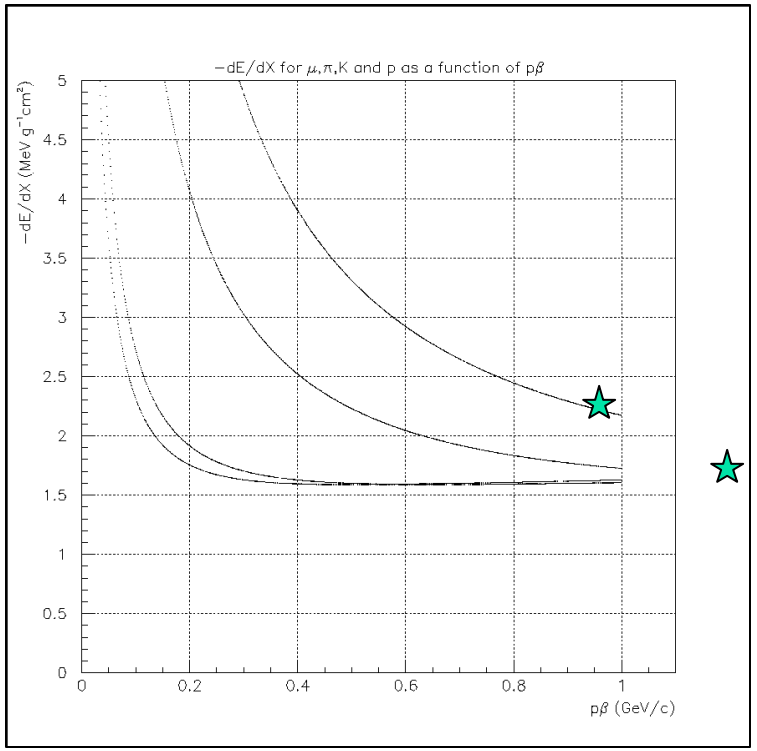

dE/dX measurement

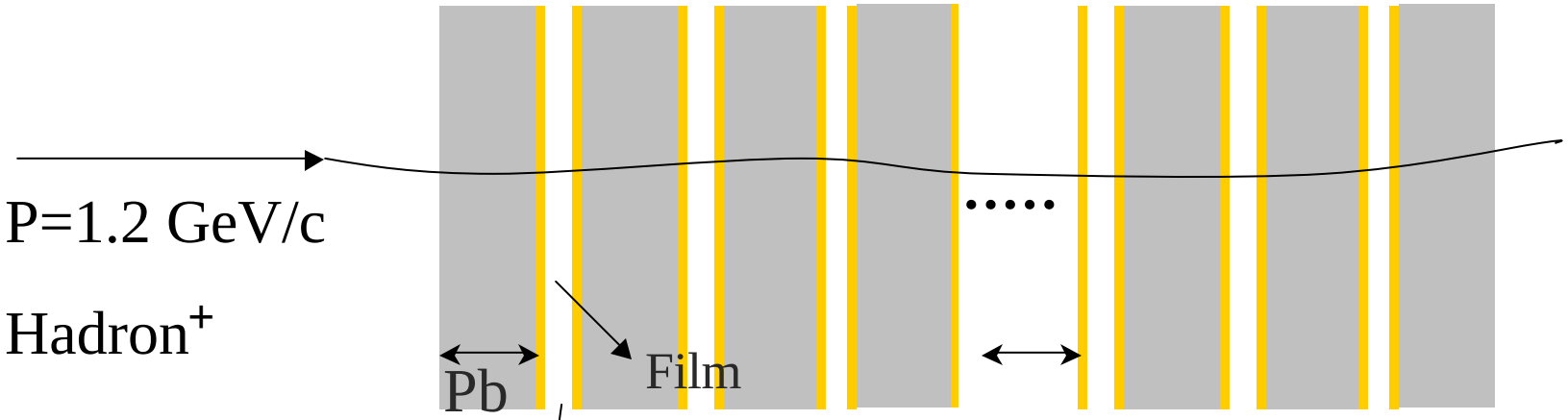

dE/dX = β measurement

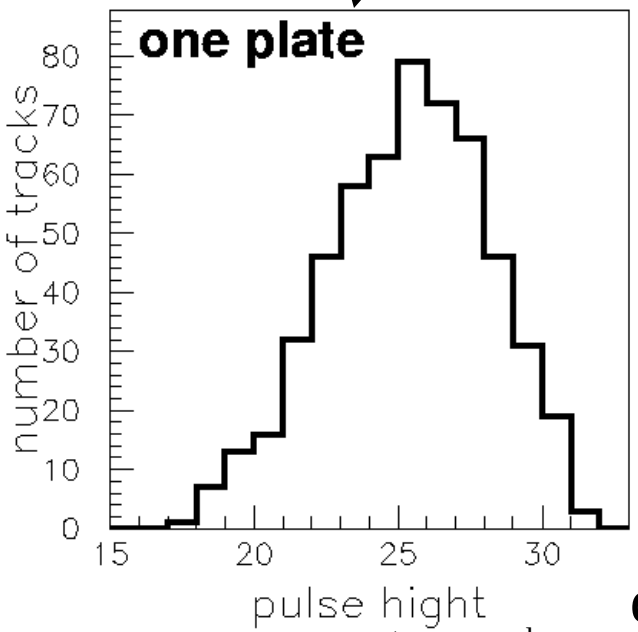

PH sum of 1st and 2nd layer

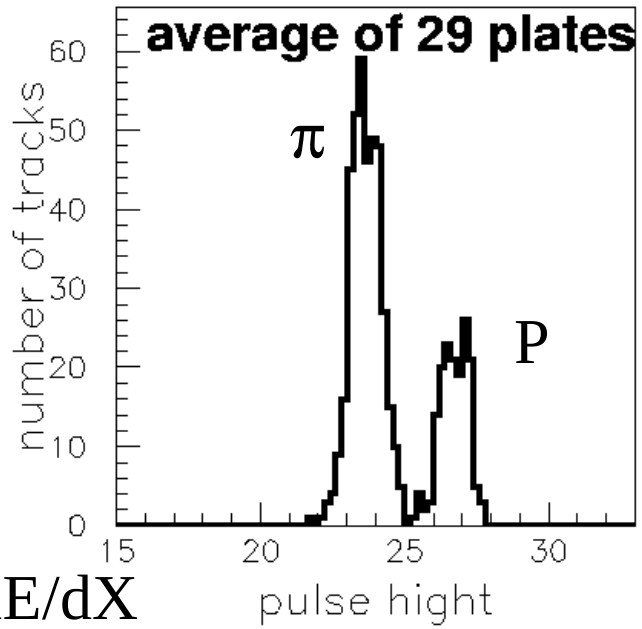

Av_{PH} : averaged over 58 layer

dE/dX

Momentum measurement

pβ measurement using Multiple Scattering

Low dE/dX

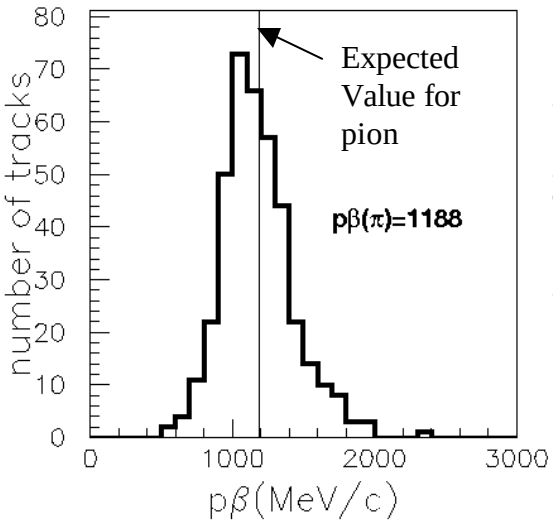

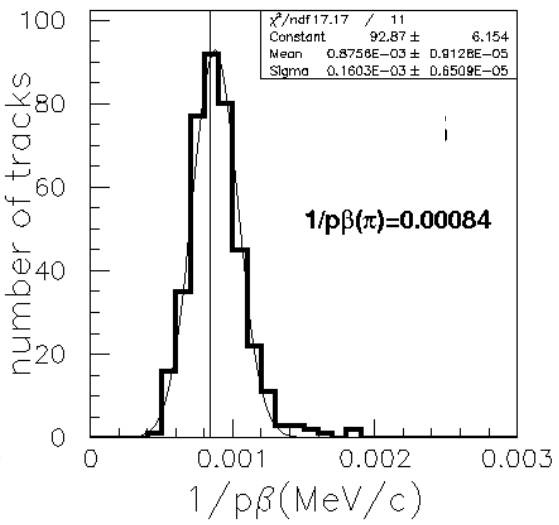

Consistent with Pion

Resolution $\sigma_{p\beta}$ ~16%

Higher dE/dX

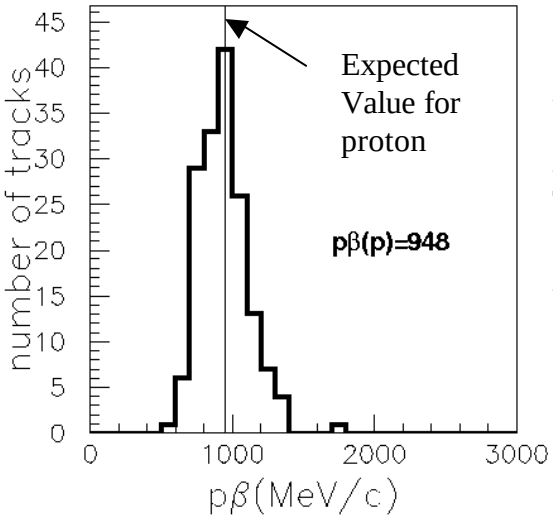

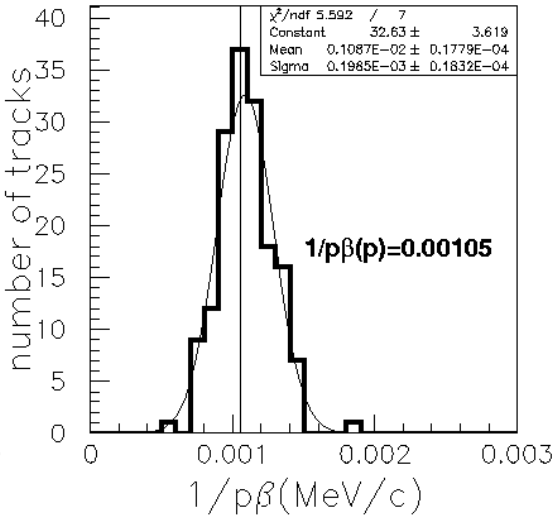

Consistent with Proton

Summary of the event reconstruction with OPERA

- High precision tracking ($\delta x < 1\mu m$ $\delta\theta < 1 mrad$)
  - Kink decay topology
  - Electron and γ/π^0 identification
- Energy measurement
  - Multiple Coulomb Scattering
  - Track counting (calorimetric measurement)
- Ionization (dE/dx measurement)
  - π/μ separation
  - e/π^0 separation

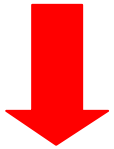

Topological and kinematical analysis event by event

Magnetized iron calorimeter

NuTeV and Minos exps

Charged-current interaction in the NuTeV detector

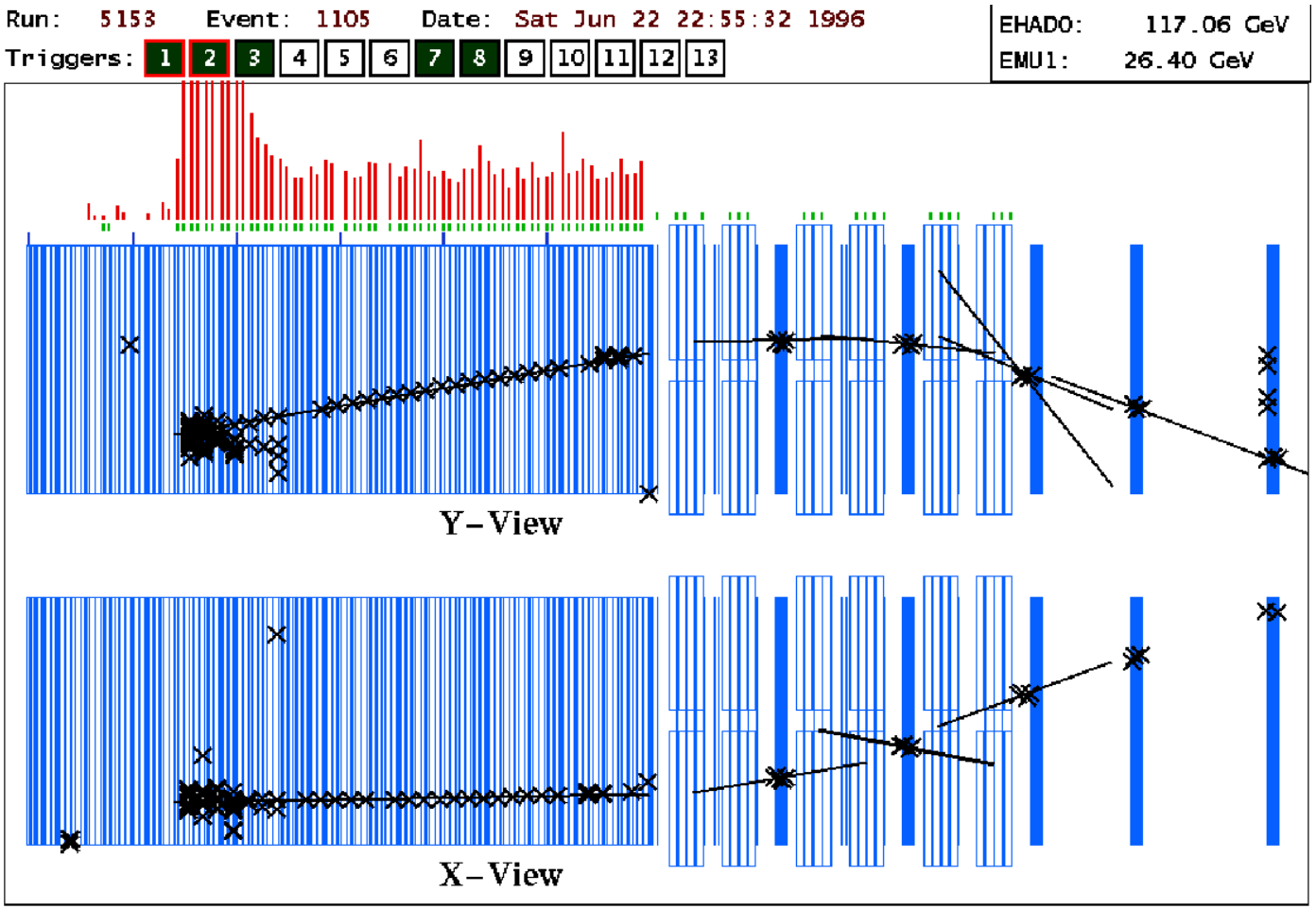

Neutral-current interaction in the NuTeV detector

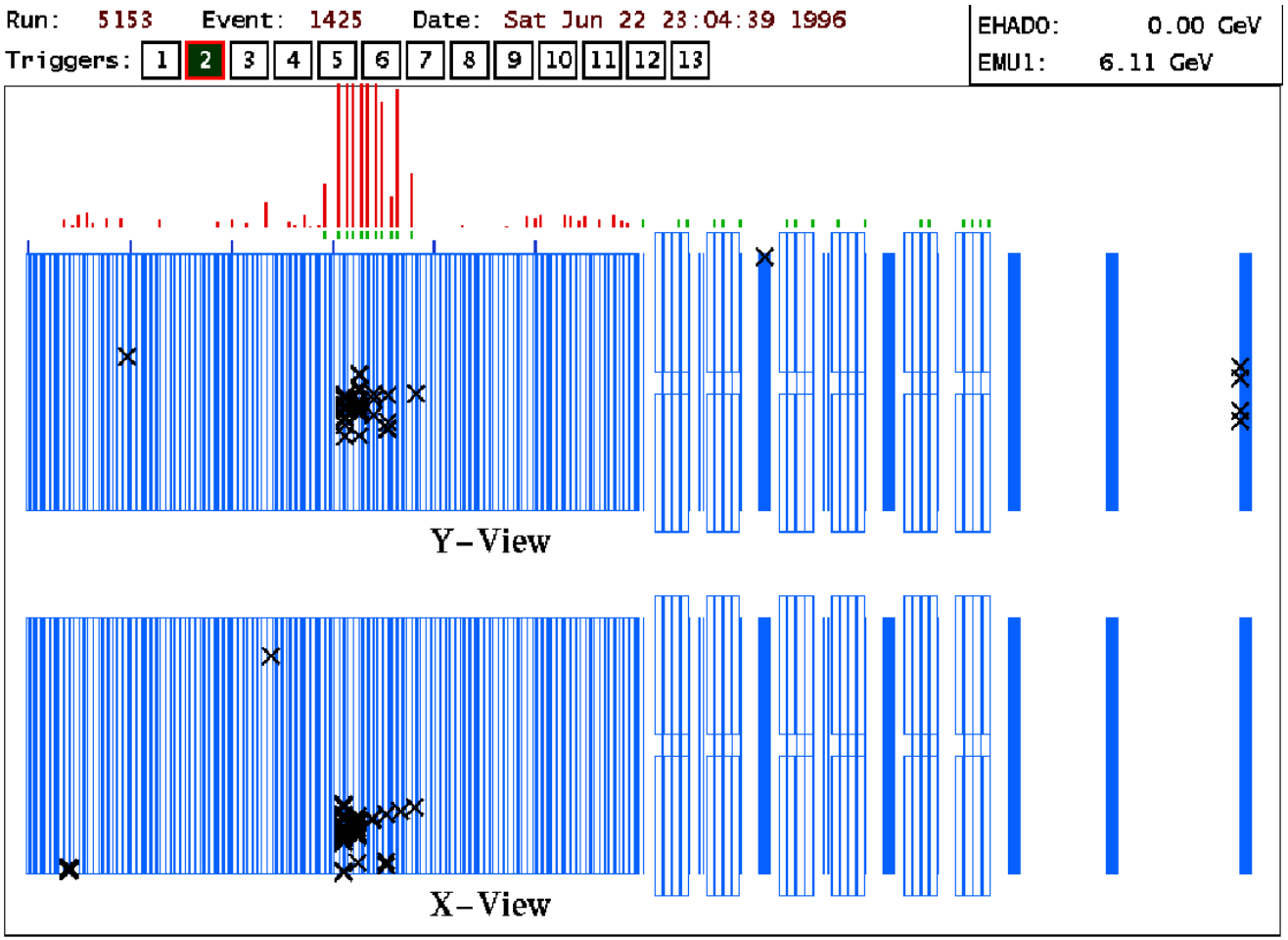

CC vs NC

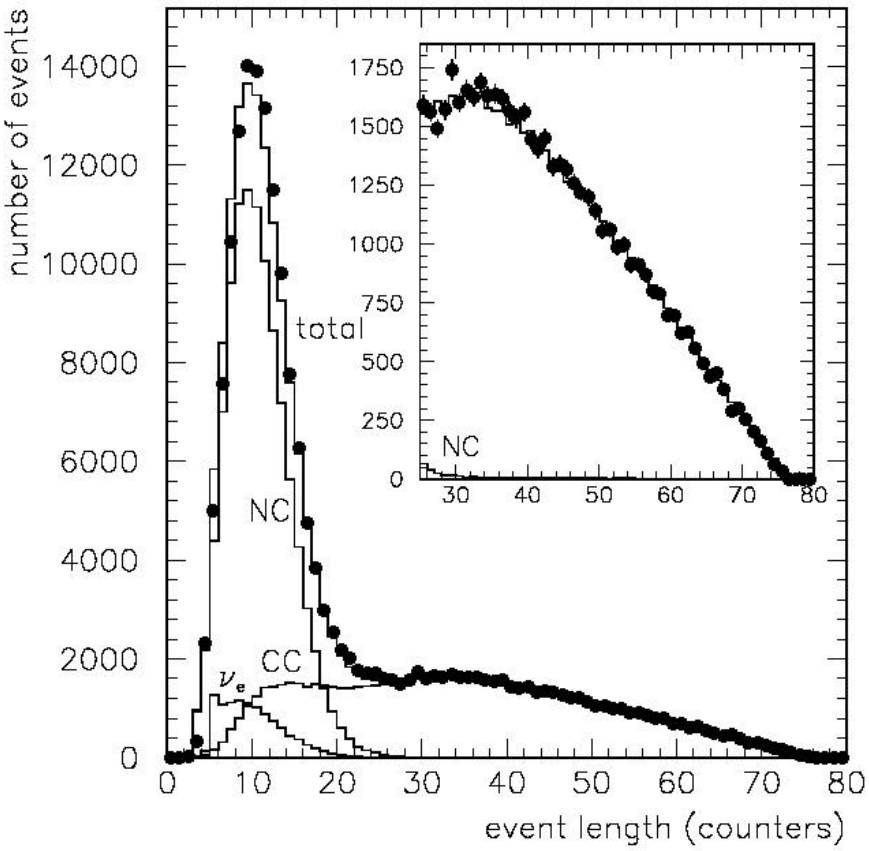

If event length>20 counters

$\Rightarrow$ CC candidate

If event length<20 counters

$\Rightarrow$ NC candidate

$$R_{exp} = \frac{SHORT\ events}{LONG\ events} = \frac{L \leq Lcut}{L > Lcut} = \frac{NC\ candidates}{CC\ candidates}$$

in ν and $\bar{\nu}$ beams (1.62 and 0.35 million events)

CC↔NC contamination

"Short" Sample Contamination

- SHORT ν_μ CC's (20% ν, 10% $\bar{\imath}$
  muons exit, range out (high y)

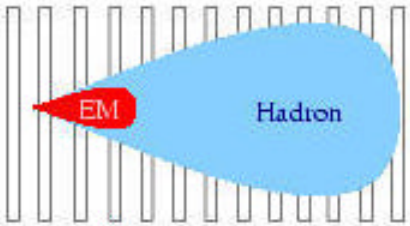

- SHORT ν_e CC's (5%)
  $\nu_e N \rightarrow eX$

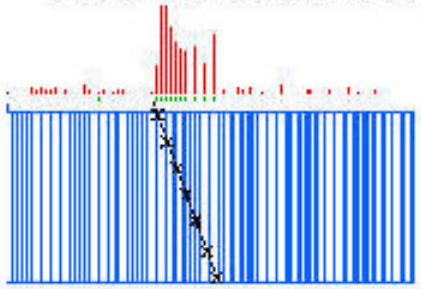

- Cosmic Rays (0.9%,4.7%)

"Long" Sample Contamination

- LONG ν_μ NC's (0.7%)
  punch-through effects

MINOS far detector

- 8 m octagonal steel & scintillator tracking calorimeter
  - Sampling every 2.54 cm
  - 4 cm wide strips of scintillator
  - 2 sections, 15m each
  - 5.4 kton total mass
  - 55%/√E for hadrons
  - 23%/√E for electrons
- Magnetized Iron (B~1.5T)
- 484 planes of scintillator
  - 26,000 m^2

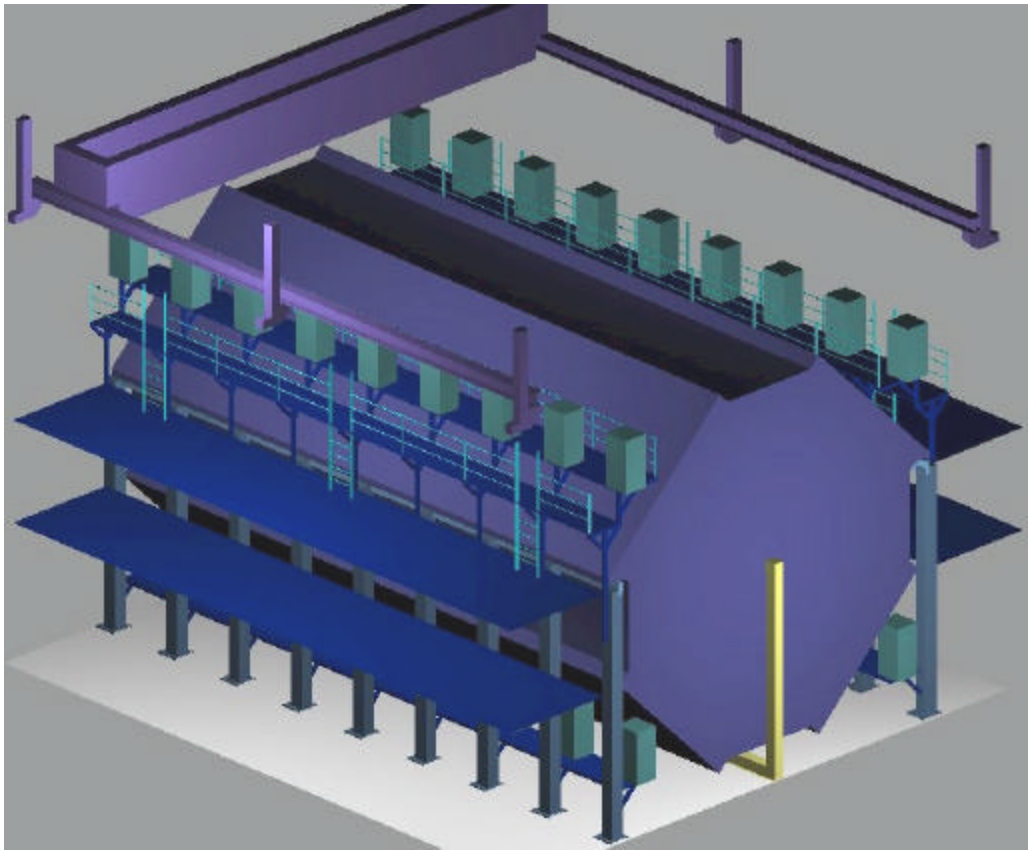

One Supermodule of the Far Detector…

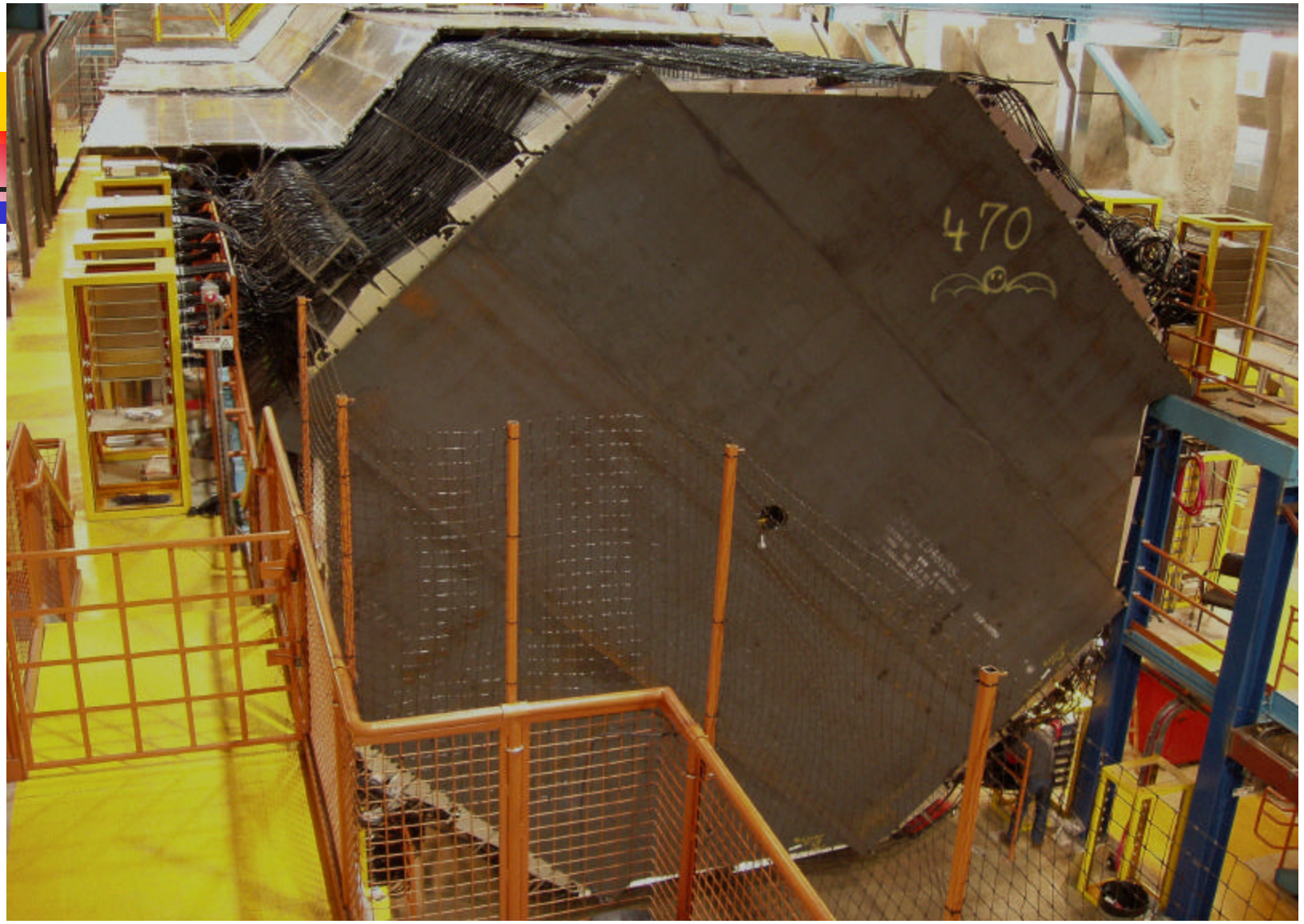
470

Detector technology

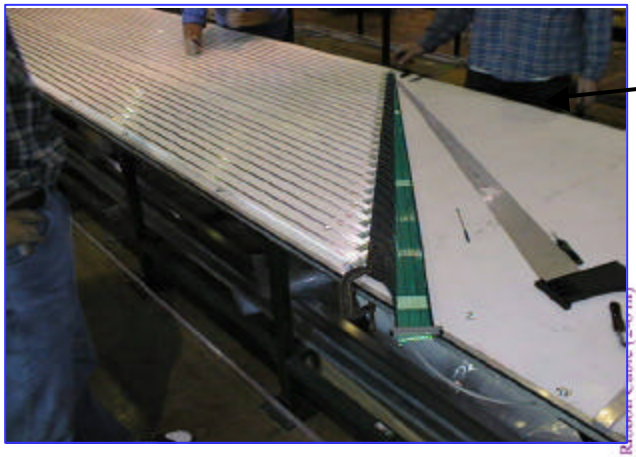

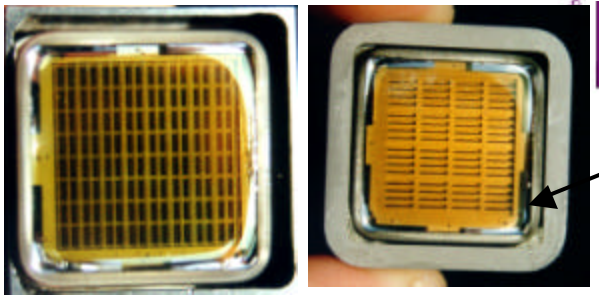

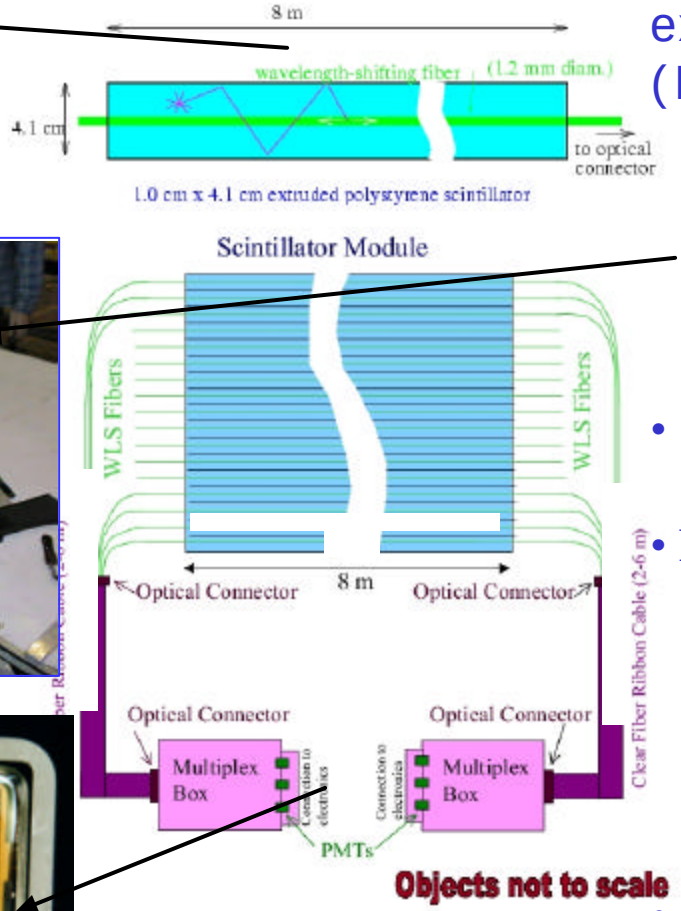

- Scintillator strips are extruded polystyrene (Itasca Plastic)
  - PPO (1%) and POPOP (0.03%) fluors
  - Co-extruded TiO_2 reflective coating
  - Fiber groove
- Kuraray 1.2mm WLS Fibers
  - (Y-11 175ppm)
- PMTs:
  - Far Detector: Hamamatsu R6000-M16 multi-anode PMTs (16 channels), 8 fibers/pixel.
  - Near Detector: “M64”, one fiber per pixel.
- Viking “VA”-based front-end electronics.

Cosmic ray muons in MINOS

- Downgoing Cosmic Ray Muon
- Current rate of CR muons ~ 2 Hz
- Magnetic field not yet on (curvature measurable up to ~70 GeV)

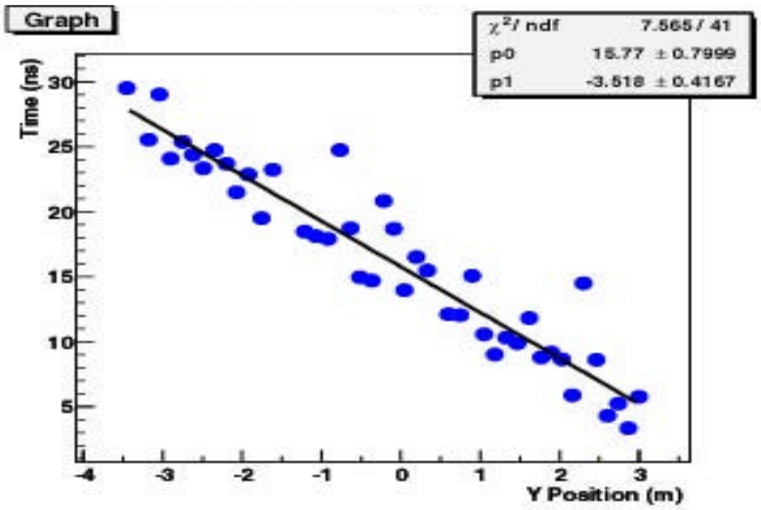

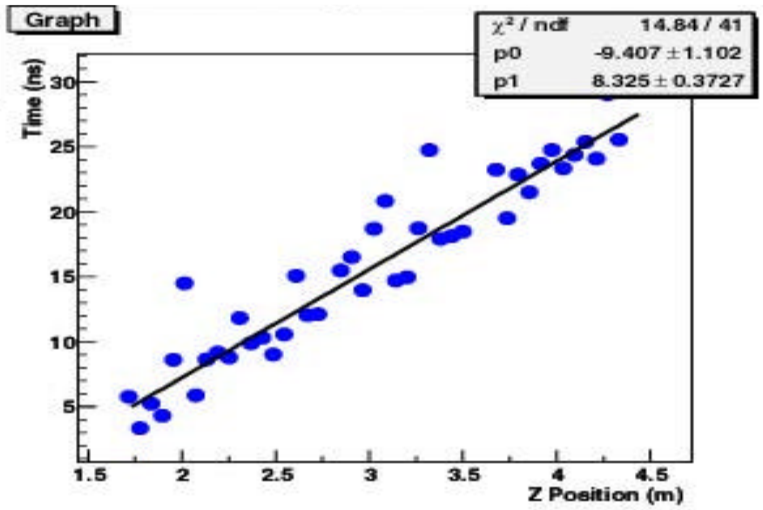

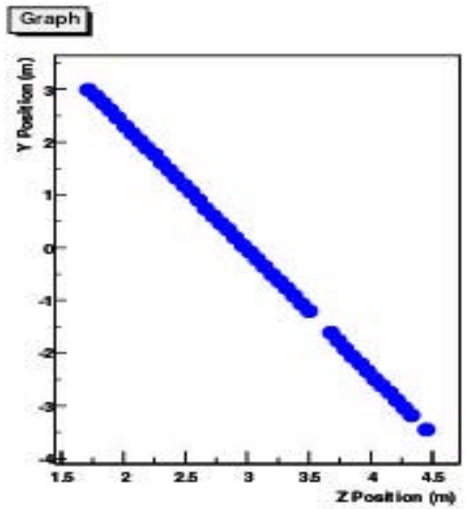

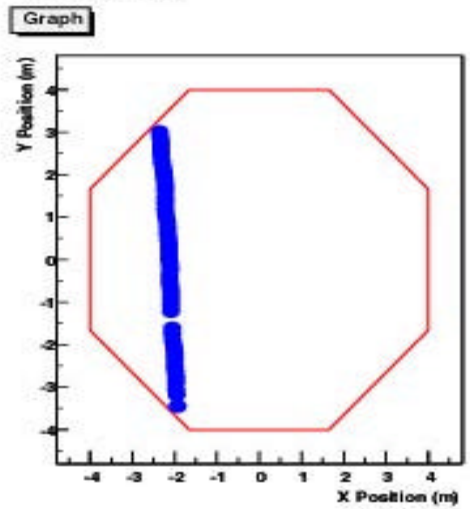

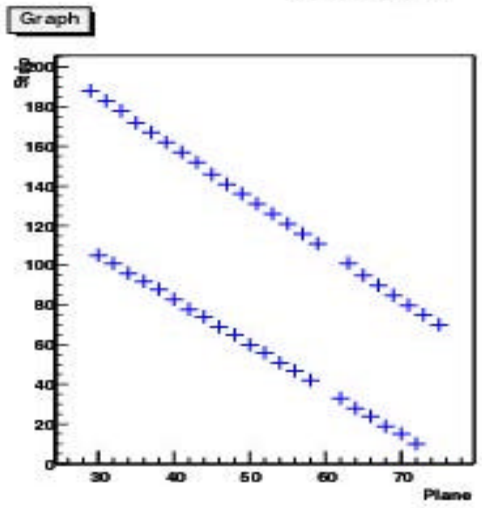

Calibrating with cosmic rays

- Cosmic ray muons are used to **measure the light output** of the scintillator system in all detectors.
- The cosmic-ray muons are used to **intercalibrate** the three detectors.
- **"Clean" muons** (no showers) are selected for **light calibration** and for each muon the light output is corrected for the pathlength to the equivalent light for 1 cm pathlength.
- PMT **gains are corrected** using light injection data.
- On average ~ **8.5 pe's/cm** (corrected for path-length and for muon energy underground)

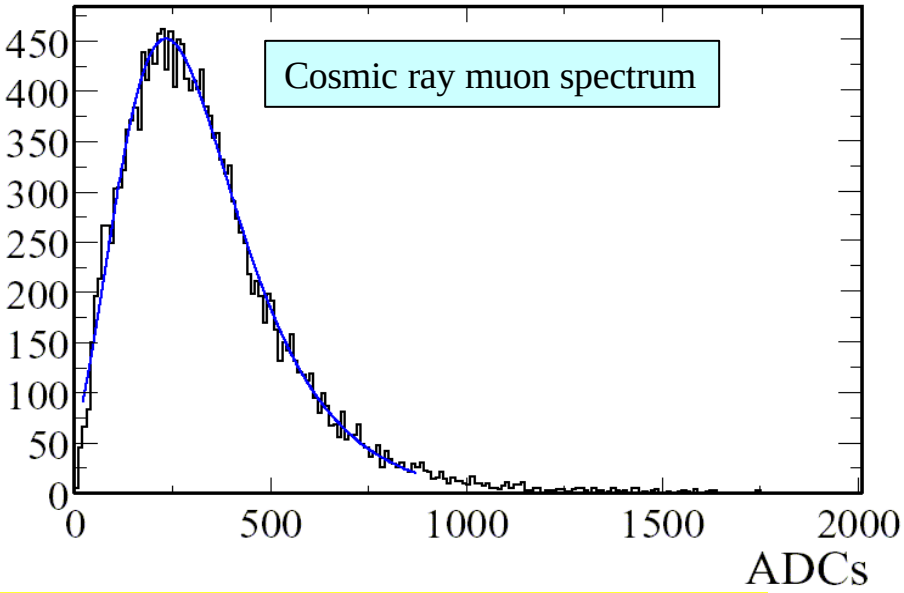

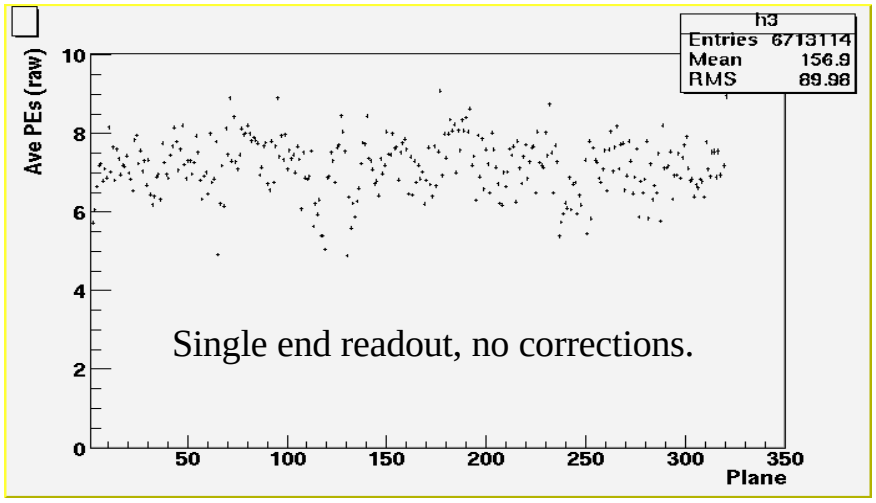

Average light output for all detector planes.

Downward Muons

- 86.8% of the muons recorded come from single muon events
- MINOS single muon rates consistent with world averages
- Strong test of muon efficiency & angular reconstruction

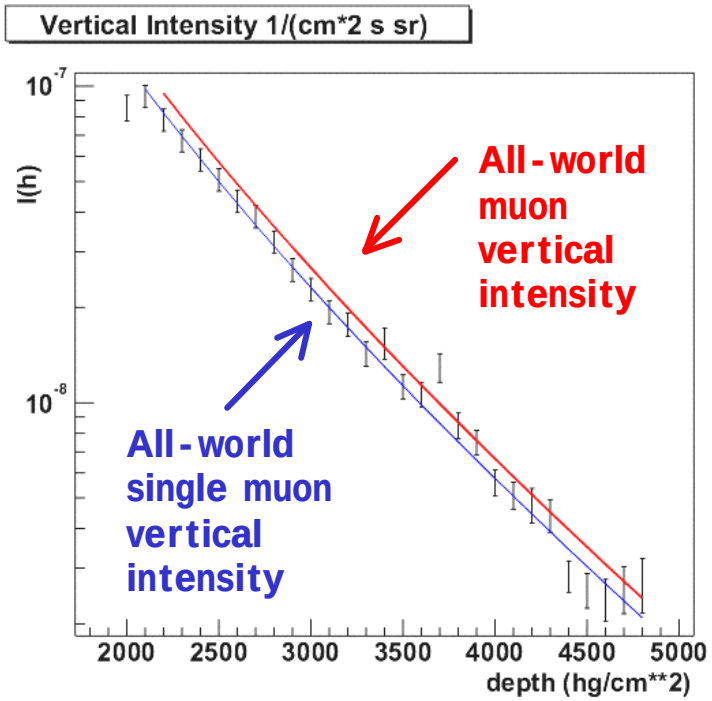

Preliminary MINOS Results
(No field data)

Time resolution in MINOS

- The time resolution of the MINOS scintillator system is determined primarily by the decay time of the Y11 fluor in the WLS fiber ~ 8 ns.
- The time resolution for each scintillator strip is expected to be ~2.5 ns based on the photoelectron statistics for muons.
- Current measurement of resolution using downgoing muons in the far detector is σ=2.6 ns/plane.
- The direction of muons can be determined with ~ 10 planes for contained vertex events.
- To distinguish upgoing from down-going through-going muons ~ 20 planes are needed.

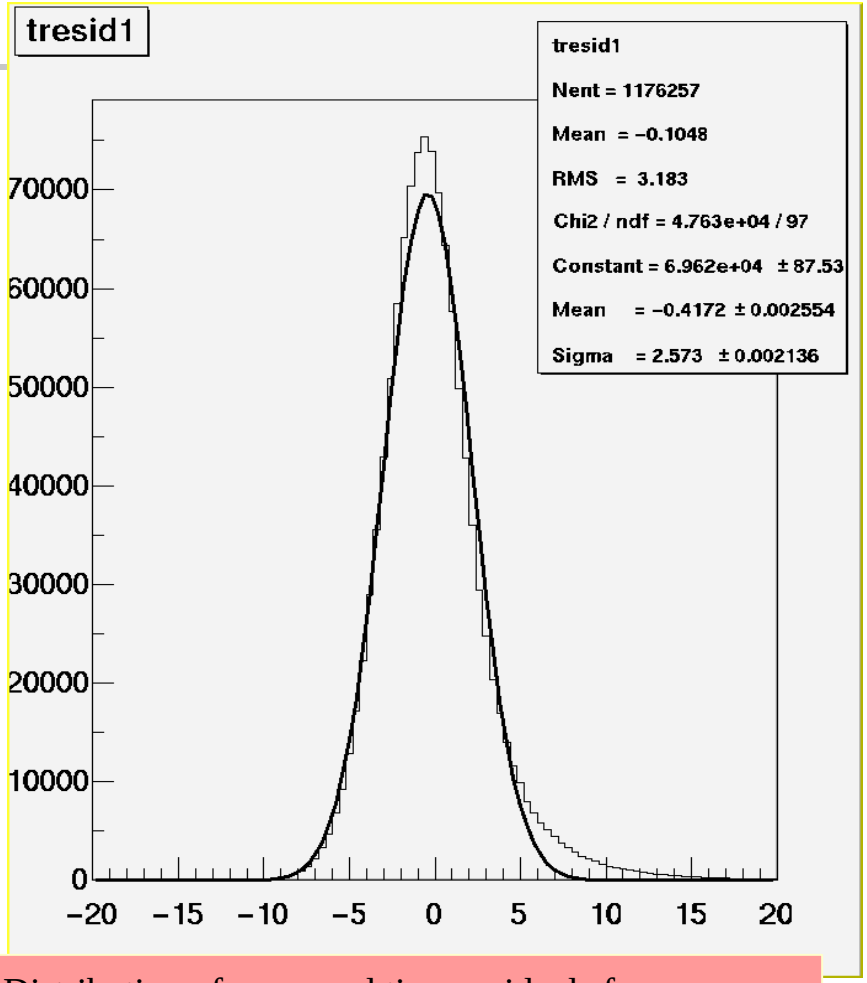

Distribution of measured time residuals for muons Passing through all strips in the far detector. The Time resolution of 2.6 ns is calculated from this data.

Direction Determination

- Use **Y direction timing** and direction cosines at vertex to identify upward-going muons

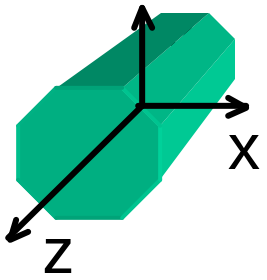

- **Tight 1/b** (=c/v) distribution indicates good timing
- **Negative 1/b** values indicate upward-going muons
- **Peak at 1/b = -1** clearly seen

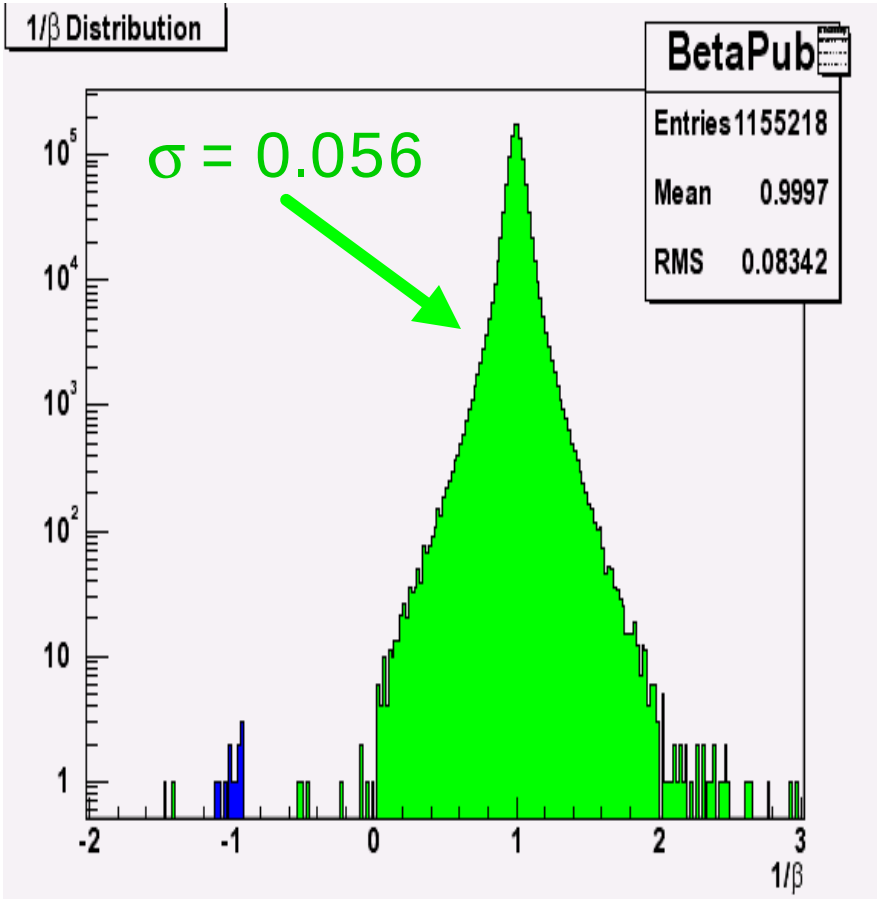

Example Event
μ+ with p = 5.4 GeV/c

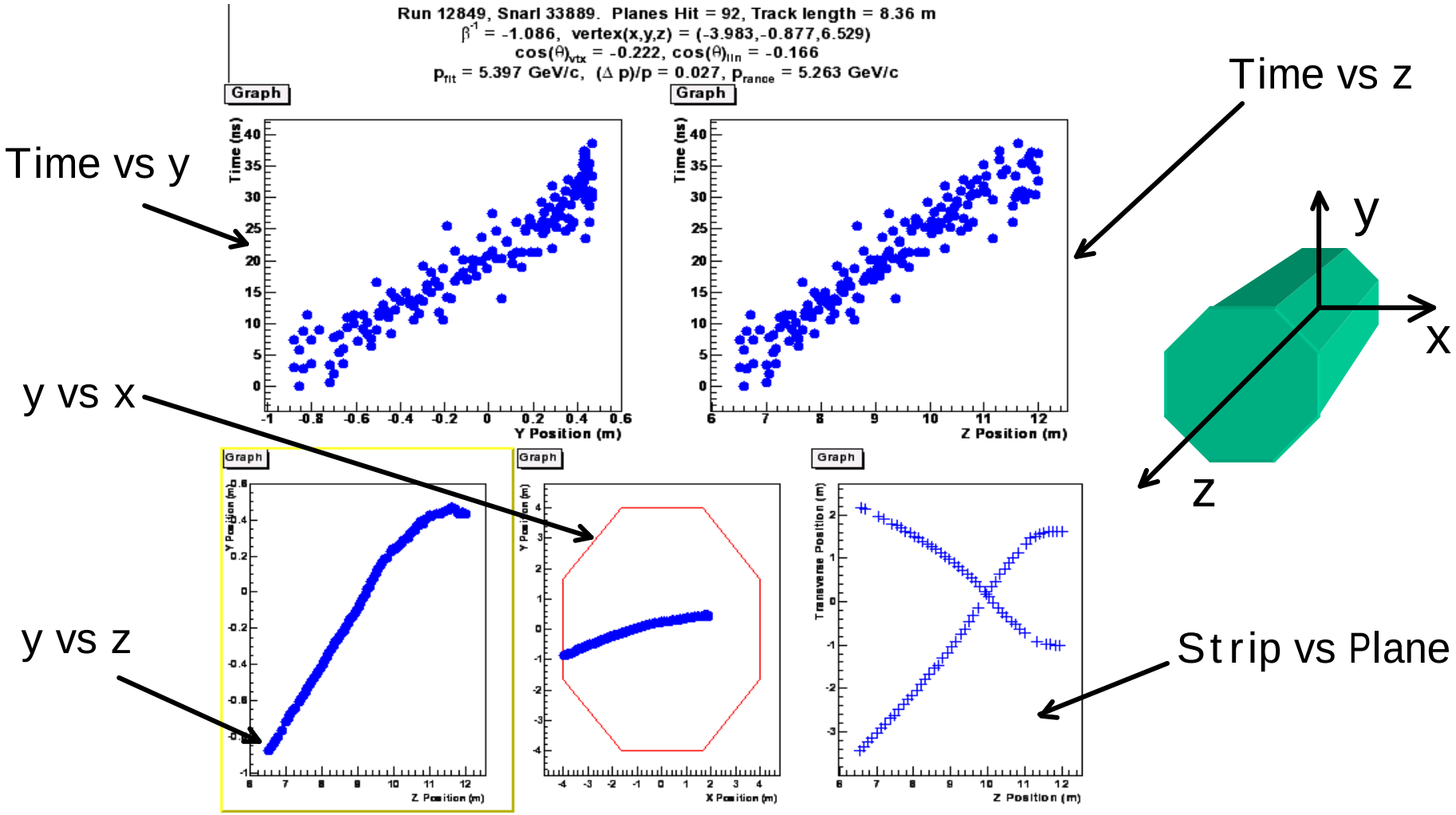

Charge and momentum of upward-going μ

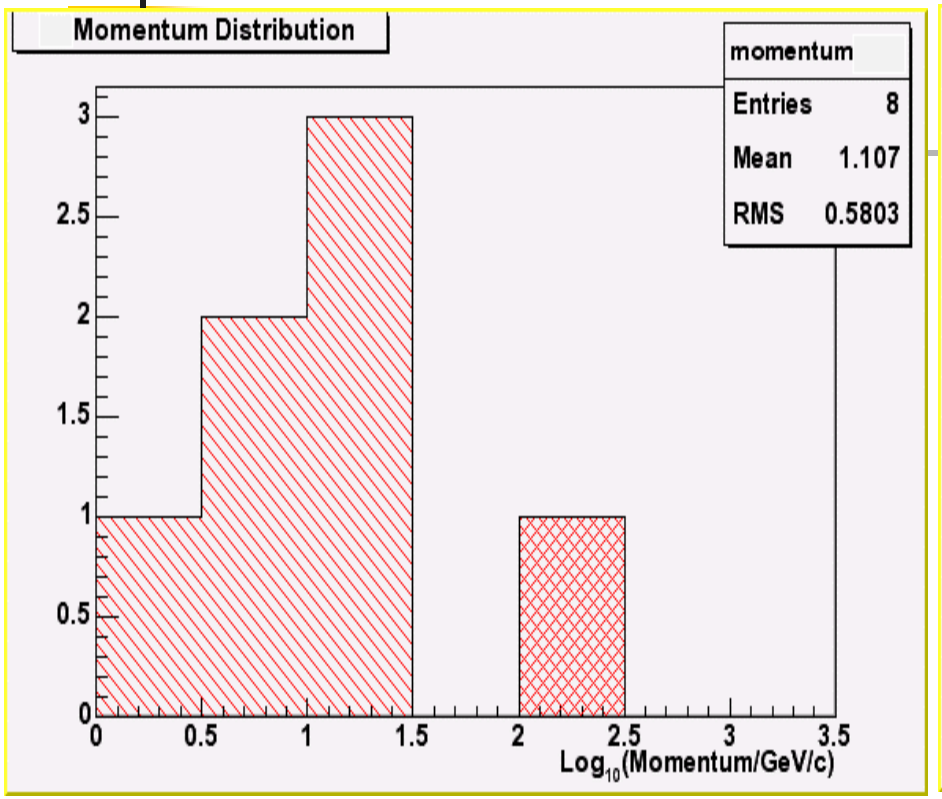

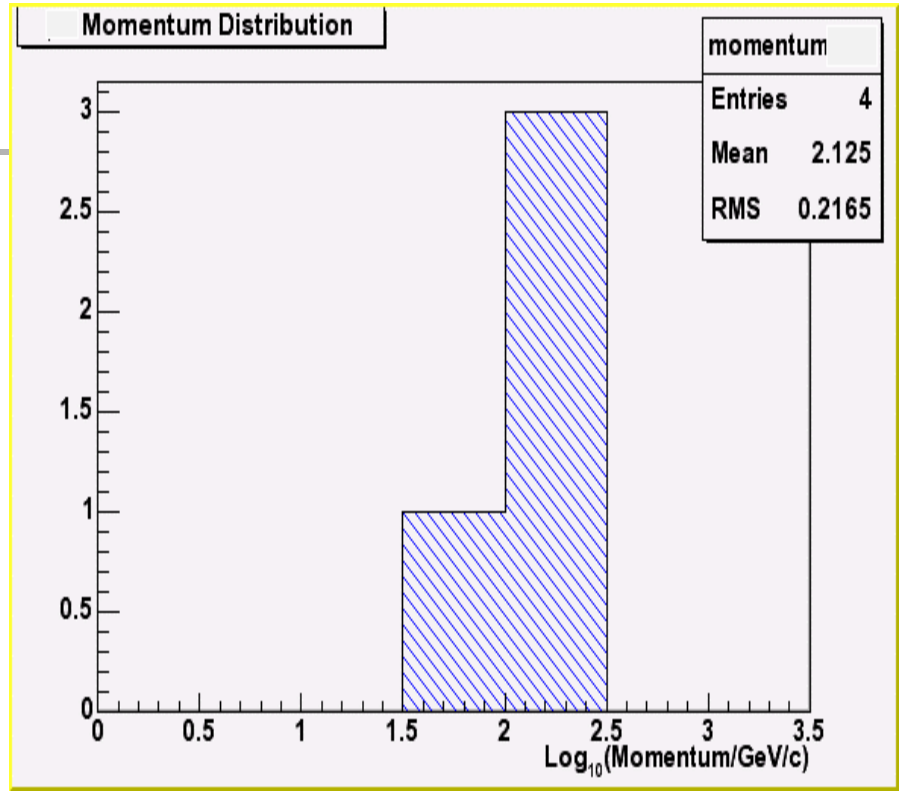

One Sign

The Other Sign

- All muons are assigned a charge, based on the most likely hypothesis.
- Above 100 GeV, the charges and the momenta are not very reliably determined at this time.
- Below 70 GeV, charge and momenta are generally well determined.

A medium energy contained event

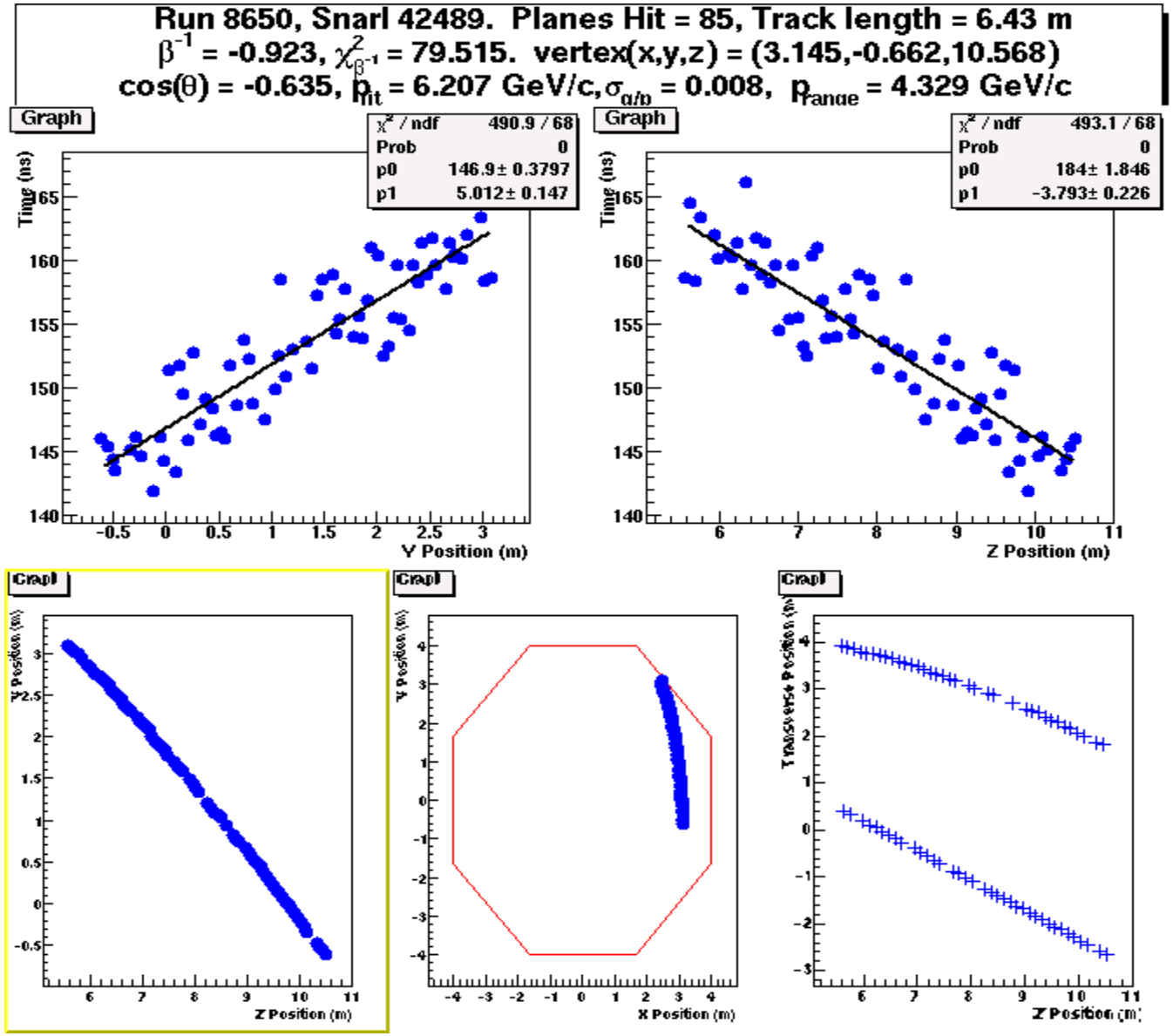

$\overline{\nu}_\mu$ interaction

Neutrino L/E

L/E for all reconstructed **contained**-vertex neutrino events in MINOS **(5 years**). Histogram is no-oscillations while triangles are with nominal oscillations.

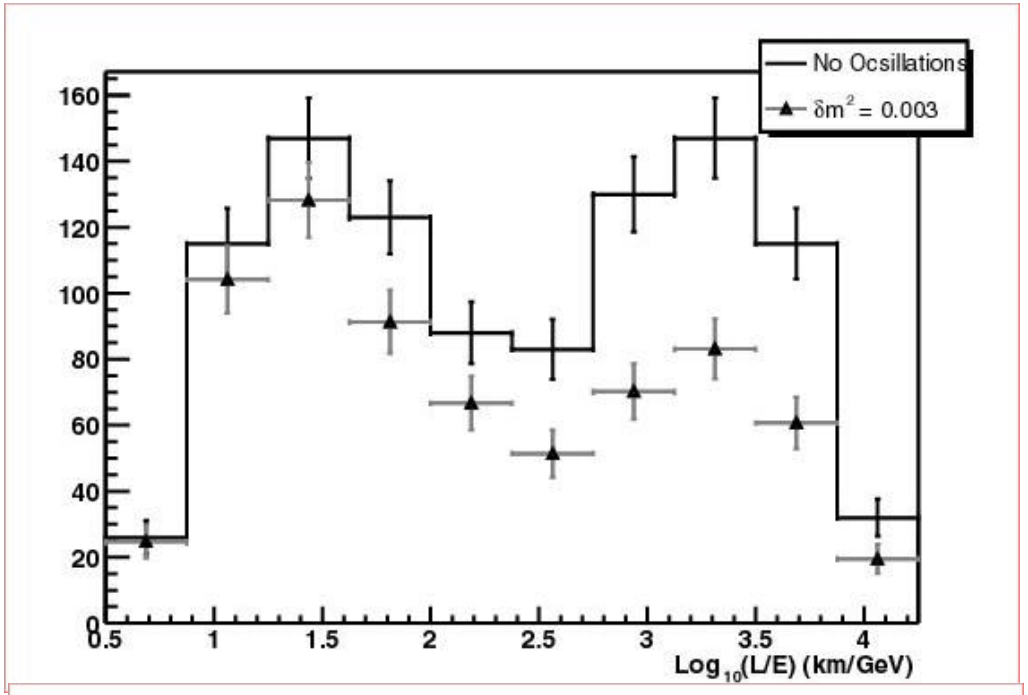

Ratio of **no-oscillation/oscillated L/E** for all reconstructed **contained**-vertex neutrino Events in MINOS **(5 years)**

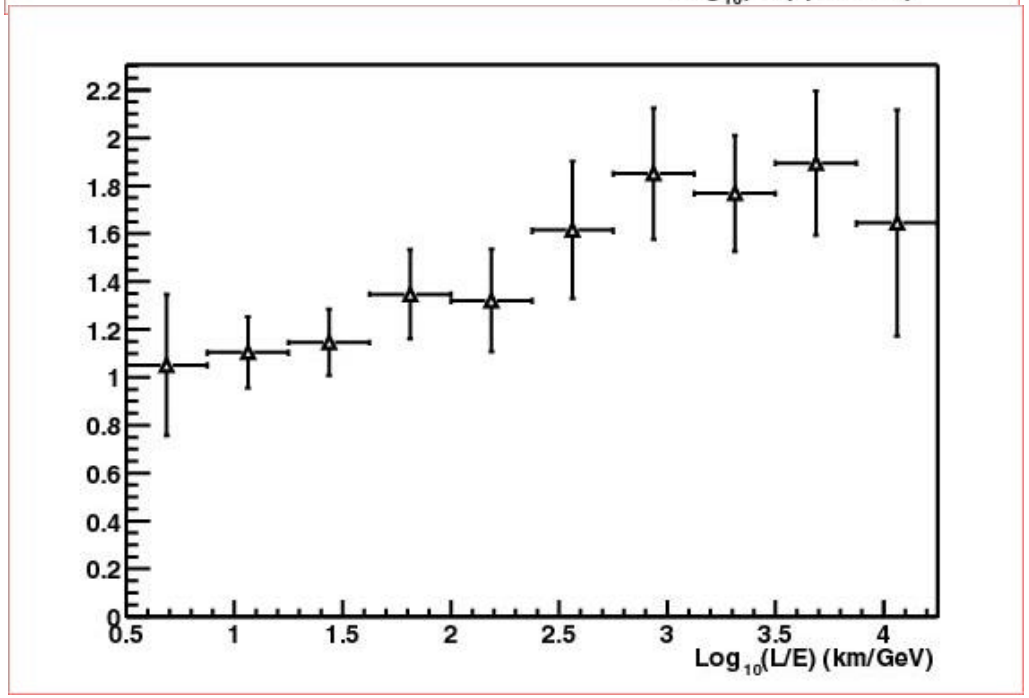

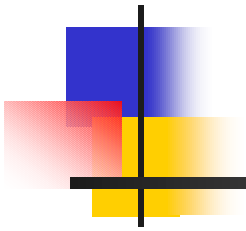

Low Z calorimeter

Proposed for future low energy neutrino beams

Low Z sampling calorimetry concept

Low z absorber in a calorimeter

$\Rightarrow$ maximize detector mass for a given X_0 sampling

or X_0 increases for fixed mass

improved resolution for e. m. showers key for π^0/e separation

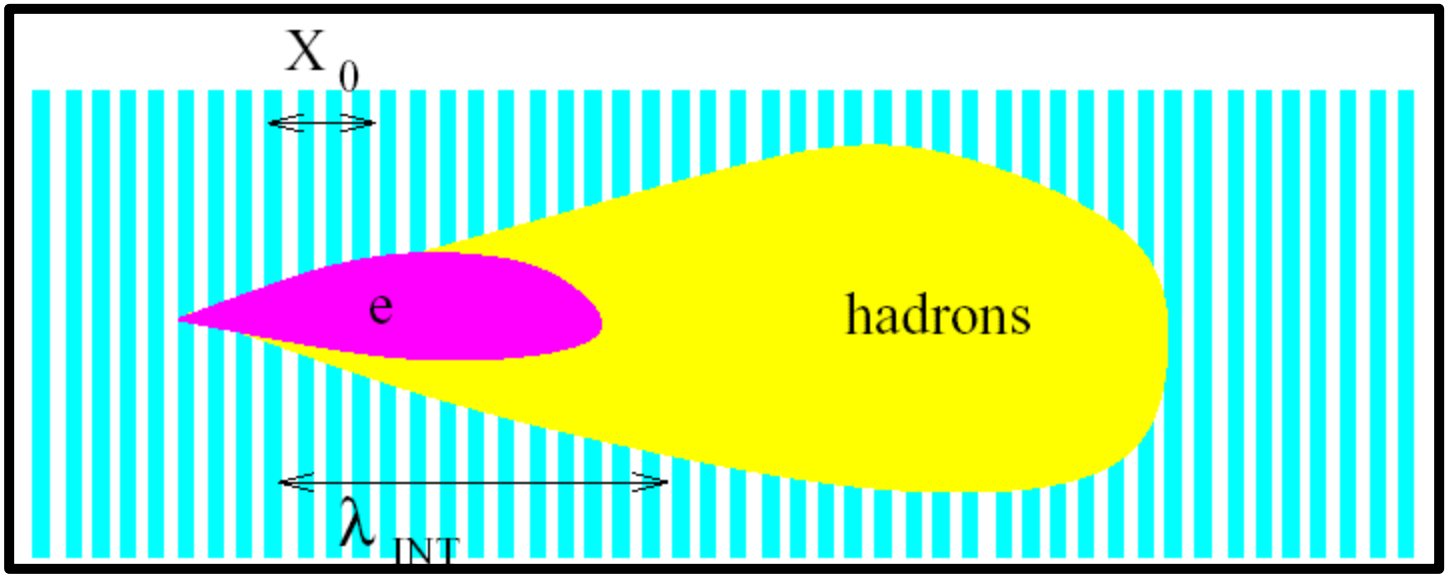

Constructing the detector

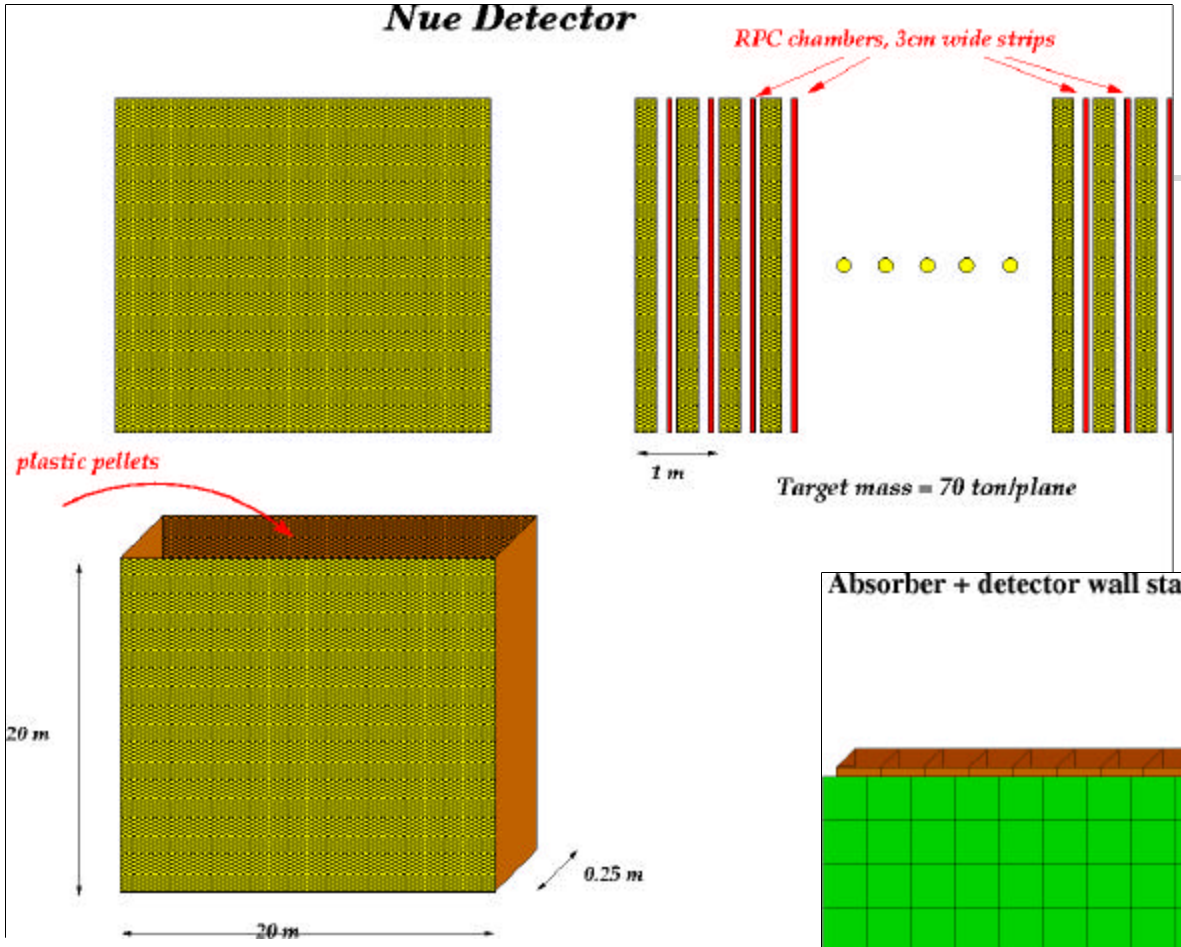

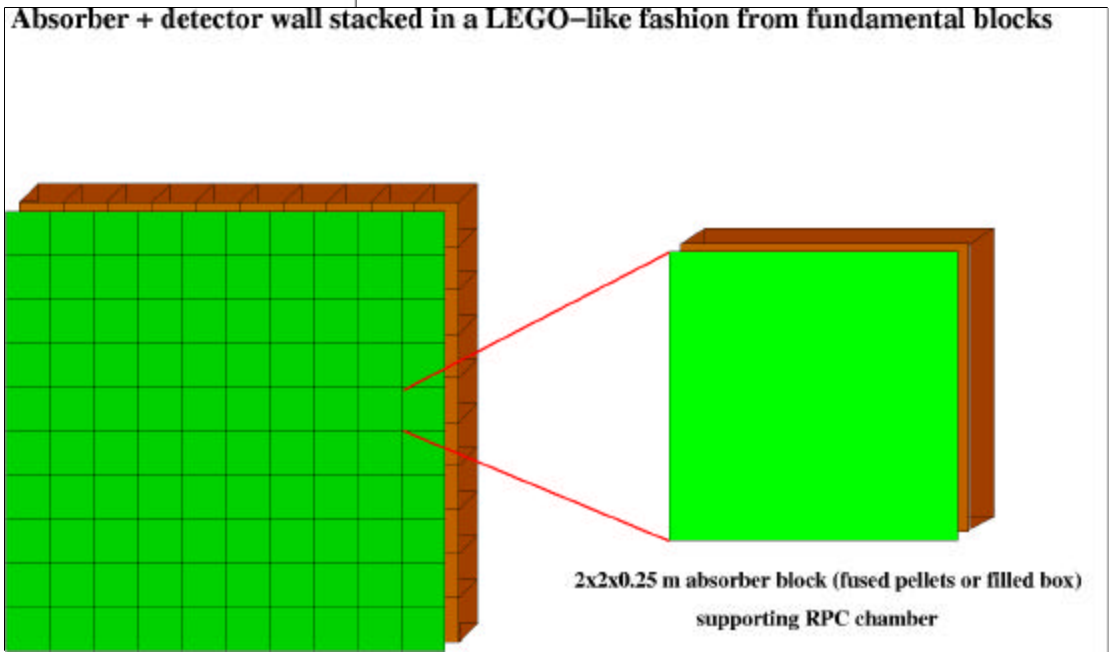

Signatures in a low Z detector

In theory…

- With long X_0, two photons should rarely be degenerate
- Other final state particles well separated

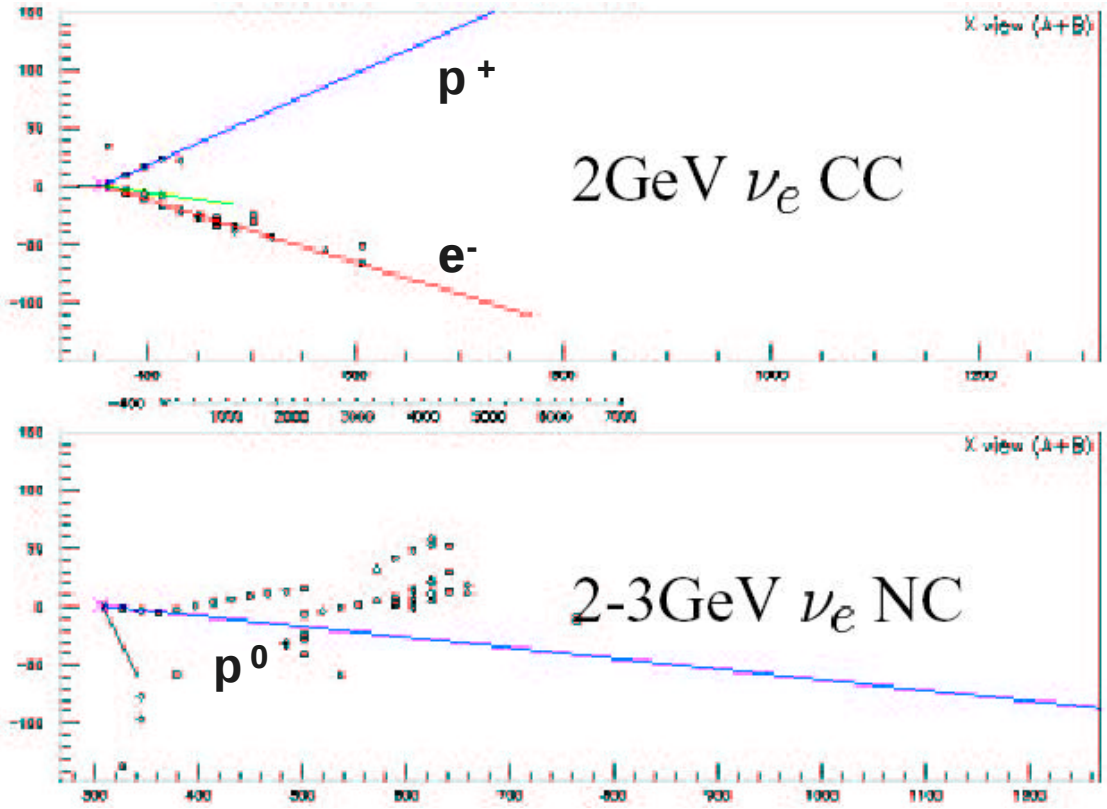

Conclusion

Detector Technology	Largest Mass to Date (kton)	Event by Event Identification			+/-?	Useful Neutrino Energy Range
		ν_e	ν_μ	ν_τ		
LAR TPC	0.6	✓	✓		Not yet	huge
Water C.	50	✓	✓			huge
Emulsion/Pb/Fe	0.27	✓	✓	✓	✓	huge
Plastic/RPC	-	✓	✓			<10GeV
Steel/Scint.	5.4		✓		✓	>.5GeV